AN ESTUARINE PLUME AND COASTAL OCEAN VARIABILITY:

DISCERNING A LAND-SEA LINKAGE IN MONTEREY BAY, CALIFORNIA

A Dissertation

Presented to the Faculty of the Graduate School

of Cornell University

In Partial Fulfillment of the Requirements for the Degree of

Doctor of Philosophy

by

Andrew M. Fischer

January 2009

AN ESTUARINE PLUME AND COASTAL OCEAN VARIABILITY:

DISCERNING A LAND-SEA LINKAGE IN MONTEREY BAY CALIFORNIA

Andrew M. Fischer, Ph. D

Cornell University 2009

Growing populations and climate change along the coastal regions of the world are an increasing reason for concern. Human alterations and land-use change have the potential to influence the ecology of the coastal ocean. Here I examine a link, an estuarine-lagoon, between land and the coastal ocean in Monterey Bay, California. The results show that the discharge plume from the Elkhorn Slough estuary represents a significant link between land and coastal ocean. The discharge plume extends ~1 km offshore in a south-westerly direction and is <1 km wide. The discharge plume is a resolvable feature when compared against the background of ambient Monterey Bay coastal waters, during the rainy months of December and January. The discharge plume is associated with elevated concentrations of dissolved organic matter and nitrate. Particulate matter appears to settle quickly through the water column and is transported in a southwesterly direction with the littoral currents, while the finer sediments and dissolved organics are transported northward to a phytoplankton bloom incubation region.

Fatty acid analysis of filtered water samples showed biologically distinct waters types between the Elkhorn Slough plume and the receiving waters of the coastal ocean. A remarkable feature of the biological content of the plume is the abundance of bacteria-specific fatty acids which correlate well with the concentrations of colored dissolved organic matter (CDOM). Results also showed that plume waters

contained higher concentrations of diatoms and cryptophytes, while the coastal ocean waters showed higher relative concentrations of dinoflagellates. Bacteria and cryptophytes can serve as nutrition for mixotrophic species of dinoflagellates.

Lastly, using three different algorithms from the Moderate Resolution Imaging Spectrometer, I describe the seasonal and inter-annual spatial patterns of phytoplankton abundance within Monterey Bay. Statistically, all three algorithms performed equally well compared with in situ chlorophyll concentrations, but they describe different spatial patterns of phytoplankton abundance. The patterns described by the fluorescence line height (FLH) algorithm, which measures the natural fluorescence of phytoplankton, appear to coincide more closely with previously described oceanographic bloom phenomena. Spatial patterns of using the FLH algorithm also show higher concentrations of phytoplankton in the vicinity of the land-based nutrient sources from Elkhorn Slough discharge.

BIOGRAPHICAL SKETCH

Andrew Fischer was born to Austrian immigrants in Glenridge, New Jersey, USA. At the age of 8 he was thrown into the clear blue waters of the Mexican Caribbean and experienced, first-hand, the vast and diverse undersea world. In high school he received his SCUBA certification and Divemaster credentials and began leading diving tours to numerous sites throughout the Mesoamerican Barrier Reef System. This experience and interest in marine life led him to study Biology as an undergraduate at Emory University in Atlanta, Georgia. Realizing the growing concerns between human interactions and the marine environment, he then moved to Seattle, Washington and obtained a Masters degree in marine resource management. There he studied techniques to restore marine water quality contaminated by land-based runoff. After a few years of working for various state governmental organizations, he moved to Cornell to conduct his doctoral research under the guidance of Drs. Charles Green, Drew Harvell, William Philpot, and John Ryan. His research interests brought him to the California coast and the Monterey Bay Aquarium Research Institute where he studied the dynamics of the coastal ocean and its linkages to the surrounding watersheds.

Andrew is married to his long-time companion, Sarah. Ella who was born in 2007, has added inspiration to both his and Sarah's lives.

For Clifford

ACKNOWLEDGMENTS

TABLE OF CONTENTS

LIST OF FIGURES

LIST OF TABLES

CHAPTER 1

RIVERINE AND ESTUARINE PLUMES AND COASTAL OCEAN VARIABILITY

IN MONTEREY BAY, CALIFORNIA

1.1 Introduction

The condition of the coastal ocean is the result of a balance between the intense interaction of natural marine, terrestrial and atmospheric processes. Numerous connections influence biological distributions, productivity and biodiversity. The coastal zone is also an important habitat providing human and ecosystem services (Costanza et al., 1997). For example, almost half of all fishes and marine mammals live in the coastal ocean. The coastal ocean occupies only 18% of the Earth's surface, however, it provides about a quarter of the primary productivity, 14% of global ocean production and more than 90% of the global fish catch (Sloan et al., 2007). As a result of these services, human population and growth have concentrated on coastal regions of the world and the number of people living within 100 km of a coastline is expected to increase by 35% over 1995 populations levels by 2025 (Center for Climate Research of the Earth Institute at Columbia University). Human pressures on coastal resources add an additional level of complexity to an already complex and dynamic system. Due to the multiple and intense interactions, which occur across multiple spatial and temporal scales, measuring, monitoring and managing the link between land-based activities and the coastal ocean is particularly challenging. Understanding land-sea linkages and how anthropogenic activity on land may influence patterns of phytoplankton abundance in the coastal ocean requires understanding of least two components of this coastal system: 1) land-based pathways of material to the coastal ocean and 2) the variability of phytoplankton abundance patterns in the coastal ocean.

1.2 Riverine and Estuarine Plumes

The transport and fate of land-based input into the coastal ocean has typically been studied by examining sediment discharge patterns (Milliman and Syvitski, 1992; Milliman and Meade, 1983) and nutrient flux from rivers (Boyer et al., 2008; Jickells, 1998). Along the California coast, the riverine transport pathways have been studied in some detail (Warrick et al., 2007; Farnsworth and Milliman, 2003; Inman and Jenkins, 1999). Warrick et al. (2004a) describe the dispersal dynamics of southern California riverine plumes entering the coastal ocean. They show that much of the riverine discharge is initially inertia dominated. Outside the distance of the inertial effects, strong wind stress and local currents are responsible for advection of river plumes. Plume waters near river mouths in this region can contain elevated concentrations of nutrients and are excessively turbid (Mertes et al., 1998), however the sediments undergo rapid initial settling within ~1km of the river mouth and are then transported into the surrounding basins by nepheloid layers (Warrick 2004b). Washburn et al. (2003) describe the spatial scales and persistence of stormwater plumes entering Santa Monica Bay from Balona and Malibu Creeks. The plumes typically extend 4-7 km offshore and 10 km along shore and persist for about three days as they respond to wind forcing and Coriolis acceleration. Riverine plumes entering Santa Monica Bay introduce toxic pollutants, pathogenic bacteria and viruses leading to the failure of nearshore waters to meet California water quality standards for urban runoff outlets 90% (Noble et al., 2003).

As in many regions of the world with Mediterranean climates, riverine discharge into Monterey Bay is driven by episodic winter rainfall, which can produce ephemeral, torrential discharges from the regions creeks and rivers. Late September through April is the rainy period along the central coast of California coast. Northwest

storms bring on average 60 cm of rain to Monterey Bay. Rainfall is largely absent the rest of the year. Rivers, which remain separated from the bay during the dry season, breach their coastal sand bars and introduce sediments and other materials into the coastal ocean.

Another conduit that links the land with the coastal ocean is the estuarine-lagoon system. Along the California coast, these estuarine lagoon systems have been formed by a combination of tectonic activity and sea-level rise. The physical exchange between estuarine-lagoons and the coastal ocean was characterized by Stommel and Farmer (1952). The process is often referred to as "tidal pumping" and the classical model is described in Fischer et al. (1979). Tidal pumping is a type of nonlinear flow produced by tidal currents, which are largely oscillatory, and is produced because tidal currents interact with bathymetry in non-linear, complex ways. This is usually manifested by differences in the strength of maximum ebb and flood currents. Chadwick and Largier (1999a) examined the importance of tidal pumping in controlling the exchange of water at the bay-ocean boundary of San Diego bay. They show that, in accordance with the classical tidal model, the horizontal dynamics at the mouth of San Diego Bay are governed by an asymmetry between the jet-like nature of the ebb flow and the sink-like nature of the flood flow. The flood tide is characterized by water being drawn from a wide region around the mouth of the estuary (radial sink), whereas the ebb tide is characterized by the formation of a jet ejecting water offshore.

Typically, estuarine-lagoons along the California coast, that have had limited alteration to their hydrological regime, exhibit limited exchange with the coastal ocean. Many of these lagoon systems are closed to the coastal ocean much of the year

by wave-built sand spits (Emmett, 2000). These sand spits may be breached during episodic flooding events and wave activity after winter storms. Elwany et al. (1998) showed that the inlet in San Dieguito lagoon in Del Mar, Southern California will remain open naturally 34% of the time and the tendency of this lagoon to remain open is vastly smaller during years of dry weather (12%) versus times of above-average rainfall (66%). When open, the hydrological regime and flow out of these estuarine-lagoons are subject to the inertial influence of tidal exchange and freshwater input from rivers and creeks. Many estuarine-lagoon systems along the central and southern California coast have been subject to some form of hydrological manipulations. These manipulations include diking, ditching, dredging and filling for residential, commercial, and agricultural development. As much as 91% of California's coastal wetlands were lost during the 150 years following statehood and settlement, 85% of tidal wetlands in the San Diego region (Zedler, 1996) and 78% in the San Francisco Bay are have been eliminated by development (Nichols et al., 1986). Estuarine lagoon entrances have also been forced to remain open and dredged for the purposes of recreational and commercial boating traffic and harborage. Plumes from these systems also discharge into the coastal ocean, but their contribution and dynamics have not been well characterized.

1.3 Coastal ocean variability

Oceanographic variability of the coastal waters of MB can be characterized as having three climatological periods: a spring/summer upwelling season, a summer/fall oceanic season and a winter Davidson Current season (Pennington and Chavez, 2000). Coastal upwelling and associated high productivity occurs between February and July (Breaker and Broenkow, 1994; Pennington and Chavez, 2000) and is associated with

upwelling favorable (northwesterly) winds. During the "cold water phase" or "upwelling period" cold filaments generated at Point Año Nuevo, north of the bay, and at Point Sur, south of the bay are advected into MB and are a major source of cold, nutrient-rich waters (Broenkow and Smethie, 1978, Breaker and Broenkow, 1994, Rosenfeld et al., 1994). From August to October, coastal upwelling relaxes and conditions in MB are more influenced by the onshore movement of oceanic waters associated with the California Current and correspond to the period of weaker and variable winds (Breaker and Broenkow, 1994). The winter months of November through January coincide with the occurrence of the northward flowing Davidson current (Breaker and Broenkow, 1994). Atmospheric pressure conditions bring southwesterly winds to the California coast which causes this northward surface current inland of the California Current. These winds are also responsible for producing surface convergence near the coast (Breaker and Broenkow, 1994).

It is essential to improve the understanding of coastal ocean variability since a majority of productivity occurs in the coastal ocean and this area of the ocean is also most utilized and impacted by humans. Satellite remote sensing of the coastal ocean provides one of the most cost effective methods to quantify coastal ocean dynamics and variability. Recurrent sampling by satellite imaging allows for addressing ocean features and phenomena on time scales from single events to their seasonal and interannual variability. Recent advances in satellite and airborne remote sensing, such as improvements in sensor and algorithm calibrations, processing techniques (Franz et al., 2006) and atmospheric correction procedures (Wang and Shi, 2007) have provided for increased coverage of remote sensing ocean color products for coastal regions. These improvements have allowed for a more accurate assessment of the spatial patterns and variability of phytoplankton abundance in coastal waters.

1.4 Research objectives

The objectives of this research are to understand transport pathways between the Monterey Bay and the surrounding coastal watersheds and if there is a discernible influence of land-based activity on phytoplankton ecology in the bay. This work is particularly focused on understanding the physical link between Monterey Bay and the Elkhorn Slough, an estuary linked to the Bay by year round tidal flux. Active agricultural fields are prevalent around the slough and share its drainage basin. The slough-bay exchange channel is also linked to the Old Salinas River channel, which drains runoff from agricultural lands. Thus, the potential for anthropogenic nutrient influence on the bay is considerable. In addition, this work focuses on the use of satellite remote sensing to best characterize the variability of phytoplankton abundance in the Bay. Once these questions are addressed then we can begin to make inferences regarding the relative influence of land-based activities on coastal ocean phytoplankton dynamics. Specific questions which were addressed are as follows:

Question 1) *What is the structure, dynamics and composition of the discharge plume from the Elkhorn Slough?* Is the spatial structure and are the constituents of the discharge plume resolvable features in the background of the coastal ocean? Do the plume constituents respond to forcing events, such a tides and rainfall? What is the fate of the plume and its constituents?

Question 2) *Can we use fatty acid and pigment analysis to characterize the biological composition of water samples from a discharge plume and its receiving coastal waters?* What is the biological content of the Slough plume and the coastal ocean? What is the relative contribution and fate of these biological materials?

Questions 3) *What are the seasonal and interannual spatial patterns of phytoplankton abundance in the coastal waters of Monterey Bay?* Which standard product from the MODIS sensor best characterizes phytoplankton? Can the spatial patterns of phytoplankton biomass be explained in terms of natural variability or land-based input?

The use of innovative sampling techniques is emphasized due to the difficulty of resolving dynamic features in the coastal ocean. In this research, I employ the use of Autonomous Underwater Vehicles (AUVs), underway mapping systems (UMS). Both the AUV and UMS platforms are multidisciplinary systems of sensors that can move rapidly through large regions of the ocean, effectively capturing synoptic views of structure for studying highly dynamics processes in the coastal ocean. Fatty acids are also an innovative approach useful for evaluating the relative importance of the input from such biological materials as bacteria, algae and terrestrial plant matter (Tolusa et al., 2004). Such biomarkers have also been used to assess the health of ecosystems and the degree to which they have been influenced by terrestrial or urban sources (Colombo et al., 1997; Budge and Parrish, 1998). While fatty acid analysis has been typically conducted on sediments and animal tissues, here I use the fatty acid analysis approach on filtered water samples to distinguish different water types. Lastly, using newly developed atmospheric correction algorithms (Wang and Shi, 2007; Franz et al, 2006), I utilize satellite imagery from the MODIS sensor to evaluate algorithms for characterizing phytoplankton abundance in the coastal ocean.

CHAPTER 2

THE STRUCTURE, COMPOSITION AND DYNAMICS OF A CENTRAL

CALIFORNIA ESTUARINE DISCHARGE PLUME

2.1 Introduction

The main conduits that link land and sea along the California coast are riverine and estuarine-lagoon systems. The dynamics at each of these interfaces is unique. Riverine discharge into the coastal ocean is episodic, with large winter storms contributing the majority of annual freshwater and sediment flux (Inman and Jenkins, 1999). Exchange between estuarine-lagoon systems and the coastal ocean is influenced primarily by the mechanism of tidal pumping. Through this process, ocean waters are drawn into an estuary, mix with estuarine waters and discharge back into the coastal ocean as some form of mixed water mass. Since estuarine-lagoon systems receive input from rivers and creeks and are exposed to the tidal influence of the ocean, they are affected by both terrestrial and marine conditions. Most studies of land-sea interaction along the California coast focus on the physical aspects of direct input from riverine plumes (see Chapter 1). Few characterize estuarine-lagoon exchange, and even fewer studies have looked at this exchange from other than a physical aspect.

Here I characterize the discharge plume from the Elkhorn Slough (ES), an estuarine-lagoon system, linked to the coastal ocean of Monterey Bay. I conducted a series of field surveys to describe the structure, composition and dynamics of its discharge plume as it exits the slough at ebb tide. I sampled physical, chemical and biological properties of the plume using an autonomous underwater vehicle (AUV), an underway mapping systems (UMS) and drifters. Both the AUV and UMS platforms

are multidisciplinary systems of sensors that can move rapidly through large regions of ocean, effectively capturing synoptic views of structure for studying highly dynamic processes in the coastal ocean. My primary objectives were; 1) to see whether the spatial structure and constituents of the plume were resolvable features in the background of the coastal ocean, 2) determine the fate of the plume constituents, and 3) to determine whether plume constituents respond to forcing events. In this chapter I focus on the physical and chemical aspects of the ES discharge plume. Biological aspects are addressed in a subsequent chapter.

Transport of materials from estuarine lagoons into the coastal have a direct influence on ocean biogeochemistry (da Cunha et al, in press), coastal sediment budgets (Inman and Jenkins, 1999; Eittreim, 2002) and, coastal phytoplankton blooms (Kudela and Cochlan, 2000) and pollutants (Bay et al., 1999; Noble, et al, 2003). Due to development pressures in surrounding watersheds, estuarine-lagoons along the California coast are increasingly acting as repositories for direct point charges of contaminants, indirect pollutant input through non-point land sources and atmospheric pollutant deposition. Hydrological manipulations at the mouth of these lagoons have changed the quantity and composition of materials transported to the coastal ocean. Studying the transport and fate of these materials is essential for understanding the influence of anthropogenic alterations to coastal ecosystem ecology. It is also necessary for responsible management of coastal resources, especially those within a national marine sanctuary and in proximity of major agricultural and urban centers.

2.2 Study area

Elkhorn Slough (ES), a 9.8 km^2 estuarine-lagoon system, is located on the eastern side of Monterey Bay mid-way between Monterey and Santa Cruz
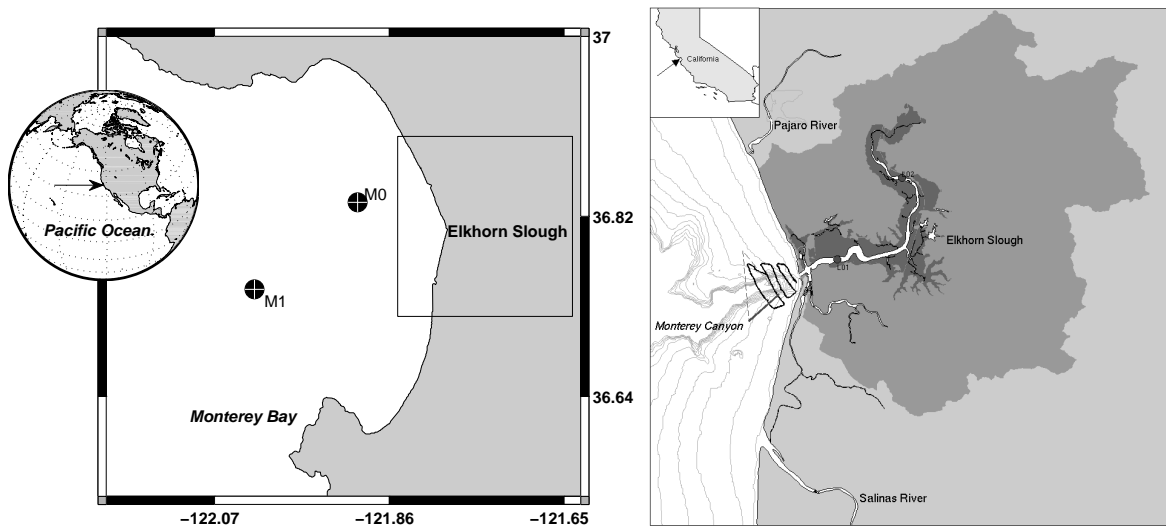
Figure 2.1. The location of the Monterey Bay and the Elkhorn Slough watershed in relation to the geography of the bay (left panel). M1 and M0 are the locations of the offshore and nearshore moorings. The right panel depicts the Elkhorn Slough (ES) watershed. Dark grey indicates the watershed drainage area and green indicates wetland areas. The underway mapping grid is shown as a black line. The autonomous underwater vehicle sample area is shown as a red triangle. L01 and L02 are the locations of the Land/Ocean Biogeochemical Observatory (LOBO) moorings in the lower and upper portions of the slough.

(Figure 2.1). ES is a complex shallow waterway comprised of a main channel, extensive mud flats, Salicornia marsh, and small tidal channels. It is about 10 km long, with depths ranging from 8 m at the Harbor entrance, to 0.5 m near its head. The average depth is approximately 3 m. The main channel has a width of about 200 m to 90 m. Its 181 km^2 watershed is characterized by rangeland, oak woodland, coastal maritime chaparral and coastal cropland supporting a variety of high value vegetables, flowers and fruit. The crop farms in ES watershed have been characterized as having some of the most severe erosion problems in the western United States due to crop choice (e.g. strawberry and flower row crops), highly erodible soils types (Arnold loamy sand, Elkhorn fine sandy loam, Santa Ynez fine sandy loam and Alviso silty

clay loam) and steepness of the farming terrain (Rein, 1999). Historically, an average of 33 tons of soil per acre was lost annually from sloped cropland and washed by storm water onto neighboring lands, county roads, and into drainage canals and streams, and ultimately into Elkhorn Slough (USDA, 2005).

Originally, ES was a sluggish lagoon with limited influence from the coastal ocean. The opening and closing of the sand spit separating it from the coastal ocean was regulated by winter storm activity. However, since the 1800s, the ES has been subjected to significant alterations, changing its hydrodynamics and the dynamics of its discharge plume. In the 1800s, lands surrounding ES were altered through the construction of ditches and dikes to make the low-lying marshes suitable for agriculture. In approximately 1900, a 150-hectare area near the mouth of the Slough was diked to form evaporative salt ponds. The Army Corps of Engineers significantly changed the hydrology of Elkhorn Slough in 1946 by cutting through the sand spit separating the slough from Monterey Bay. Since then, the slough has been subject to semi-diurnal tidal forcing. The tidal forcing between the bay and the ES is characterized by a tidal asymmetry, which is due mainly to the relatively narrow opening through which tidal waters must flow when compared to the large area of marsh and mud flats, as well as the retardation of tidal flow by frictional effects (Broenkow and Breaker, 2005). As a result, the duration of the ebb tide is reduced relative to that of the flood tide, and this results in faster ebb currents than would otherwise occur. This asymmetry and increased currents has led to increased erosion of the banks and tidal creeks within ES, and the widening has caused marsh vegetation to be lost from its edges (Wasson et al., 2001). These alterations have also led to a greater than 2-fold increase in the tidal prism (the volume of water exchanged between the slough and its parent body of water over a tidal cycle) and an increase in the tidal

11

currents in the main channel of the slough. A 1956 survey by Johnson (1973) reported

a tidal prism of 2.65 x 10^6 m^3. Smith (1974) estimated a tidal prism of 4.7 x 10^6 m^3.

In 1993, Breaker and Broenkow (2005), using the same methods as Smith (1974),

estimated the tidal prism as 6.0 x 10^6 m^3. Maximum tidal currents in the main channel

of the slough have increased from approximately 1.5 knots in 1971 to 3.0 knots today.

Recent estimates of the erosional sediment losses from the slough have ranged from

3.5 x 10^4 m^3 year^{-1} (Crampton, 1994) to 8 x 10^4 m^3 year^{-1} (Malzone, 1999).

Observations of bank erosion indicate average losses of 40 cm year^{-1} (Wasson et al,

2001). Based on aerial surveys, losses of the surrounding wetlands have increased

significantly over the past 50 years (Lowe, 1999).

        The discharge from ES constitutes one of the largest inputs into Monterey Bay.

The amount of water exchanged between ES and the bay, based on tidal prism

estimates, is 2.2 x 10^9 m^3, three times as much water as is discharged by all the rivers

(San Lorenzo River, Soquel Creek, Aptos Creek, Pajaro River, Salinas River) entering

MB. The exchange between the ES and the coastal ocean is manifested as a

pronounced discharge plume that appears turbid during the ebb tide, while the

incoming tide introduces relatively clear water from Monterey Bay. The plume is

particularly evident during the winter months when the hydrological regime is further

influenced by fresh water input from the surrounding creeks and runoff from the

surrounding watershed. Carneros Creek, at the head of the slough, contributes the

largest influx of freshwater into ES, an average of 2,800 acre feet (3.4 x 10^6 m^3)

annually.

2.3 Field program

The discharge plume of the ES was sampled on December 9 and 10, 2004 and on January 6, 10, 20 and 21, 2005 during the ebb stage of the tidal cycle (Figure 2.2). The surface expression of the plume was measured by a near surface underway mapping system (UMS) deployed from a Boston Whaler. The surface UMS is set of instruments measuring water clarity (light transmission), temperature and salinity, chlorophyll fluorescence, color dissolved organic matter (CDOM) fluorescence, and nitrate concentration. The individual instruments used to measure these parameters were a WetLabs Cstar, SeaBird 45, WetLabs WetStar, WetLabs CDOM fluorometer
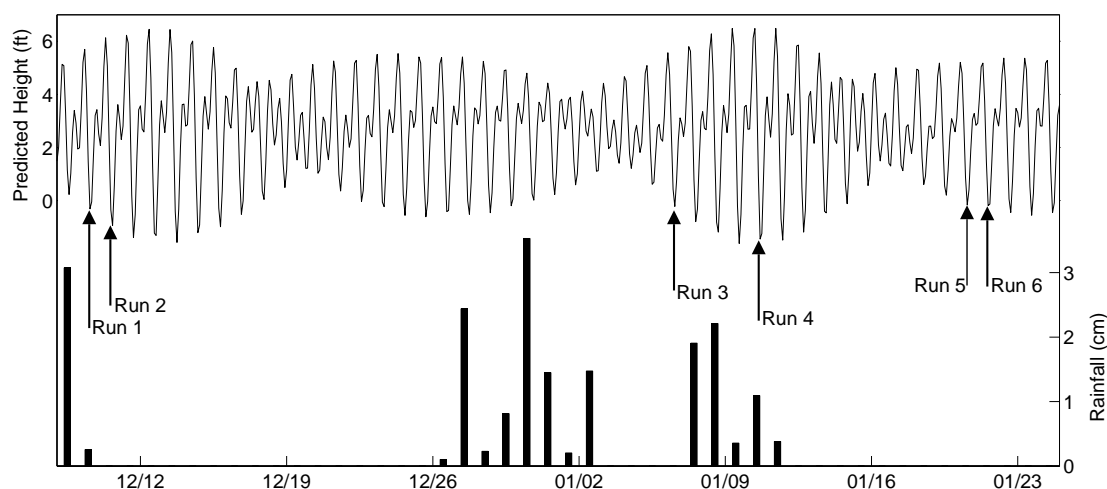
Figure 2.2 Elkhorn slough discharge plume was sampled during the ebb tide on December 9 (run 1) and December 10, 2004 (run 2), January 6 (run 3), 10 (run 4), 20 (run 5), 21 (run 6), 2005. Sampling occurred during winter month and sometimes after rain events.

and an In Situ Ultraviolet Spectrophotometer (ISUS)(Johnson and Coletti, 2002), respectively. Water samples were pumped through the instruments from 0.3 m below the surface. The speed of the boat was regulated to avoid air bubbles in the system. The ES plume was sampled between four to six times on each day during the outgoing

tide. The boat followed a regular sampling grid (see Figure 2.1) designed to capture the full extent of the plume. The average time to complete each sampling pass was 76 minutes.

MBARI's autonomous underwater vehicle (AUV) was deployed from the RV Zephyr in conjunction with the UMS surveys to monitor physical and bio-optical conditions through the volume of the plumes. The speed of the AUV during surveys was ~1.5 m/s, and the vehicle pitch through a sawtooth sampling pattern was 30°. The AUV followed a triangular surface track (see Figure 2.1). The average duration of each triangular sampling track was 58 minutes. This pattern was repeated four to seven times each sampling day through the ebb stage of the tide. These sampling attributes provided synoptic high-resolution sections through plume waters. The AUV was equipped with a multidisciplinary sensor suite for measuring physical, chemical and optical properties. I present observations from three sensors: a SeaBird SBE 25 CTD that measured temperature and conductivity, a HOBI Labs HS-2 sensor that measured optical backscattering at two wavelengths and chlorophyll fluorescence, and an in situ ultraviolet spectrophotometer (ISUS) sensor that measured nitrate concentrations (Johnson and Coletti, 2002). To represent properties within the volume, a two-dimensional interpolation of the sampled volume was created for each measured variable via Delaunay triangulation in MATLAB.

Drifters were deployed to describe the plume surface flow patterns. The drifters, consisting of a PVC pipe with foam flotation, were attached to a drogue to ensure that the movement of the drifter coincided with the flow of the water and not that of the wind. The PVC pipe housed a Garmin GPS receiver which, in addition to

logging its geographic position every 30 seconds, recorded local time, distance between logged points, speed and magnetic direction.

To describe the background conditions of the coastal ocean and plume receiving waters, data from two moorings, one at the mouth of Monterey Bay (M1) and the other in the nearshore waters of the northern shelf (Figure 2.1) were examined. The observations include temperature, salinity and nitrate at M1 and temperature and salinity at M0. Temperature and salinity were measured by Sea-Bird microcat conductivity, temperature, depth (CTD) sensors at 3.5, 10, 20, 40, and 60 m. Nitrate was measured by an in situ ultraviolet spectrophotometer (ISUS). Hourly data of nitrate, salinity and temperature from surface waters (1 m) from M1 and M0 were downloaded from the MBARI LiveAccess server (http://dods.mbari.org/lasOASIS/main.pl?). For this study, monthly averages between the years 2002-2007 and 2005-2007, respectively, were calculated for each of the stations.

To understand the plume source region, data from two moorings, part of the Land/Ocean Biogeochemical Observatory (LOBO), which measured components of biogeochemical processes in ES, were examined. Temperature and salinity (conductivity) were measured by Sea-Bird Electronics (SBE-16plus and SBE-37) and YSI environmental (6600). Nitrate was measured by an in situ ultraviolet spectrophotometer (ISUS). Hourly temperature, salinity and nitrate data of surface waters (0.5 m) from mooring L01 in the lower portion of ES and L02 in the upper portion of ES were downloaded from the LOBO Network Data Visualization (LOBOViz 3.0) (http://www.mbari.org/lobo/loboviz.htm) website. Data processed from these stations spanned the years 2003-2007 and 2004-2007, respectively. Monthly averages were calculated at each of these stations. Rainfall data was

acquired from the University of California Integrated Pest Management Program website for Freedom, California http://www.ipm.ucdavis.edu/WEATHER. From these data, the average monthly rainfall (cm) was calculated for the years 1970-2005.

Data from the Moderate Resolution Imaging Spectroradiometer (MODIS) on the Aqua satellite was also used in this study. MODIS data was processed from Level 1A using the SeaDAS software, applying calibrations for ocean remote sensing developed by the MODIS Ocean Biology Processing Group. True color images, from cloud free days during the sampling period, were created using the 645nm (red), 555nm (green) and 469nm (blue) bands. These bands have the spatial resolutions of 250, 500 and 500m, respectively. The true color images further describe the background ocean conditions of the coastal ocean and provide a snapshot of turbid riverine plumes.

2.4 Results

2.4.1 Monterey Bay background conditions

Figure 2.3 shows the average monthly nitrate, salinity and temperature changes for the surface waters of the upper (L02) and lower (L01) portions of the ES estuary. The bottom panel shows the monthly average rainfall at a rain gage station located in Freedom, California, 9.6 kilometers from the head of ES. Changes in the properties of the upper and lower portions of ES closely reflect the properties measured at M0 and the influence of land-based run-off. Higher rainfall during winter months introduces freshwater runoff into ES that is cooler and relatively high in nitrate. As the rains subside during the spring and cease during the summer, this flux of nitrate decreases and water becomes more saline, warmer and lower in nitrate. In comparison, the monthly average properties at M1 do not reflect this influence. Nitrate, temperature

16
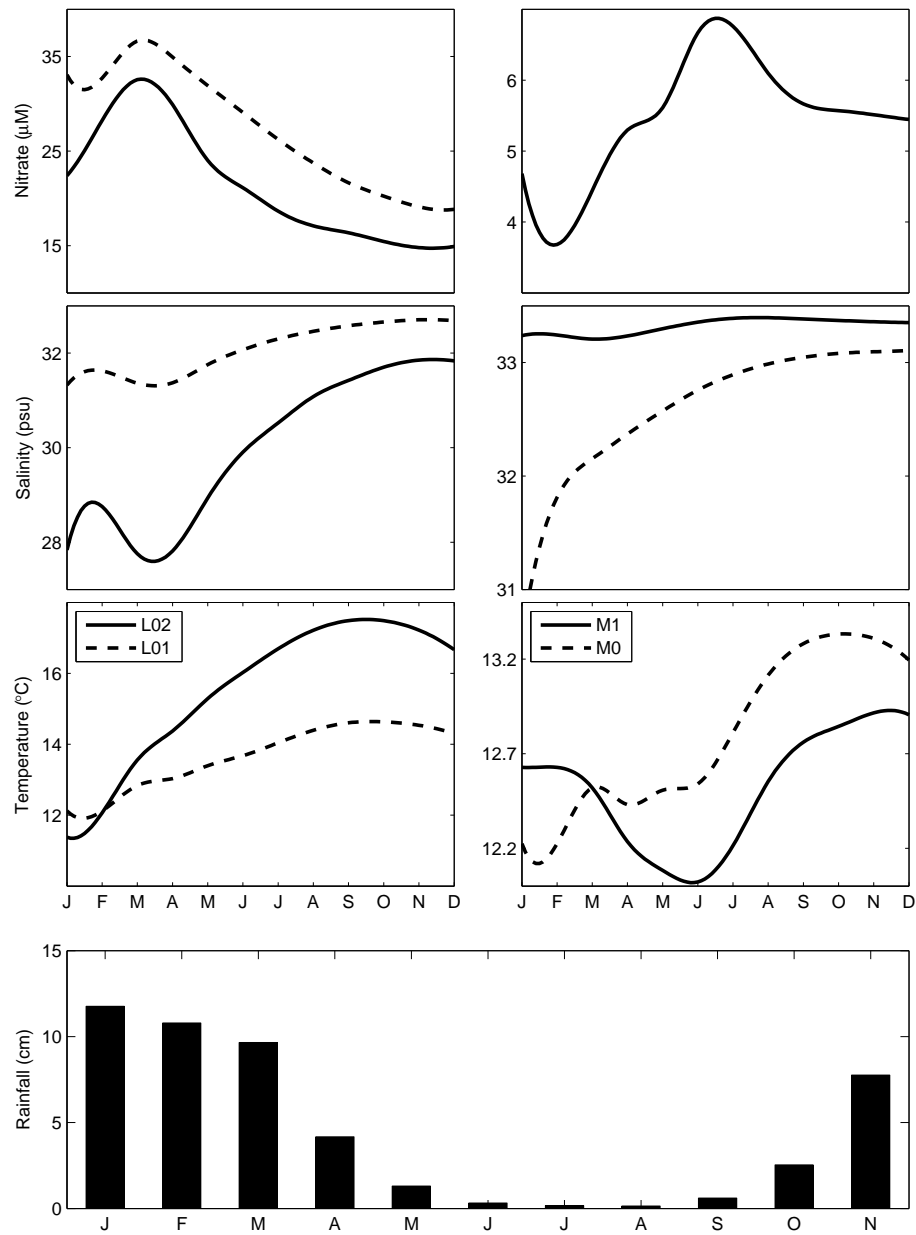
Figure 2.3 Monthly average measurement of nitrate, salinity and temperature from the time series stations L02, L01, M0, and M1, and monthly average rainfall.

and salinity more closely reflect the climatological conditions of Monterey Bay (Chapter 1) as influenced by the California Current and upwelling favorable winds. Primarily, the upwelling favorable winds, which occur during the spring and summer introduce sub-surface waters that are relatively higher in nitrate, are cooler and more saline. As winds subside onshore movements of the California Current bring warmer, fresher water that is lower in nutrients than upwelled water.

This land-sea linkage is visible from space during the winter when rainfall is greatest (Figure 2.4). Imagery collected by MODIS shows high levels of suspended particulate matter in MB surface waters, indicated by lighter colors in the true color
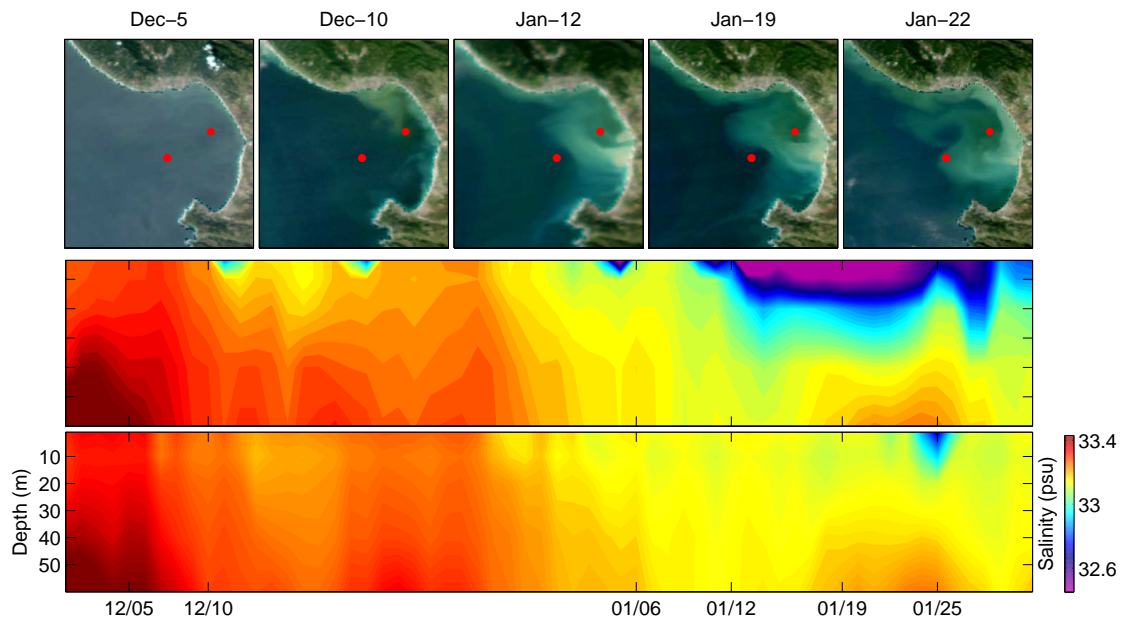
Figure 2.4 True color images from the Moderate Resolution Imaging Spectromoter (top panel) during the winter of 2004-2005, showing the introduction of fresh, sediment laden waters from watersheds surrounding Monterey Bay. Profiles from moorings M0 (middle panel) and M1 (bottom panel) illustrate the influence of this flux on the salinity of the nearshore coastal waters.

images. Between December 10, 2004 and January 12, 2005 sediment laden waters are introduced into the coastal ocean. The plumes shown in this imagery coincide with periods of increased rainfall during the sampling period (see figure 2.2). Rainfall during the winter of 2004-2005 was 82cm, 20cm above the average of 59cm (1971-2005). One quarter of the yearly rainfall that year (~20cm) fell between December 1st and January 16th, during the sampling period. This rainfall likely led to episodic discharge events from the Pajaro and Salinas Rivers and the breaching of sand bars across the river mouths, which are directly north and south of the mouth of the ES. Salinity profiles at M0 verify that this particulate flux was associated with a freshened lens of surface waters in the upper 20m. This freshening of the surface began near January 12, 2005 and persisted through the end of the sampling period. This discharge is largely not as evident at the offshore at M1 mooring.

2.4.2 Plume Horizontal Structure and Composition

Summary statistics of plume surface properties as measured by the UMS are shown in Table 2.1. Temperature across all sampling dates ranged from 12.1 to 18.3°C and averaged 13.5°C. Salinity measurements ranged from 21.4 to 33.3 psu and averaged 32.4 psu. Nitrate concentrations ranged from 7.3 to 283 μM and average 25.5 μM. Chlorophyll fluorescence in the ES plume as measured by relative fluorescence units (rfu's) ranged from 0.09 to 0.61 and averaged 0.17, while color dissolved organic matter (CDOM) fluorescence, which ranged from 0.02 to 4.3, averaged 0.3 rfu's. Optical transmission values ranged from 0.98 to 84% and averaged 35.2%.

Table 2.1 Parameter statistics of the Elkhorn Slough plume. The values represent an average over the 6 sampling dates. *Indicates mean lowest 5%.

Parameter	Min	Max	Mean	St. Dev	Range	Mean Highest 5%
Temperature	12.1	18.3	13.5	0.6	6.2	15.9
Salinity	21.4	33.3	32.4	0.75	11.9	30.5
Fluorescence (rfu)	0.09	0.61	0.17	0.04	0.52	0.29
CDOM (rfu)	0.02	4.3	0.3	0.3	4.3	1.3
Transmission (%)	0.98	84	35.2	1.1	21.3	6.6*
Nitrate	7.3	283	25.5	18.7	275.5	79.8

Correlations between constituents measured by the underway-mapping system are shown in Table 2.2. The greatest correlation between constituents describing the horizontal structure of the plume is a positive correlation between CDOM fluorescence and nitrate ($r = 0.93$). Other strong correlations between constituents are between salinity and CDOM fluorescence ($r = -0.71$) and salinity and nitrate

Table 2.2 Correlation coefficients (r) between constituents measured by the UMS T=Temperature, S=Salinity, Tr=Transmission, N=Nitrate, C=CDOM ($p<0.001$).

Date	T-S	T-Tr	T-N	S-Tr	S-N	Tr-N	T-C	S-C	C-N	C-Tr
12/9/04 *n=1570*	-0.19	-0.25	0.18	0.57	-0.91	-0.55	0.16	-0.91	0.97	-0.70
12/10/04 *n=5309*	-0.36	-0.40	0.55	0.47	-0.64	-0.78	0.40	-0.59	0.94	-0.83
01/06/05 *n=4516*	0.22	0.04	0.03	0.70	-0.76	-0.76	-0.20	-0.87	0.93	-0.78
01/10/05 *n=3536*	0.36	0.11	0.10	0.65	-0.41	-0.12	-0.08	-0.67	0.92	-0.34
01/20/05 *n=827*	-0.16	-0.26	0.26	0.29	-0.34	-0.20	0.01	-0.47	0.91	-0.17
01/21/05 *n=3882*	0.08	-0.19	0.48	-0.03	-0.59	-0.19	0.24	-0.78	0.91	-0.09
Mean	-0.01	-0.16	0.27	0.44	-0.60	-0.43	0.09	-0.71	0.93	-0.48

(r = -0.60). Negative correlations between salinity and CDOM indicate that lower

salinity waters from ES carry elevated concentrations of CDOM and nitrate.

Additionally, these lower salinity waters with higher CDOM are associated with lower

optical transmission. A property plot of the salinity, CDOM fluorescence and nitrate

shows a clear progression from lower salinity waters that are higher in CDOM

fluorescence and nitrate (plume waters) to higher salinity waters that are lower in

CDOM fluorescence and nitrate (oceanic waters) (Figure 2.5).
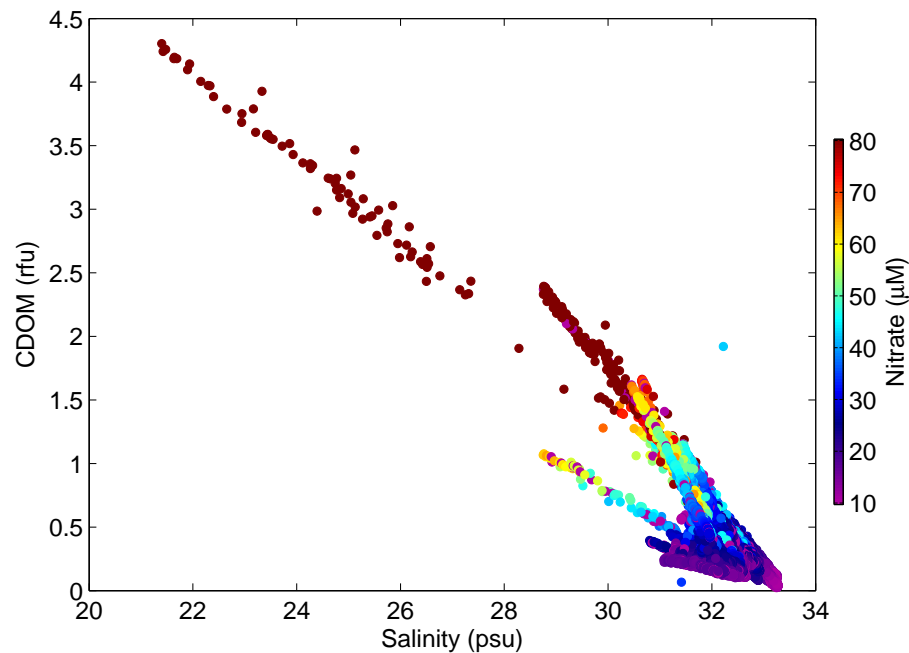
Figure 2.5 Property-property plot distinguishing plume waters as low salinity waters
with higher concentrations of nitrate and CDOM

In comparison to oceanic or bay-wide physical conditions, mean slough surface

waters are slightly warmer and fresher than those sampled offshore and contain higher

concentrations of nitrate. Monthly time series measurements in the winter months

show that Monterey Bay surface waters have an average temperature of ~13°C, a range

in salinity of 32.9-33.33 ppt and generally have nitrate concentrations of <1 μ M (Pennington and Chavez, 2000). Temperature measurements conducted with the underway system must be viewed with caution due to the existence of discharge from the thermal outfall pipe of the Moss Landing Power Plant. Heated waters used for cooling during power plant operations are discharged into Monterey Bay through discharge pipes located just to the south of the harbor entrance. This discharge, which interacts with the discharge plume of ES, is described in studies by Paduan (2003) and Fischer (2006). Values of salinity and transmission, averaged across all UMS (Figure 2.6) sampling tracks for each day, show a correlated decrease that coincides with the period of fresher surface waters and increased sediment loading in the mooring profiles shown in figure 2.4. Other measured plume constituents (temperature, nitrate, chlorophyll and CDOM fluorescence), however, did not reflect this change.
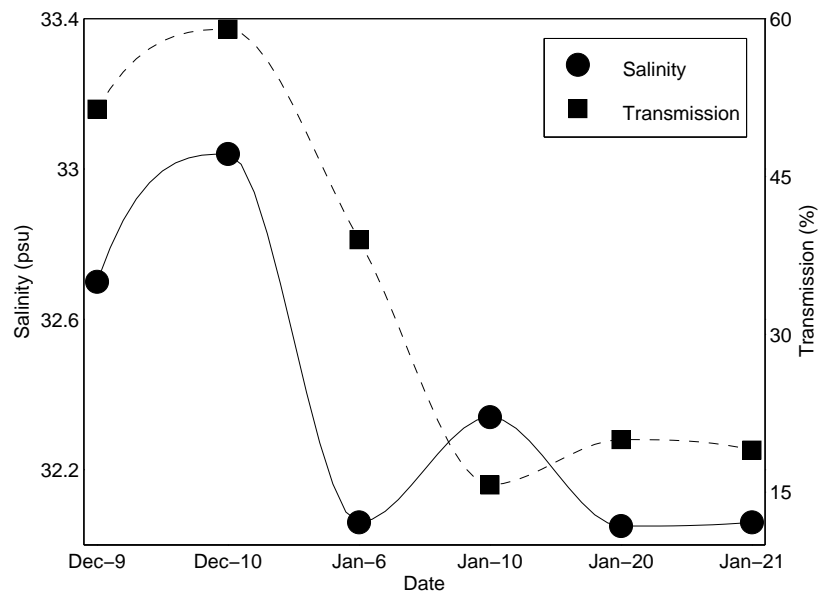
Figure 2.6 Surface daily mean values from the underway mapping system reflecting the mean changes in salinity and transmission during the sampling period.

Spatial mapping of UMS data, when viewed with relative scale bars over the course of the sampling period, reveals synoptic characteristics of plume surface properties. A detailed graph of the tidal period during which the UMS passes were conducted is shown in figure 2.7 and spatial maps of plume surface properties are shown in figures 2.8-2.13. In general, the strongest plume signature appears as increases in relative fluorescence of CDOM and low transmission due to sediment loading which also appears to be coupled with elevated concentrations of nitrate. Lower salinity water is also a consistent marker of the plume during the winter sampling period.
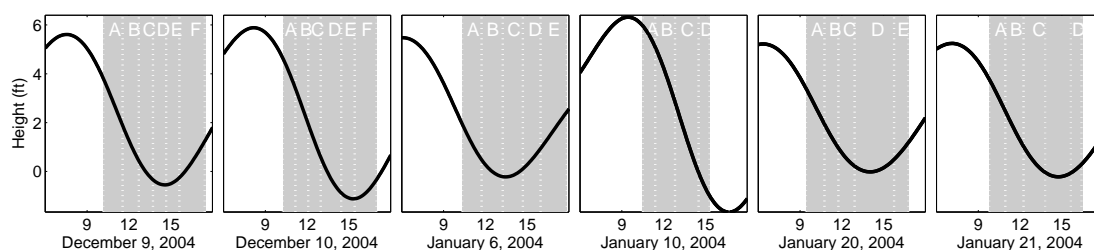
Figure 2.7 The stage of the tide at Elkhorn slough highway 1 bridge (local time) together with the period (grey box) during which observations were acquired. Individual passes over the sampling area with the underway system are indicated by the white lines and letters.

Salinity maps (Figure 2.8) show the evolution of a fresher plume of water exiting the slough during ebb tide. This is most evident in panels C-E for Dec-9-2005, panels D-F on Dec-10-2005, panels B and C on Jan-6-2005, panel D on Jan-10-2005, panels D and E on Jan-20-2005, and panel D on Jan21-2005 (highlighted by the gray boxes). These less saline waters also are associated with higher levels of chlorophyll fluorescence (Figure 2.9). A similar pattern of plume evolution is apparent in the mapped constituents of the fluorescence of CDOM (Figure 2.10) and nitrate (Figure
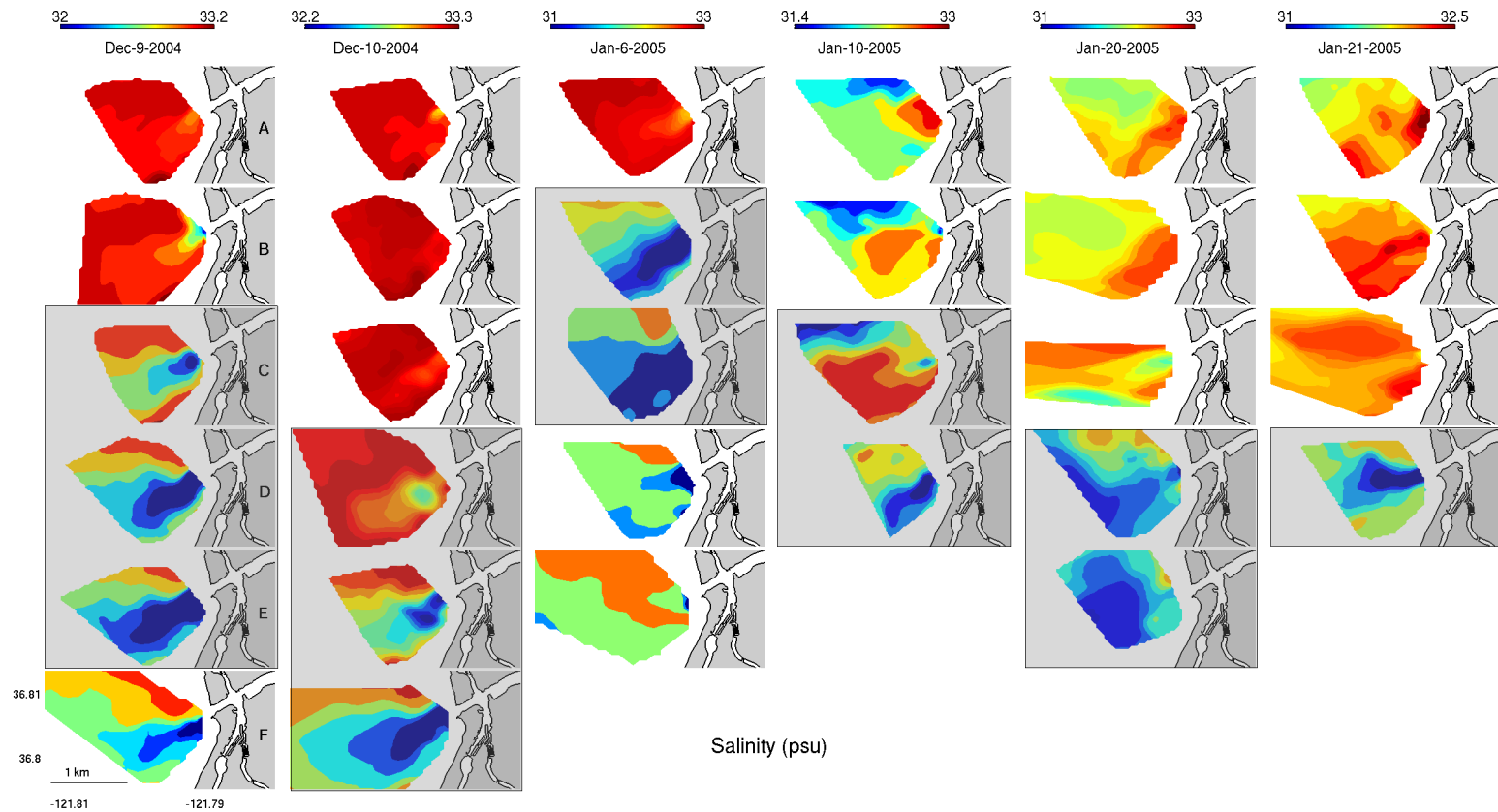
Figure 2.8 Horizontal surface structure of the Elkhorn Slough discharge plume shown as practical salinity units (psu). Each row corresponds to the lettered sampling passes shown in figure 2.7 for the respective date. The scale bar equal one kilometer. Gray boxes highlight surface plume evolution throughout the ebb tide (see text).
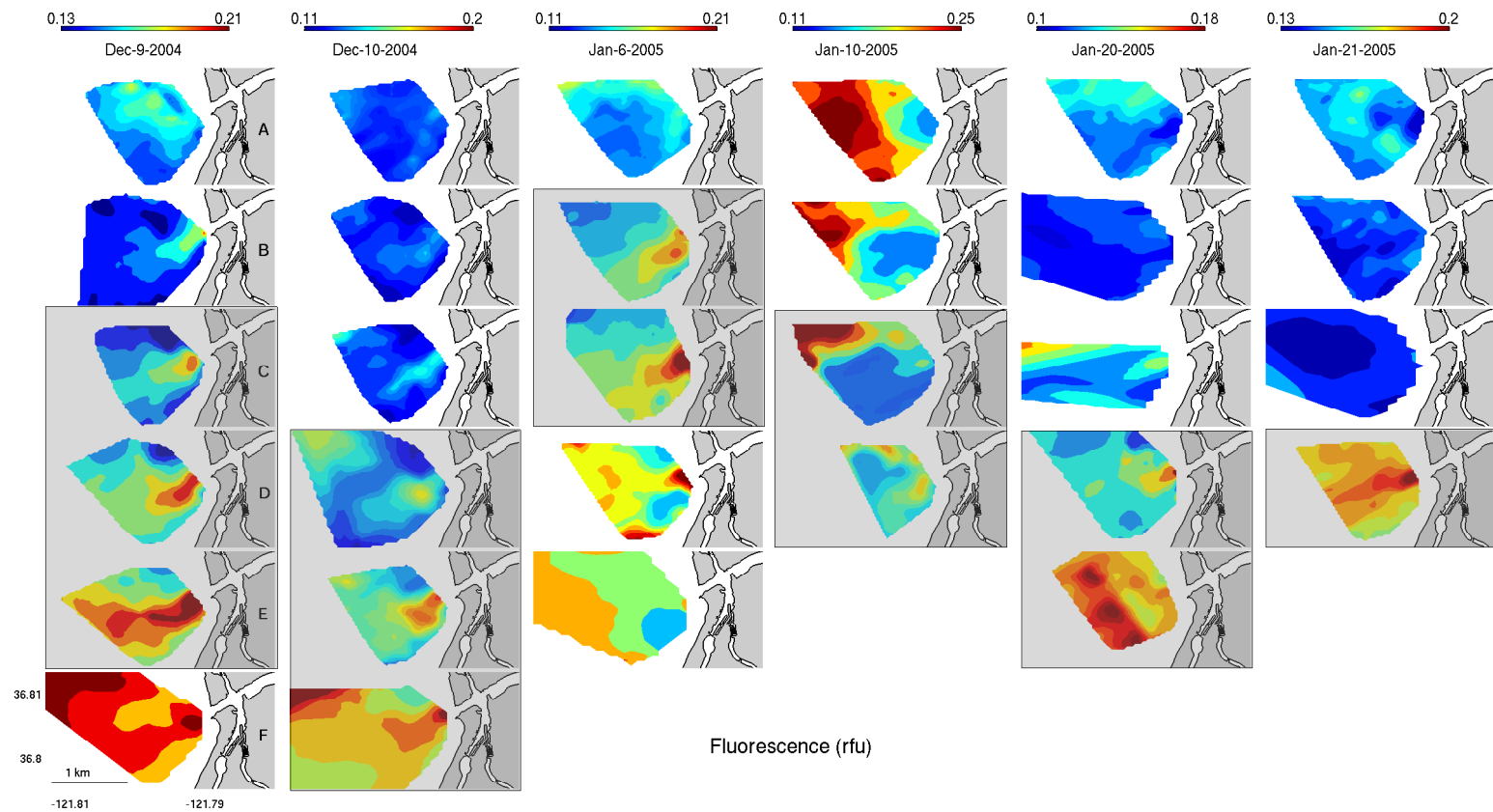
Figure 2.9 Horizontal surface structure of the Elkhorn Slough discharge plume shown as relative fluorescence units (rfu) of chlorophyll. Each row corresponds to the lettered sampling passes shown in figure 2.7 for the respective date. The scale bar equal one kilometer. Gray boxes highlight surface plume evolution throughout the ebb tide (see text).
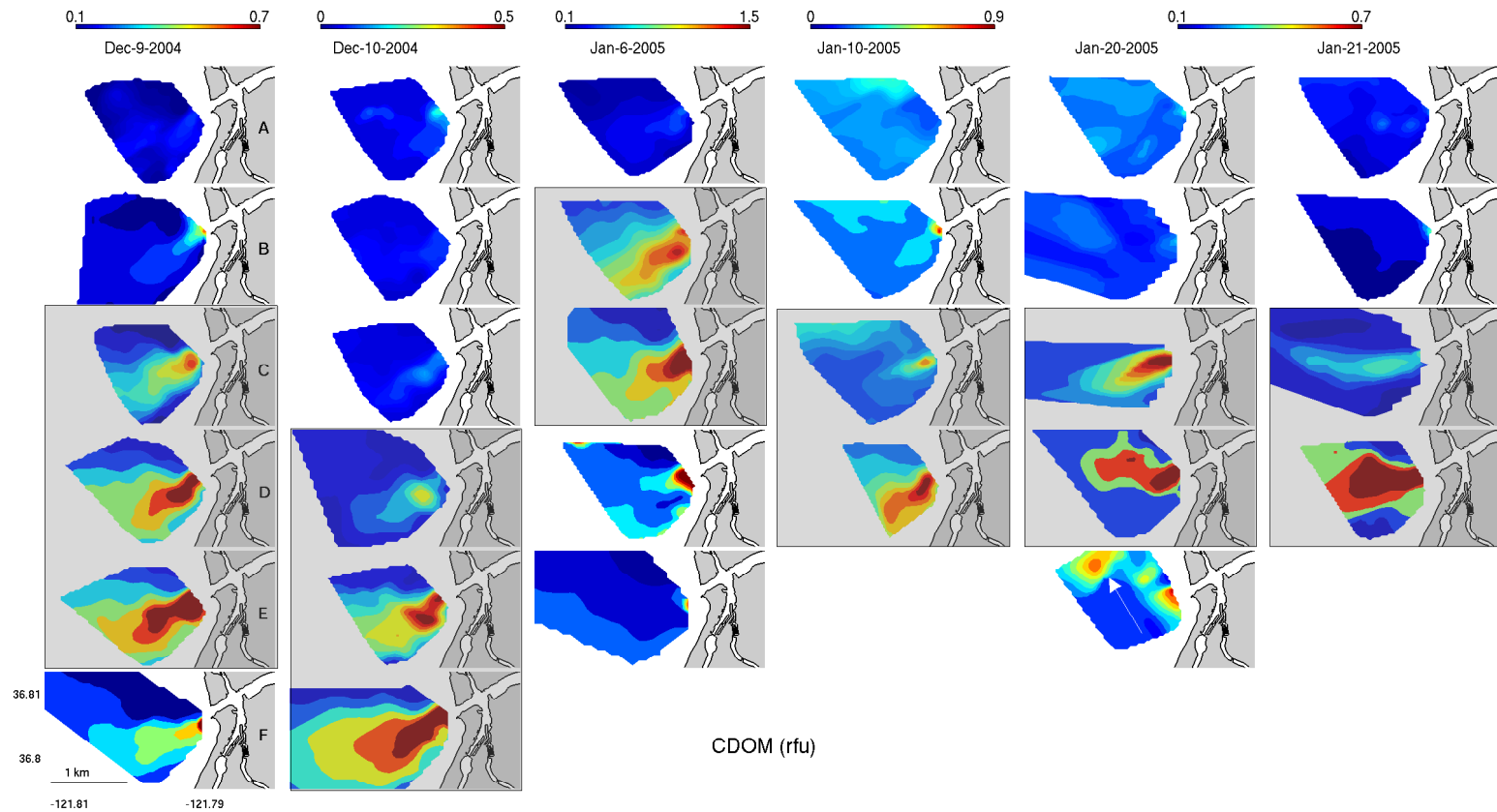
Figure 2.10 Horizontal surface structure of the Elkhorn Slough discharge plume shown as relative fluorescence units (rfu) of color dissolved organic matter. Each row corresponds to the lettered sampling passes shown in figure 2.7 for the respective date. The scale bar equal one kilometer. Arrow indicates the northward transport of plume waters. Gray boxes highlight surface plume evolution throughout the ebb tide (see text).
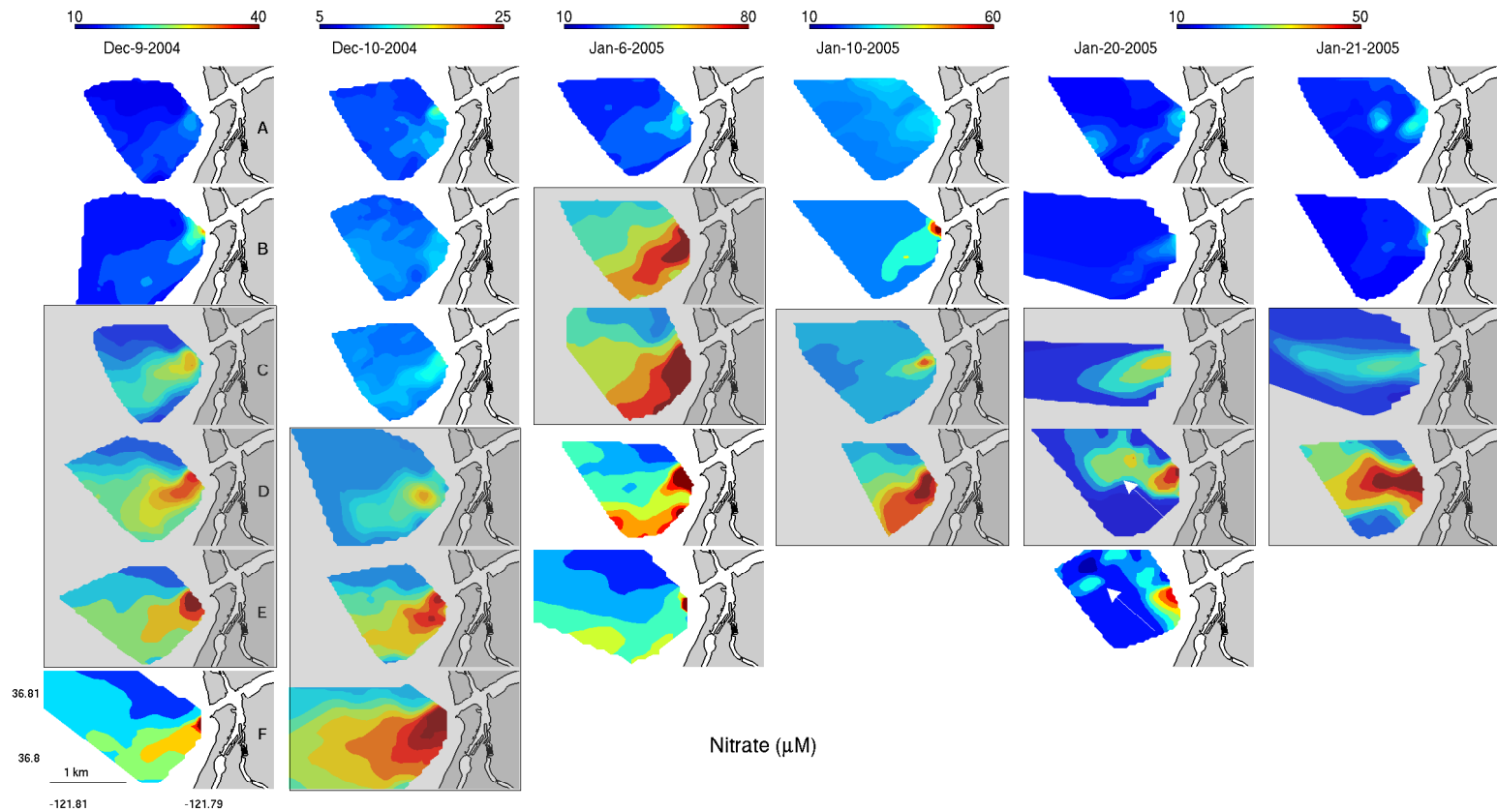
Figure 2.11 Horizontal surface structure of the Elkhorn Slough discharge plume shown as nitrate. Each row corresponds to the lettered sampling passes shown in figure 2.7 for the respective date. The scale bar equal one kilometer. Arrows indicate the northward transport of plume waters. Gray boxes highlight surface plume evolution throughout the ebb tide (see text).
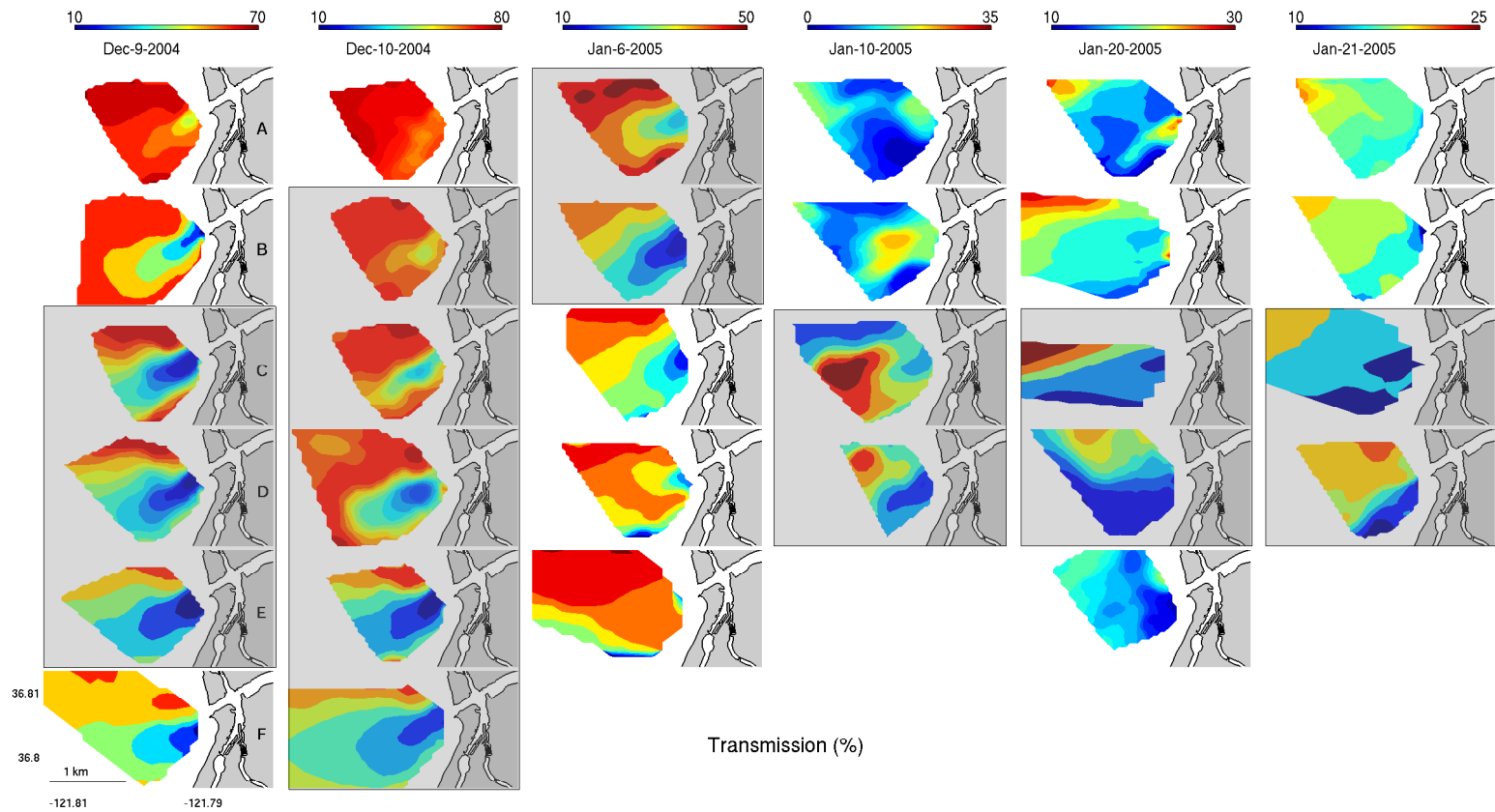
Figure 2.12 Horizontal surface structure of the Elkhorn Slough discharge plume shown as percent transmission. Each row corresponds to the lettered sampling passes shown in figure 2.7 for the respective date. The scale bar equal one kilometer. Gray boxes highlight surface plume evolution throughout the ebb tide (see text).
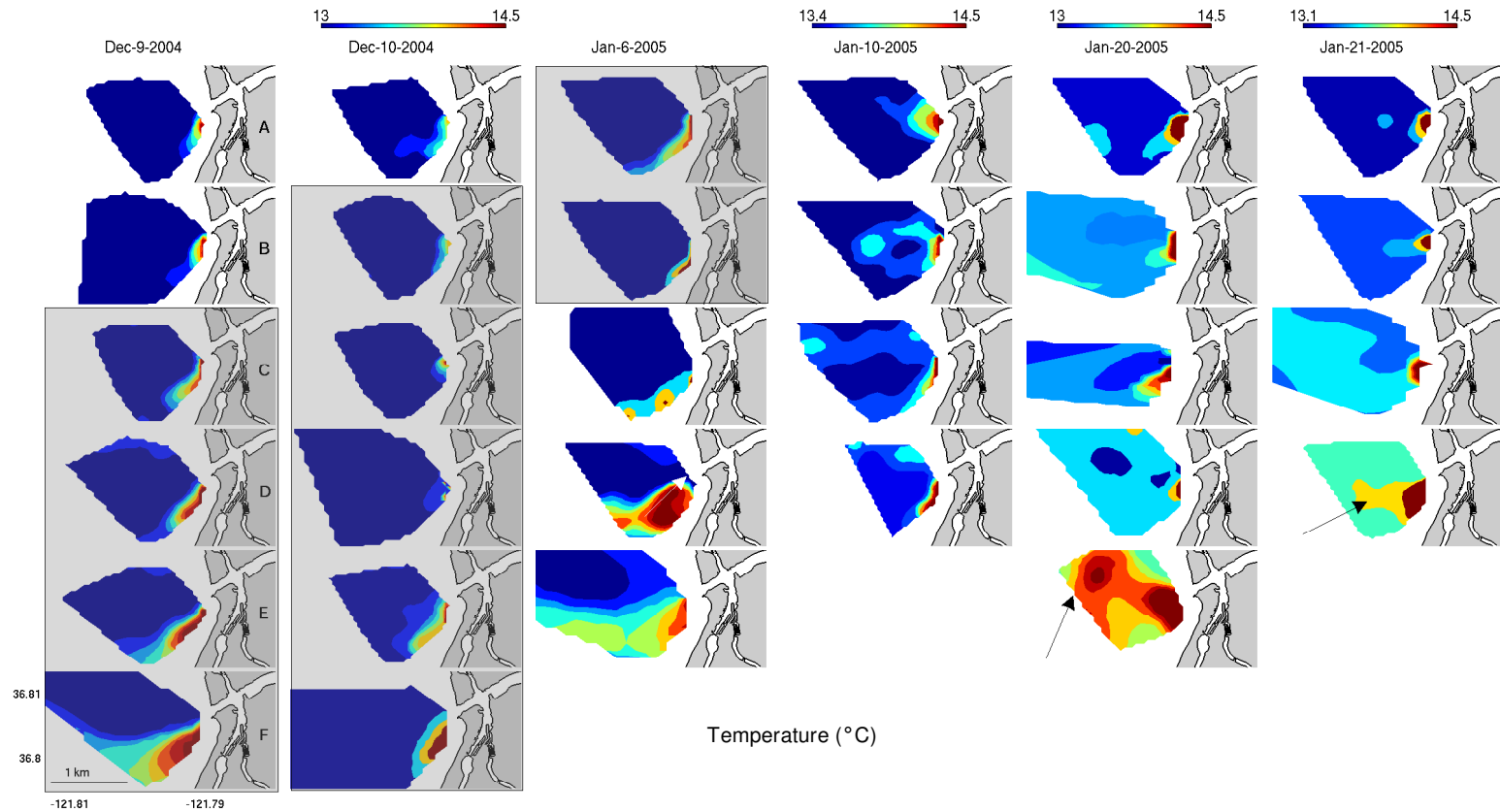
Figure 2.13 Horizontal surface structure of the Elkhorn Slough discharge plume shown by sea surface temperature. Each row corresponds to the lettered sampling passes shown in figure 2.7 for the respective date. The scale bar equal one kilometer. Dark arrows indicate the transport of warmer plume/outfall waters northward. Gray boxes highlight surface plume evolution throughout the ebb tide (see text).

2.11; (Dec-9-2004, panels C-E; Dec-10-2005, panels D-F; Jan-6-2005, panels B and C; Jan-10-2005, panels C and D; Jan-20-2005, panel C and D; Jan-21-2005, panel C and D). Visually, nitrate and CDOM fluorescence appear to be the most consistent indicators of plume. Transmission (Figure 2.12) also shows the horizontal surface expression of the plume except on Jan-10-2005 and Jan-20-2005 when low transmission waters appear prior to the ebb tide, indicating that other coastal processes might be influencing turbidity in the vicinity of the harbor entrance. CDOM fluorescence and transmission also do not consistently show correlated horizontal structure across all sample dates. For instance, while CDOM, on January 20, 2005 in panel E, and nitrate in panels D and E show a traces of plume water being carried northward in the prevailing along shore current, this is not evident in the transmission plot. The horizontal structure of sea surface temperature in the vicinity of the slough entrance is dominated by the thermal outfall pipe from the Moss Landing Power Plant (MLPP) (Figure 2.8). Warmer surface waters produced by the MLPP outfall discharge are evident in each of the panels in Figure 2.8. The warmer waters can be entrained into the out going tidal currents and transported to the south and west along shore. Spreading of the MLPP warmer outfall waters is most evident in panels C-F on Dec-9-2004 and panels D-F on Dec-10-2004. In some cases, warmer waters from this thermal output were transported northward along shore (Jan-20- 2005, Panel E and Jan-21-2005, Panel D). Mean values, over the entire sampling period from the underway data, plotted against tidal height show that highly correlative constituents of nitrate and the relative fluorescence of CDOM increase with an increase in height of the ebb tide (Figure 2.14), with maximum concentrations occurring at or after maximum ebb tide.
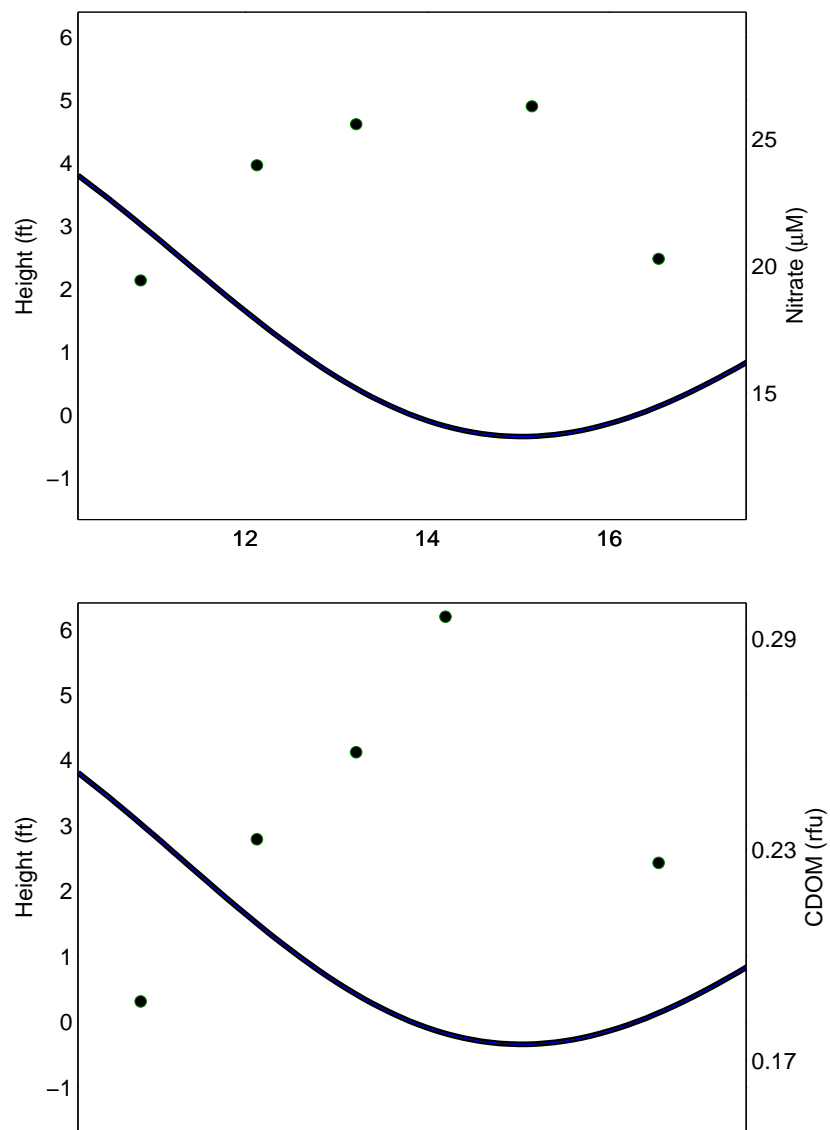
Figure 2.14 Tidal-phase averaged concentrations of nitrate and CDOM (dots) plotted against the average predicted tidal height (line) from all surveys.

2.4.3 Vertical structure and composition

Values of salinity and optical backscatter, averaged across the surface volume

of water (2-15m) for all AUV sampling tracks for each day, also reflect the changes in the background conditions of the nearshore coastal ocean. A decrease in salinity and an associated increase in optical backscatter occurred during the sampling period with lowest salinity and highest backscatter occurring on January 20 and 21 (Figure 2.15). Despite the background changes, the AUV resolved the vertical structure of the
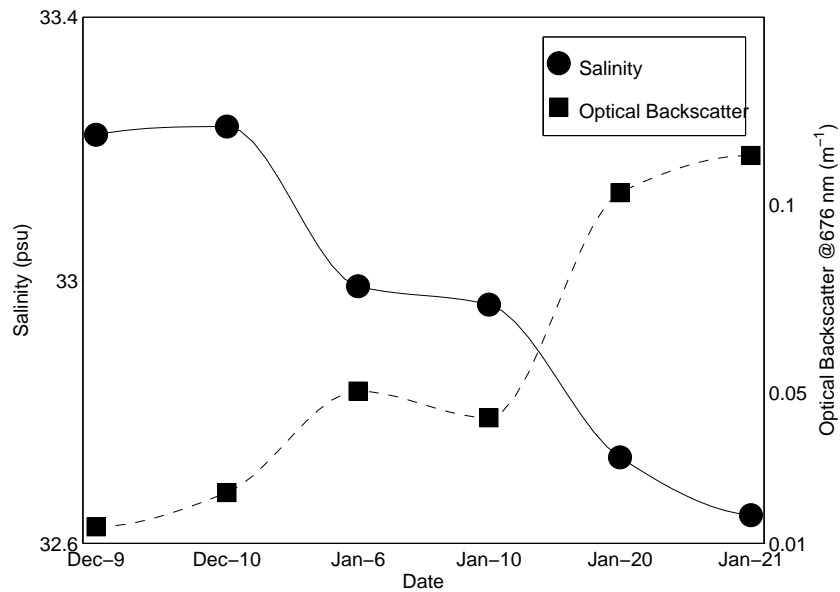
Figure 2.15 Daily mean values from the autonomous underwater vehicle volume sampling reflecting the mean changes in salinity and transmission during the sampling period.

Elkhorn slough plume. Generally, the plume appears as a surface plume extending to 5-10m depth, largely expressed during the ebb tide. A detailed graph of the tidal period during which the AUV passes were conducted appears in figure 2.16.

Spatial mapping of AUV data, when viewed with relative scale bars over the course of the sampling period, reveals synoptic characteristics of plume vertical
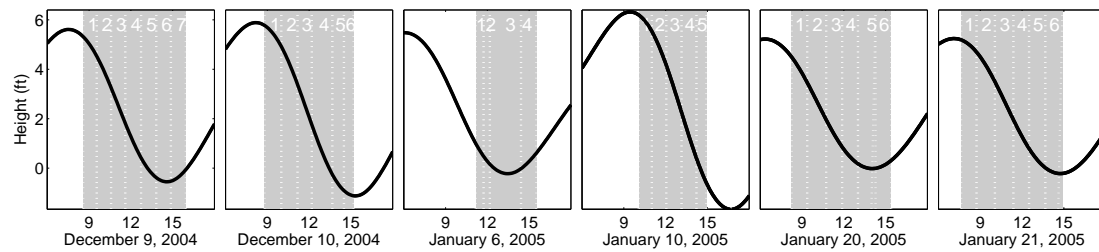
Figure 2.16 The stage of the tide at Elkhorn Slough highway 1 bridge (local time) together with the period (grey box) during which observations were acquired. Individual passes over the sampling area with the autonomous underwater vehicle are indicated by the white lines and letters.

structure and constituents. Synoptic maps of the data from the AUV passes appear in figures (2.17-2.21). The vertical structure of the plume can be more readily distinguished by slightly lower salinity waters on Dec-9-2004, panels 1-5; Dec-10-2004, panel 5; Jan-6-2005, panel 1-2; Jan-10-2005, panel 4; Jan-20-2005, panels 4-6 and Jan-21-2005, panels 3-6 in Figure 2.17 (highlighted with gray boxes). By January 20th a distinct lower salinity surface lens has established itself throughout the entire sampling area, though the plume structure is still evident throughout the ebb tide.

High optical backscatter (Figure 2.18) coincident with low chlorophyll fluorescence (Figure 2.19) is indicative of higher particulate sediment loads in the water column. This is most clearly defines the extent of the plume on Dec-9-2004, panels 3-5; Dec-10-2004 panel 4-5; Jan-10-2005, panel 5; Jan-20-2005, panels 3-6. Instead of forming a surface lens, the particles seem to fill the entire vertical sampling domain. This is most evident on Jan-20-2005, panels 4 and 5 on the southern flank of the sampling triangle (S in Figure 2.18). On Jan-21-2005, panel 5 and 6, sediments are shown to rapidly settle away from the surface waters and develop a subsurface turbid layer (T in Figure 2.18). Chlorophyll fluorescence (Figure 2.19), on several occasions,

33

appears to be highest at the northwesterly corner of the sampling triangle. This is consistent with observations of a convergence zone forming between the outgoing plume and the along shore counter current, just north of the harbor entrance and suggests a localized area of high biological productivity or dinoflagellate aggregation (C in Figure 2.19). Only on January 21, 2005, (X in Figure 2.19, panel 6) are plume waters exiting the slough associated with higher concentrations of chlorophyll, suggesting the possible subsurface export of biological productivity from the slough. Pulses of nitrate are also evident leaving the slough during the ebb tide with concentrations reaching over 20 μM (Figure 2.20). These surface pulses do not extend throughout the water column and are most evident on Dec-9-2004, panels 2-5; Dec-10-2004, panels 3-5; Jan-6-2005, panel 1-2; Jan-10-2005, panel 3-5. On Jan-20-2005, panel 3 and Jan-21-2005, panel 3-5, nitrate concentration is highest on the northern and western flanks of the sampling triangle. This area is still in the plume sampling domain, though the lower tidal range and reduced tidal inertia on these days may have reduced the horizontal extent of the plume and nearshore currents may have played a greater proportional role in pushing the plume to the north. Temperature was the least consistent indicator of plume waters. The temperature signature appeared as a warm surface layer mostly on the southern flank of the sampling triangle (Figure 2.20; Dec-9-2004, panel 3-5; Dec-10-2004; panel 4-5; Jan-10-2005, panels 4; Jan-21-2005, panels 2-5). However, Jan-6-2005 shows a pulse of cooler water leaving the slough, which quickly warms again with the changing tide (C in Figure 2.21). There are several reasons temperature is a poor indicator of plume waters. Temperature changes in the slough are complex (Lemos et al., 2007). They can change rapidly with air temperature and rainfall, especially within the shallow basins of the slough, and the outgoing plume temperature can also be influenced by the power plant outfall pipes (Fischer, 2006; Paduan, 2003).
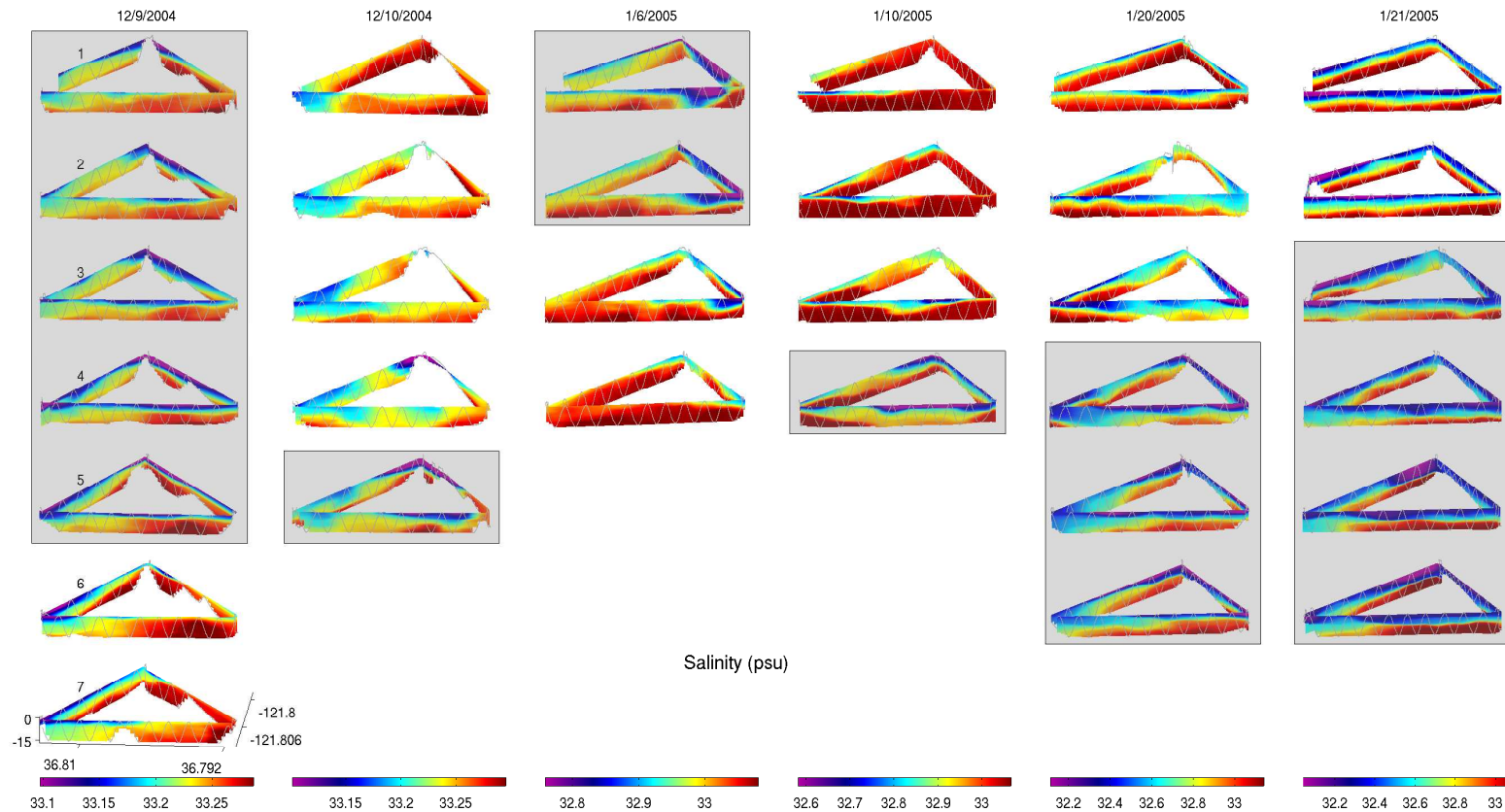
Figure 2.17 The AUV sampling triangle shown as salinity vertical profiles through the water column. The mouth of the Elkhorn slough is on the top side of each of the panels. Each run corresponds to the numbered sampling passes shown in figure 2.16. Gray boxes highlight surface plume evolution throughout the ebb tide (see text).
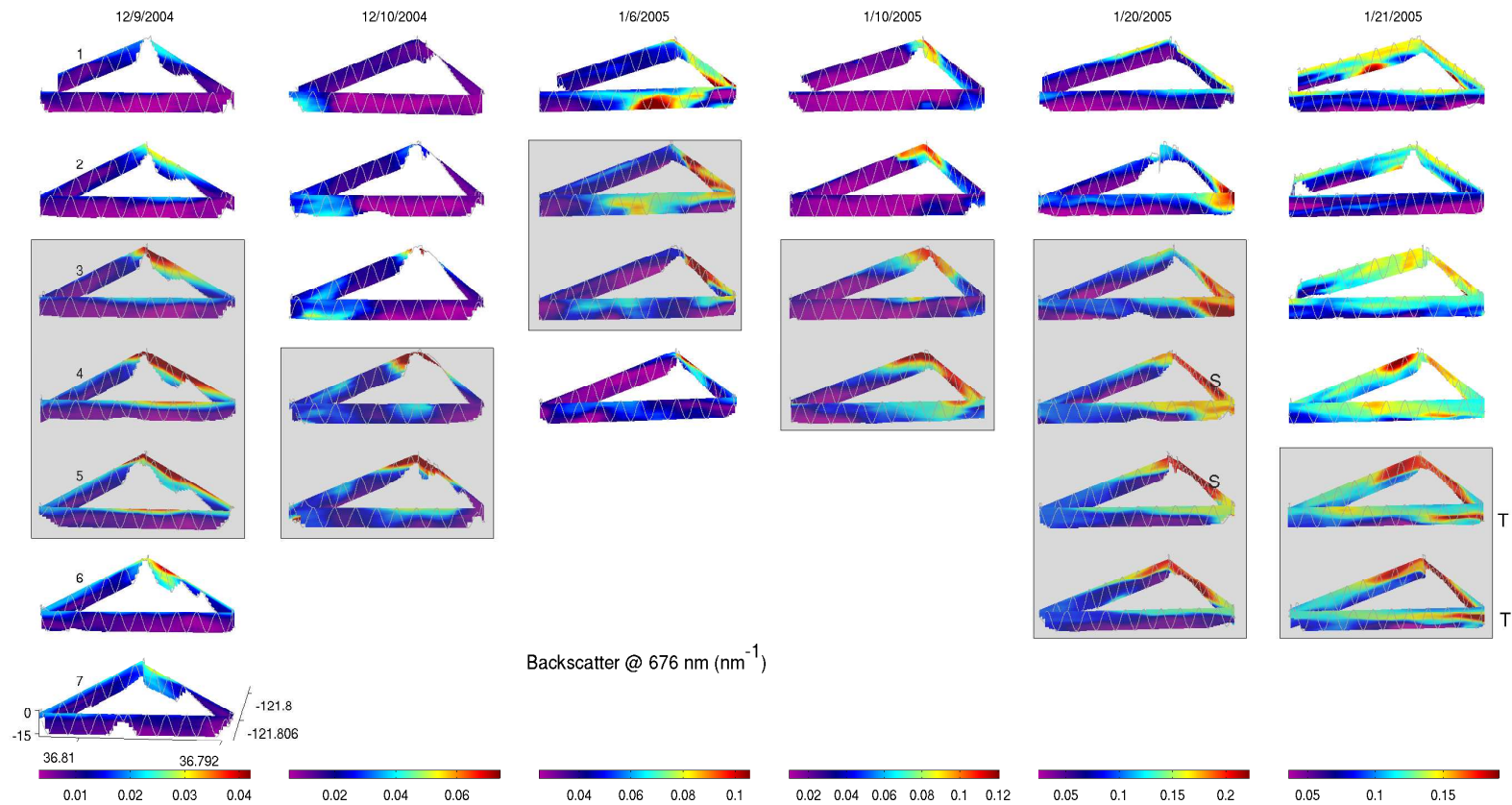
Figure 2.18 The AUV sampling triangle shown as suspended particulate matter (backscatter at 676nm) vertical profiles through the water column. The mouth of the Elkhorn slough is on the left side of the panels. Each run corresponds to the numbered sampling passes shown in figure 2.15. S indicates particulates settling out through the water column and T indicated the development of a subsurface turbid layer. Gray boxes highlight surface plume evolution throughout the ebb tide (see text).
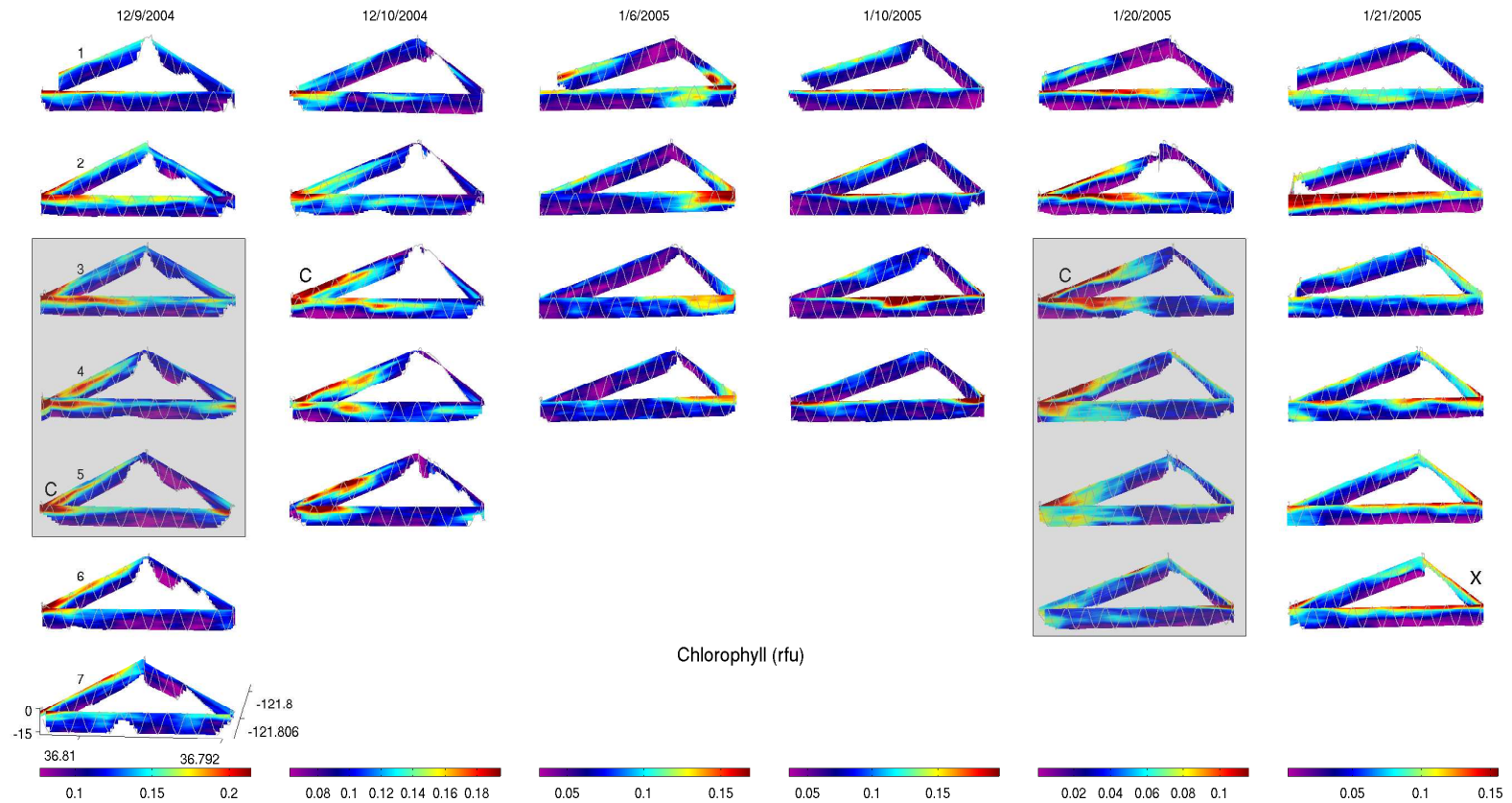
Figure 2.19 The AUV sampling triangle shown as relative chlorophyll fluorescence vertical profiles through the water column. The mouth of the Elkhorn slough is on the left side of the panels. Each run corresponds to the numbered sampling passes shown in figure 2.16. C indicates a high chlorophyll in a convergence zone. X indicates the presence of biological export from the slough to the coastal ocean. Gray boxes highlight surface plume evolution throughout the ebb tide (see text).
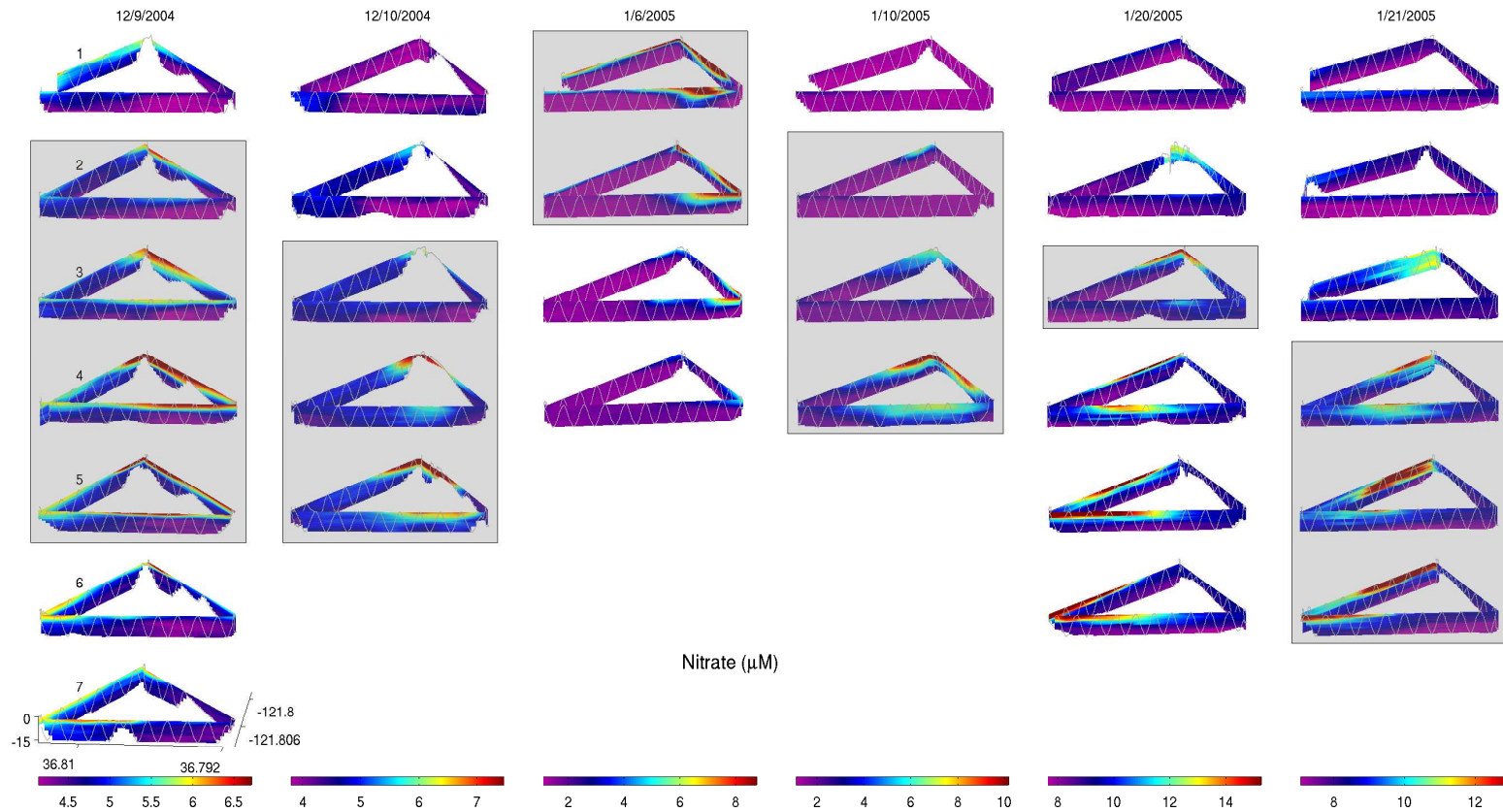
Figure 2.20 The AUV sampling triangle shown as nitrate (uM) vertical profiles through the water column. The mouth of the Elkhorn slough is on the left side of the panels. Each run corresponds to the numbered sampling passes shown in figure 2.16. Gray boxes highlight surface plume evolution throughout the ebb tide (see text).
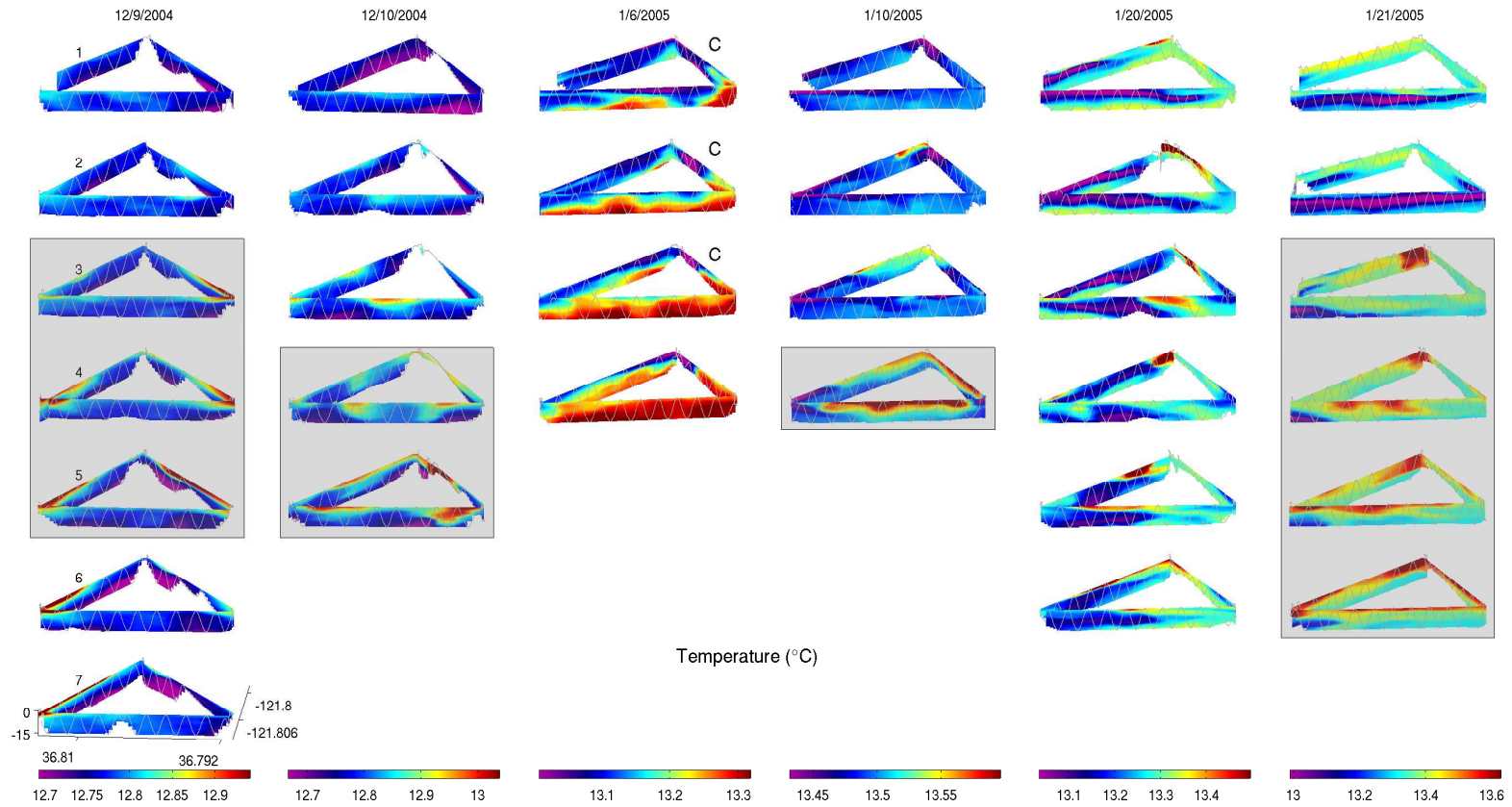
Figure 2.21 The AUV sampling triangle shown as temperature vertical profiles through the water column. The mouth of the Elkhorn slough is on the left side of the panels. Each row corresponds to the numbered sampling passes shown in figure 2.16 for the respective date. Gray boxes highlight surface plume evolution throughout the ebb tide (see text).

2.4.4 Plume Speed and Direction

Drifters deployed in the harbor mouth show that, during ebb tide, the plume followed a trajectory southwest along the coast, eventually becoming entrained in the northward bay circulation. The mean drifter speed as measured by all drifters was 19.7 cm s^{-1}. On average, the maximum velocity of currents within the vicinity of the harbor entrance across all days sampled was 282 cm/s. Once entrained in the northward bay circulation system, the drifter current speed slowed to an average of 16.5 cm/sec (Figure 2.22).

All the drifters deployed and recovered during the winter sampling period were subjected to only one partial tidal cycle (black-dotted lines in Figure 2.22, top panel). However, drifters deployed near the Pajaro River and Elkhorn Slough in July and August of 2007, respectively (red-dotted lines in Figure 2.22, top panel), persisted through several tidal cycles and showed mean transport to the northern bay. This suggests that the influence of the plume constituents can extend into northern bay waters during the late summer.

2.4.5 Plume Forcing and Dynamics

Here I calculate the kelvin mouth and plume numbers, plume lift-off depth and inertial radius using parameters extracted from the UMS and AUV surveys and drifters studies. These parameters provide a metric of the degree of influence of tidal inertia versus Coriolis forcing on plume structure, whether the plume is surface or bottom advected, and the extent of influence of plume interial effects. Garvine (1995) was the first to classify buoyant discharge plumes in order to help provide a universal metric of comparison among plume types. This classification can help us understand how the transport and fate of plume constituents are influenced by tidal pumping,
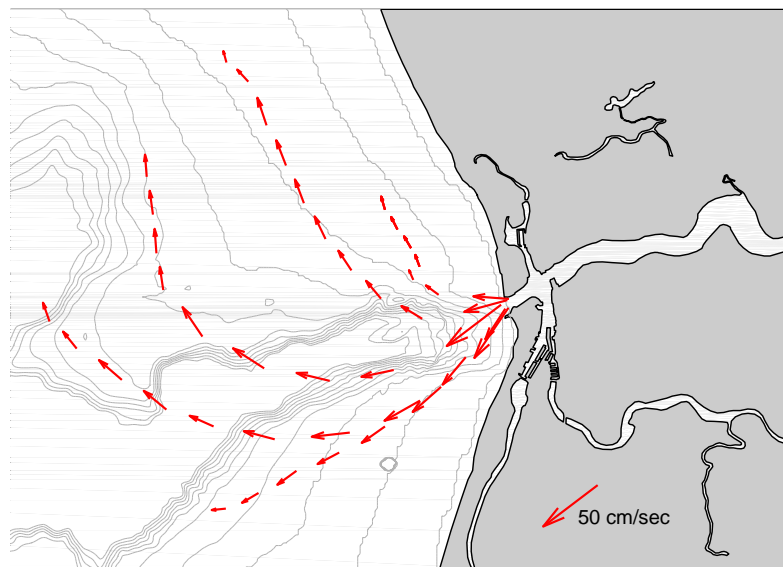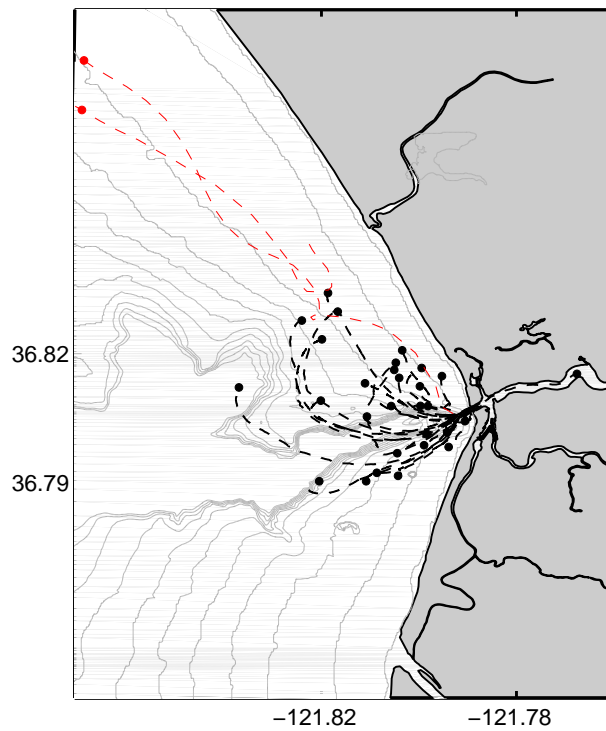
Figure 2.22 Drifters exiting the Elkhorn Slough and becoming entrained in the north-ward flowing bay circulation. The top panel shows path of all drifters deployed during the study. The bottom panel shows the drifter tracks and relative current speed from drifter deployed on January 6, 2005.

along shore current and Coriolis forcing, as the delivery of physically different types of water masses to the coastal ocean may be strongly influenced by the trajectory and forcing of the plume.

According to Garvin (1995), the physical classification of plumes (and their behavior) depends on the relative magnitudes of the convective and Coriolis accelerations, wind and bottom stress and horizontal baroclinic pressure gradients. With plume variables such as plume length, width, depth and current velocity, additional calculations can be made to further describe the general flow structure and dynamics of the plume. The "mouth" Kelvin number K_m is used to compare the relevance of inertial effects and rotational forcing at an estuarine mouth and is defined as the ratio of the width of the plume at the mouth L_m to the deformation radius L_D, which is defined as

$$L_D = (g'h_p)^{0.5} / f$$

where g' is the maximum measured buoyancy anomaly (Pond and Prickard, 1983) of the plume, h_p is the thickness of the plume (~6 m), and f is the Coriolis parameter (~8.2 x 10^{-5}/s). Therefore, for Elkhorn Slough $K_m \ll 1$ which indicates that inertial effects at the mouth are much more important relative to rotational effects of the earth. Rotational effects may be much more important in influencing larger plumes.

Secondly, the "plume" Kelvin number is defined as the ratio of plume width L_P to L_D. The L_P of the Elkhorn Slough plume was estimated to be on the order of one kilometer. This suggests that $K_P \ll 1$ and that once out of the mouth of the harbor, the

ES plume is still significantly influenced by inertia. In summary, the ES plume can be characterized as a relatively small-scale, jet-like structure that is primarily advection dominated and produces strong boundary fronts (Garvine, 1995).

As observed by the AUV profiles, the outflow of the Elkhorn slough exits as a buoyant surface layer "floating" above the ambient but denser nearshore waters. Yankovsky and Chapman (1997) describe a method of calculating the plume "lift-off" depth for surface advected plumes such as this. The plume lift-off depth is defined as

$$H_b=(2Q_p \, f / g')^{0.5}$$

where Q_p is the total transport of brackish water in the ES plume, defined here as the tidal prism (Broenkow and Breaker, 2005) divided by the mean current velocity sampled by the drifters in the plume. The average lift-off depth for the six sampling days was 12.28 m. This indicates, as was observed in the winter months, that the ES plume is detached from the bottom and is surface advected. Lastly, knowing that inertial forces are important to plume dispersion and that it is a surface advected plume, Garvine (1995) suggests that the discharge momentum flux will influence a spatial scale approximately equal to the inertial radius L_i, which is defined as

$$L_i = u_f / f$$

where u_f is a representative velocity within the plume, measured directly from drifters, which during the six sampling periods averaged 28cm/s (1 km/hr). The ES plume

inertial radius is ~8 km suggesting that the extent and influence of the plume may extend far offshore.

The mean values for each of these parameters were calculated for each of the six sampling days. The results are summarized in Table 2.3. Based on observations and these calculations, the ES plume is a relatively small-scale plume feature whose flow dynamics relies on tidal inertia and possibly inertia from freshwater inflow from creeks and rivers during the winter months. Small-scale plumes, such as those characteristic of discharges from engineering structures and narrow river mouths, have nonlinear flow dynamics and include sharp frontal boundaries (Garvine, 1995). The inertia effects as calculated here can influence an area up to 8 km from the harbor entrance.

Table 2.3 Plume parameters calculated from observations of the Elkhorn Slough discharge plume.

Parameter	Name	Elkhorn Slough values	Signifigance	Reference
K_m	"Mouth" Kelvin	$\ll 1$	Inertia > rotation (at mouth)	Garvine, 1995
K_p	"Plume" Kelvin	$\ll 1$	Inertia > rotation (within plume)	Garvine, 1995
h_b	Plume "lift-off" depth	~12.28m	surface advected plume	Yankovsky and Chapman, 1997
L_i	Inertia radius	~8 km	Inertia length scale	Geyer et al., 2000

2.4.6 Key Processes

Further analysis of the UMS and AUV data suggest forcing by rainfall and tides. Surface plume composition, particularly salinity and nitrate show response to rain events and the flux of land-based constituents to the coastal ocean, while the

magnitude of the tide modulates the plume extent and dynamics. Partitioning of particulate and dissolved constituents is also evident when examining vertical plume structure with AUV data. The plume forcing parameters described in the previous section showed little overall correlation to either tidal height or rainfall events. Inertial radius, or extent of the plume correlated poorly to tidal height ($r^2 = 0.005$) and 3-day cumulative rainfall ($r^2 = 0.004$) or both of the variables ($r^2 = 0.05$). However, the greatest mean current speeds, measured by drifters, 64.27cm/s on Dec-9-2004, coincided with the highest inertial radius (13.41 km). The change of tidal height on this day was relatively high (1.85 m) in comparison to the greatest change in tidal height (2.4 m) on January 10, 2005. December 9th was proceeded by a period of heavy rainfall with accumulation of 7.3 cm, suggesting a combined influence of inertial forcing from tidal inertia and freshwater runoff.

Patterns of plume forcing are also evident in the contoured underway data. Salinity and nitrate anomalies (Figure 2.23), represented as differences from the spatial mean, show a difference in plume structure and inertial radius. The more clearly defined plumes on December 9 and 10 and January 6, 2006 coincide with tidal height changes of > 2 m. Less well defined plume structure is evident on days when change in tidal height change is < 2 m. Salinity and nitrate patterns in Figure 2.23 parallel each other, indicating that freshwater influx brings with it nutrient from slough, and possibly land-based sources, to the coastal ocean. The magnitude of nutrient anomalies compared with the surrounding coastal ocean values increased during the sampling time series suggesting increased nutrient input with increased amount of cumulative rainfall. The plumes on January 20 and 21, 2005, which occurred during tidal height changes of <2 m, emphasize the interaction of plume waters with the prevailing cyclonic bay-wide circulation. The surface plume, as

represented by lower salinity and the dissolved constituent of nitrate, suggests northward transport of plume waters to the northern bay, as previously shown in the underway data.

Within the plume, vertical sampling with the AUV shows partitioning of particulate and dissolved constituents (Figure 2.24). Patterns of optical backscatter / fluorescence used to describe particulate matter present through of the water column, while nitrate is used to describe dissolved constituents. The backscatter to fluorescence ratio is used to eliminate the contribution of chlorophyll scattering as measured by optical backscattering instruments. These instruments have been used to quantify phytoplankton cell dimensions for some cell shapes (Reinecker et al., 2008). While the vertical distribution of particulates on Jan-20-2005 followed the southern flank of the AUV sampling triangle, flowing to the south and dispersing throughout the water column, nitrate is observed on the northern flank of the sampling triangle, flowing to the north at the surface (Figure 2.24). The spatial maps of surface structure showed this tendency, as well. Nitrate is shown to be transported northward (Figure 2.11. Jan-20-2005, panel D), while low transmission waters were confined largely to a southerly trajectory (Figure 2.12. Jan-20-2005, panels C and D).
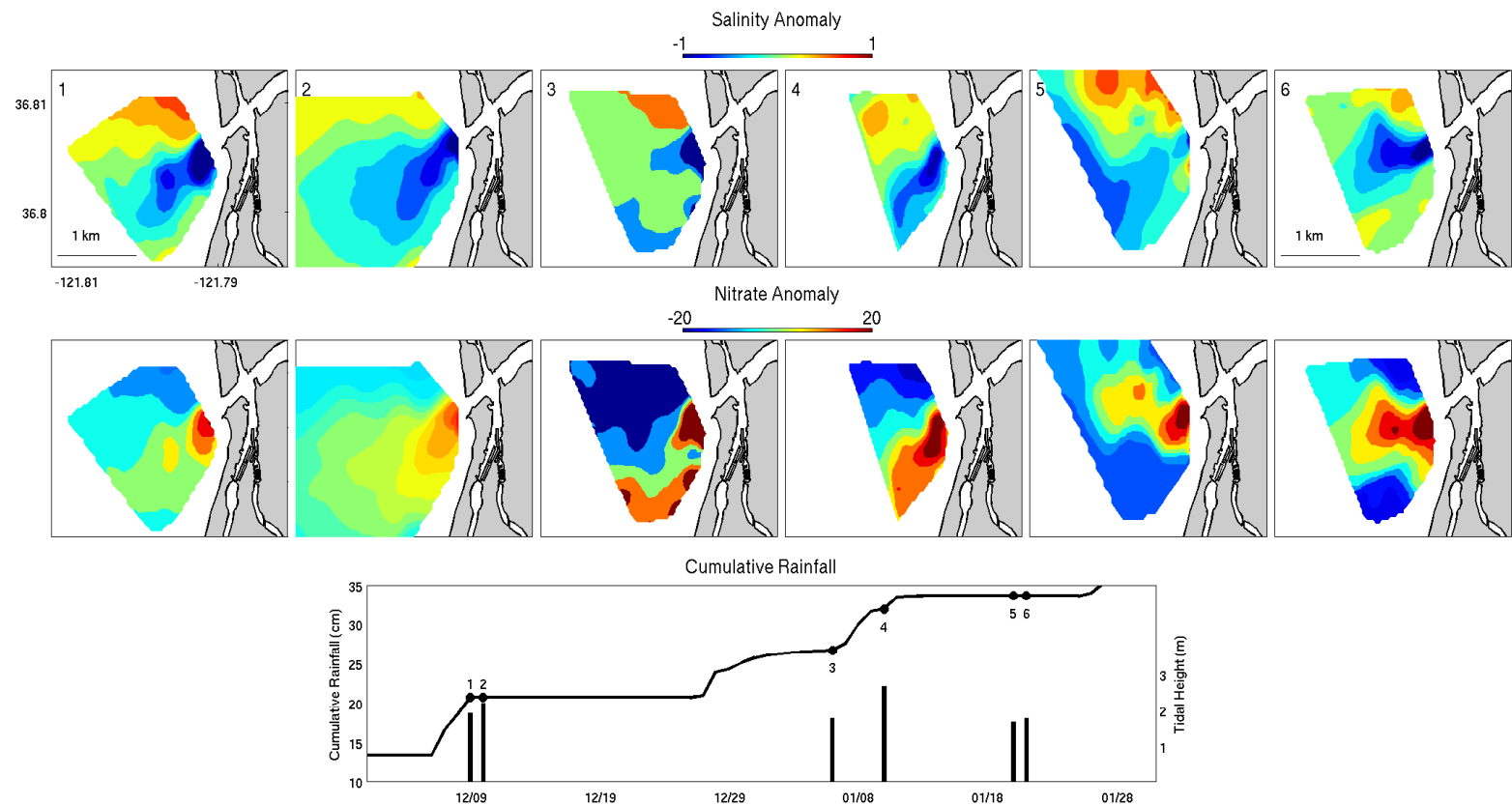
Figure 2.23 Salinity and nitrate anomalies of plume surface patterns at the same point in the tide (maximum ebb) from each of the sampling days (top and middle panels) and the cumulative rainfall and change in tidal height for each sampling day (bottom).

47
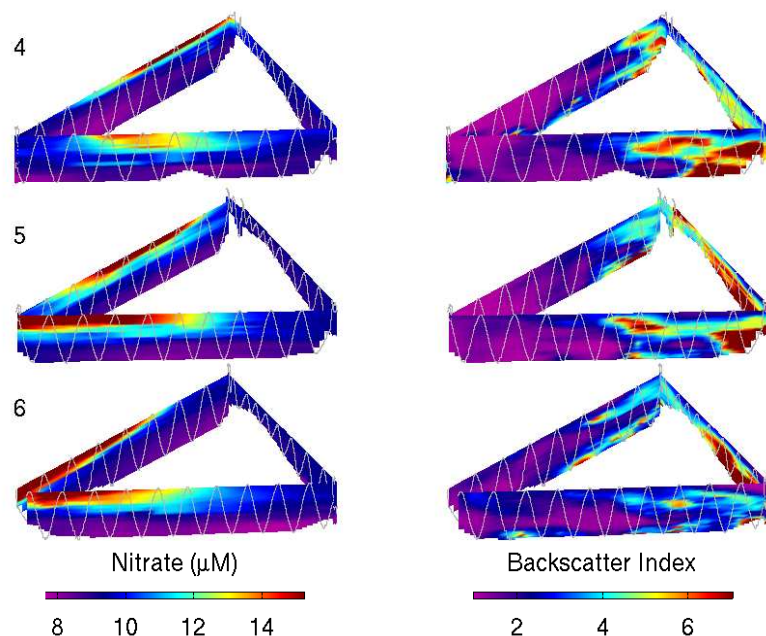
Figure 2.24 The partitioning of dissolved (nitrate) and particulate backscatter / fluorescence) constituents in the vertical structure of the slough plume during the ebb tide.

2.5 Summary and conclusions

The Elkhorn Slough exchanges waters with Monterey Bay twice daily, year-round. This exchange is nearly three times greater than the discharge of all rivers into Monterey Bay. Hydrological alterations to the slough have transformed the quantity and quality of water that empties in Monterey Bay on each ebb tide. The Elkhorn Slough now represents a significant link between the surrounding watersheds and the coastal ocean with the potential to alter coastal biogeochemcial cycling and nearshore ecology. The ebb tide discharge from the Elkhorn Slough produces a buoyant tidal jet that is distinguishable from the receiving coastal nearshore waters. The discharge plume extends ~1 km offshore in a south-westerly direction and is <1 km wide. The

discharge plume relies largely on inertial forcing from tidal activity with little influence from the earth's rotational forcing. Based on drifter observations, this inertia dissipates quickly, likely due to rapid mixing, and is quickly altered by coastal currents and the northward flowing bay circulation. A calculation of the plume inertial radius (Geyer et al., 2000), based on the current measurements and dimensions of the plume indicated that the inertial effects have the potential to extend up to 8 km offshore. However, this far-reaching extent was not observed during the sampling period. The reason for this is that the plume may either have extended beyond the geographic limits of the surveys, or that the discharge plume quickly dissipated due to rapid mixing in the highly dynamic coastal environment.

The discharge plume is a resolvable feature when compared against the background of ambient Monterey Bay coastal waters, during the rainy months of December and January. Despite interaction of bay waters with the slough through tidal fluxing, the plume that exits the slough is significantly different from the water that enters the slough. The discharge plume is associated with elevated concentrations of highly correlated dissolved organic matter and nitrate. Particulate matter, likely eroded from the banks and bottom of the slough, appears to settle quickly through the water column and is transported in a southwesterly direction with the littoral currents, while the finer sediments and dissolved organics are transported northward. The quick settling of particulate matter corroborates the results found by Warrick et al. (2004) and Warrick et al. (2007) in their studies of riverine plumes. Also, in describing a sediment budget for Monterey Bay, Eittreim et al. (2002) describe the fate of sediment input from river outflow. They show that coarse sediment moves southward along the coast in the littoral zone, while fine sediment moves to the north by advection and diffusion along the midshelf. Sediment transport directions are poleward (parallel to

the coast) in the fall and winter and equatorward in spring/summer. Since the majority

of transport occurs in the winter, the net transport of fine sediments is poleward

(Eittreim et al., 2002). The sediments from the plume appear to follow a similar

dynamic.

CDOM and nitrate input provides an important biogeochemical linkage

between MB and the ES watershed. Co-varying concentrations of CDOM and nitrate

(r = 0.93) provided the most consistent signature of plume waters across all sampling

days. CDOM occurs naturally in aquatic environments and is primarily a result of

tannins released from decaying organic detritus. Humic substances make up the

majority (50–70%) of DOM discharged into coastal ocean, and DOM is the most

important constituent of CDOM (Aiken et al., 1985). Humic substances contain

carbon, nitrogen and associated nutrients such as phosphorus and iron and they

provide a major source of nutrients and energy to coastal ecosystems (McKnight and

Aiken, 1998). The nutrients and energy bound in humic substances becomes available

to food webs during photochemical and microbial decomposition of CDOM (Mopper

and Kieber, 2002). Human activities such as logging, agriculture, effluent discharge,

and wetland drainage can affect CDOM levels in fresh water and estuarine systems.

Mainly, these activities can lead to nutrient enrichment, which can lead to

phytoplankton growth, increasing the amount of decaying phytoplankton or decaying

organic detritus. Vertical differences in the CDOM concentrations can be especially

pronounced under stratified conditions where a strong thermocline can act as an

effective barrier separating the overlying water mass (which is exposed to high solar

radiation) from the underlying water mass (which receives little or no insolation).

Therefore, the freshwater input can act as both as a source of buoyancy which, in

correlation with increased concentrations of CDOM and promoted phytoplankton

growth near the surface can act as an attenuator of visible light which inhibits growth deeper in the water column.

Nutrient pulses appear to exit the slough on ebb tide with nitrate concentrations much higher than the background signal in their coastal receiving waters. While nitrate concentrations in the plume seem to be associated with rainfall events, particulate loading from the slough into the coastal ocean appears to be related to tidal forcing, possibly a result of the erosion of the banks and the bottom of the slough. While the heavy particulates settle out quickly, fine sediment (and likely dissolve organics and nitrate) can be transported northward by the mean bay circulation to an oceanographic retention region where dinoflagellate blooms have been shown to incubate (Ryan et al., 2008a) and from which they spread throughout the bay and offshore (Ryan et al., 2005, Rienecker et al, 2008; Kudela et al, 2008).

Nutrient inputs to the coastal ocean have increased over the last several decades. Howarth et al. (2000) reports that from 1960 to 1980, the average nitrogen fluxes to the coastal waters of the United States increased by an estimated 67%. They also state that during the 1980's, nitrogen fluxes increased little if at all, but then have been estimated to have again increased steadily over the past 15 years, although less rapidly than during the 1960s and 1970s. For disturbed landscapes in the temperate zone, an average of 20 to 25% of the nitrogen inputs resulting from human activity is exported in rivers (Howarth et al., 1996, 2000; Boyer et al., 2002). Eutrophication of coastal marine ecosystems has been shown to be driven primarily by nitrogen inputs (Howarth and Marino, 2006), and impacts of nutrient inputs can lead to decreases in biotic diversity, to hypoxic and anoxic conditions and can increase the incidence and duration of some types of harmful algal blooms (NRC, 2000).

Additionally, the discharge plume waters have been shown to differ in temperature and salinity from the surrounding coastal waters into which they enter, although only slightly. The physical processes that result from the differences in temperature and salinity have the potential to influence ecosystem ecology. Features and processes, such as fronts and density stratification, are commonly associated with the accumulation of biological materials and serve to regulate distribution of nutrients and phytoplankton. The convergence of plume waters and nearshore coastal counter-currents appears to create a high chlorophyll retention region to the north of the slough entrance, creating a localized area of high biological productivity. Drifters deployed here showed a long residence time and AUV and UW data showed high relative concentrations of chlorophyll fluorescence.

The plume was sampled during various phases of the neap and spring tide cycle. The plume was more clearly defined on when the tidal height was > 2 m and the relative magnitude of constituents increased with increasing rainfall. However, this signal was confounded by the complex dynamics of the coastal ocean into which the plume enters. The coastal ocean presents a noisy background, due to a mixture of signals from mixing currents, seasonal changes of oceanographic conditions, and changes in background conditions due to riverine input. The surface structure of the plume was most well defined on December 9 and 10, 2004, as the plume entered a coastal ocean that was undisturbed by riverine input from the Pajaro and Salinas rivers. This coincided with the highest observed plume currents and inertial radii. December 9th was also preceded by the highest 3-day cumulative rainfall observed during the sampling period.

This is the first multi-disciplinary study of the Elkhorn Slough plume and its interaction with the coastal waters of Monterey Bay. The plume is an important, often overlooked link between Monterey Bay and the surrounding coastal watersheds. This is also the first multidisciplinary study of a plume from this type of system that is typical of mid-latitude regions of the west coast of North America and Mediterranean climates. The multidisciplinary approach of this study, a description of physical, chemical and biological structure, composition and dynamics, also highlight the importance of use of AUV and UMS to capture synoptic views of highly dynamic coastal ocean processes.

The transport of materials across the land-sea interface and into nearshore waters plays a role in transforming the biogeochemical processes in the coastal ocean. Changes to the hydrology of these systems and alteration of land use activities in the surrounding watershed can have important consequences regarding the quantity of constituents and dynamics of these plumes and ultimately to ecology of the coastal ocean. Climate variability and climate change are likely to have a profound effect on the delivery of materials to coastal marine ecosystems, and the continued alteration of land use patterns and hydrological modifications to estuarine systems will confound these effects. As shown here, estuarine plumes along the California coast, are important land-sea links that have been largely overlooked. It is important to further understand their role in linking estuarine watersheds to the coastal ocean.

CHAPTER 3

FATTY ACIDS AND PIGMENTS IN AN ESTUARINE PLUME AND THEIR
RECEIVING COASTAL WATERS

3.1 Introduction

It has been shown that estuarine-lagoon systems can be an important link between Monterey Bay and the surrounding coastal watersheds. Estuarine-lagoons, which are often associated with high rates of biological productivity, are a potential source of organic matter. Knowledge of the source and composition of organic matter is important to understand the role of estuarine input in coastal ocean biogeochemical cycles. Here I characterize the fatty acid and pigment content of a tidal plume leaving an estuarine-lagoon, the Elkhorn Slough, and the difference in content between the plume and coastal receiving waters of Monterey Bay. While the previous chapter focuses on defining the physical structure of the plume, as well as some of its biological content (dissolved organic matter and chlorophyll), here we focus on further defining the sources and composition of biological constituents and organic matter in plume waters. Some attention is paid to the ecological consequences of the interaction between the estuary and the surrounding watershed and the coastal ocean and the degree of mixing once the plume enters the coastal ocean.

Lipids are a major constituent of living organic matter involved in a variety of cellular functions, including membrane structure (phospholipids and glycolipids) and energy storage (triacylglycerols and wax esters) (Vance and Vance, 1985; Arts and Wainman, 1999). Lipids also constitute a source of essential nutrients and vitamins. Fatty acids (FAs), a class of lipids, are straight-chain hydrocarbons possessing a

54

carboxyl (COOH) group at one end. Since the most important fatty acids are synthesized de novo in phytoplankton and are transferred to zooplankton and other primary consumers, lipids constitute a significant part of the carbon flux through trophic levels in aquatic environments (Lee et al., 1971; Sargeant et al., 1977). In shelf areas, lipids are an important component of the productivity of the coastal ocean ecosystem because they are carbon rich with a very high energy value and are thus important metabolic fuels

Fatty acids can be generally grouped into two classes: those fatty acids that cannot be synthesized *de novo* but are essential for animal growth and development and must be supplied by food, and those that can be synthesized and are nonessential. Fatty acids without double bonds are called saturated fatty acids and those with double bonds are called unsaturated fatty acids. The morphology of fatty acids can be described by the shorthand A:Bn-C, where A equals the number of carbon atoms, B equals the number of double bonds and C equals the position of the double bonds from the carboxyl end. Enzymes, called desaturases, catalyze reactions that introduce double bonds and lead to the synthesis of unsaturated fatty acids from saturated fatty acids. The most abundant saturated fatty acids in animal and plant tissues are straight-chain saturated fatty acids with 14, 16 and 18 carbon atoms (e.g. 14:0, 16:0, and 18:0). Monounsaturated fatty acids (MUFA's) are straight chain fatty acids with one double bond. Those with more than two double bonds are called polyunsaturated fatty acids (PUFA). The lipids of all higher organisms contain appreciable quantities of PUFAs. While SFAs and MUFAs serve as efficient storage lipids (Roessler, 1990), PUFAs play an important role in cell membrane activity (Broglio et al, 2003). Marine invertebrates, including zooplankton, require PUFA with between 2 and 6 double bonds for survival and growth (Xu et al., 1994; Pond et al., 1996, Milke et al., 2004).

Fatty acids have been used as biomarkers to characterize biological processes in the world's oceans (Daalsgaard et al., 2003). Gao et al. (2006) measured the uptake of organic fish feed waste by green-lipped mussels in the vicinity of a fish aquaculture facility. Bachok et al. (2006) characterized the FA composition of healthy and bleached corals as a diagnostic indicator of coral health. They showed that health-compromised, bleached corals showed low levels of PUFAs, an essential energy reserve and metabolic precursor for growth, and high bacterial FAs. In unpolluted bays, fatty acids have been utilized to denote the relative contribution of diatoms, bacteria, dinoflagellates or terrestrial organic matter. For example, Mezaine and Tsuchiya (2000), using fatty acids, showed that organic matter from the mangrove forests in Oura Bay, Okinawa, is exported to the intertidal flat in both the rainy season and the dry season. Zou et al. (2004) used fatty acid analysis to show that a fraction of high-molecular-weight dissolved organic matter (HMW-DOM) is derived from bacteria and phytoplankton, as opposed to the previous notion that HMW-DOM was derived from direct exudation by phytoplankton. They found that this was the case across several different coastal systems despite variable organic matter inputs and environmental conditions.

Each of these studies used individual fatty acid compounds, groups of compounds and FA ratios to indicate the presence and/or sources of certain types of organisms or biological material. Generally, long chain (>C20) saturated fatty acids have been associated with vascular plants and are thought to originate from terrestrial sources (Cranwell, 1982). The PUFA 18:2n6 has been associated with terrestrial plant material (Copeman and Parrish, 2003) and 26:0 has been associated with terrestrial matter. The sum of iso- and anteiso-branched chain fatty acids, 15:0 and 17:0 have

been used to trace the presence of bacteria in aquatic systems (Fulco, 1983; Sargent et al., 1987). Bacteria specifically synthesize a series of odd-number C15-C17 (branched and normal) and also 18:1n-7 fatty acids, which are associated with membrane phospholipid material (Parrish et al, 2005; Fulco , 1983; Sargent et al, 1987; Kaneda, 1991). The presence of PUFAs suggests phytoplankton material. Various phytoplankton produce a variety of PUFAs, including 20:4, 20:5, and 22:6 (Clautre et al., 1988; Volkman, 1989). Phytoplankton also produce SFAs and MUFAs such as 16:0 (Sargent and Whittle, 1981) and 16:1n-7 (Nichols et al , 1993). The relatively high ratio of 16:1n-7 to 16:0 is often used as an algal input index (Volkman, 1989), and diatoms have been indicated by increased proportions of 20:5n-3 or by elevated ratios of $\Sigma16{:}1/16{:}0$ and $\Sigma16/\Sigma18$. The ratio of 16:1n-7/18:4n-3 has been used as an indicator of diatom food and low ratios of flagellate based nutrition (Stubing and Hagen, 2003). We can reverse the ratio 18:4n-3/16:1n-7 and use it as a basis for high ratios of flagellates, since 18:4n-3 is found in higher percentages in flagellates (Sargent et al., 1987).

Here, I use fatty acid biomarkers to describe the concentrations of terrestrial, planktonic and bacterial constituents in outflowing plume waters and receiving coastal waters. Pigments are used to characterize in more detail the planktonic content of these waters. Coastal zones are transitions between the land and the ocean and have become increasingly important areas to human society ecologically, economically and socially. Estuaries are at the land sea interface and play a considerable role in the biogeochemical cycles, and virtually all land-derived materials (water, sediments, dissolved and particulate nutrients) enter this region through surface runoff or groundwater flow. The functioning of the coastal marine environment has been linked with adjacent terrestrial processes (e.g. Skreslet, 1986; Valiela, 1992), and there is

concern that human pressures and the associated infrastructure may be changing the delicate balance between terrestrial and marine environments. The characterization and quantification of transport pathways and biological materials across the land-sea interface is important for understanding impacts to the ecology of coastal and nearshore marine environments.

3.2 Materials and methods

3.2.1 Study area and sample collection

Details of the slough, its surrounding watershed and the rapid man-made changes to the hydrological structure and functioning are described in Chapter 2. Water samples were collected during the ebb tide on January 6, 10, 20 and 21, 2005 at three locations: in the plume as it immediately exits the harbor entrance (plume water), at locations offshore (coastal waters), and between the plume and coastal waters (intermediate waters), where plume waters exiting the slough have mixed with coastal waters (Figure 3.1). The mean change in tidal height, from high-high to low-low tide, during the sample period was 1.9 meters while during the month of January; the mean change was 1.5 meters. From each water sample, between 250 and 500 ml of the water samples were filtered through 25 mm Whatman GF/F glass micro-fiber filters (nominal pore size of 0.7 um), until water stopped flowing through the filters. The filter pads were stored in clean glass centrifuge tubes in preparation for lipid extraction, fatty acid (FA) and high performance liquid chromatography (HPLC) analysis.

During water sample collection, the surface expression of the plume was mapped by a near surface Underway Mapping System (UMS) deployed from a Boston Whaler (Chapter 2). Statistics for the surface water properties in the vicinity of the

sampling location from the UMS were calculated and used for correlations with fatty acid concentrations.
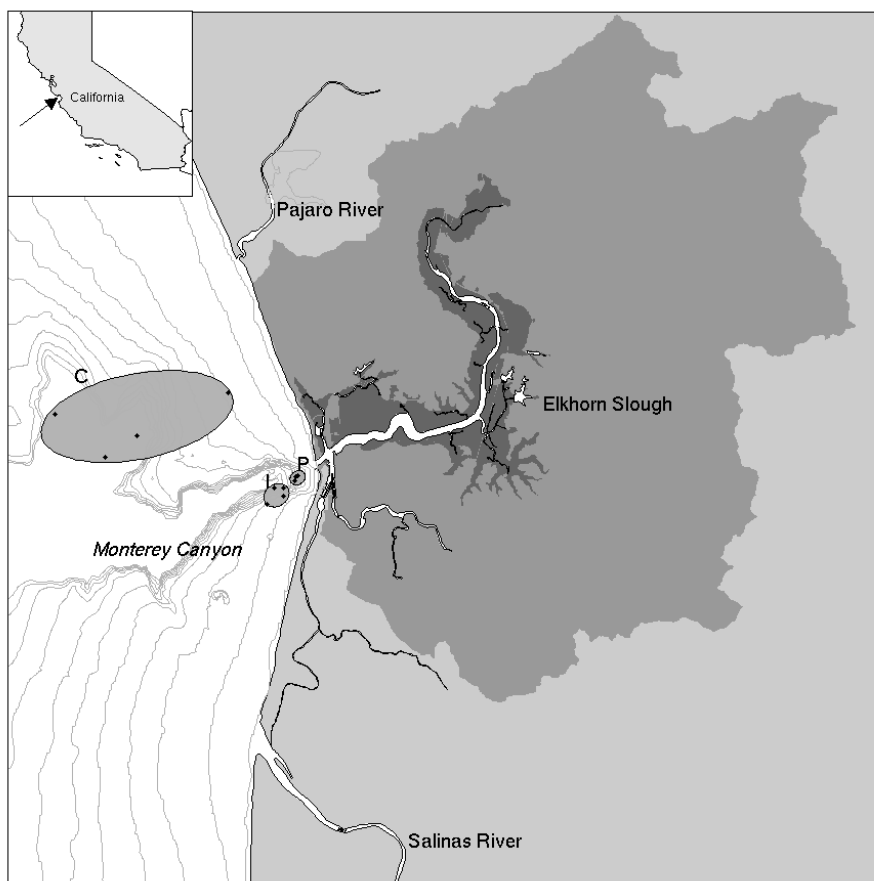
Figure 3.1 The location of the Elkhorn Slough. Dark grey indicates the watershed drainage area and green indicates wetland areas. Water sampling locations are shown in the grey ovals, C = coastal water, I = intermediate water, and P = plume waters.

3.2.2 Lipid Extraction, FA Analysis and HPLC Analysis

Lipid extraction and fatty acid methyl ester (FAME) preparation were performed as described in Parrish (1999). Lipids can be conveniently separated from other compounds in an aqueous sample due to their hydrophobic nature. Lipids were

extracted using a modified Folch procedure (Folch et al., 1957). The extraction was conducted ultrasonically in a slush bath for 4 minutes with a 2:1 mixture of methylene chloride (CH_2Cl_{l2}) and methanol (CH_3OH) with 0.5 ml of HPLC grade water, for a solvent:water ratio of 4:1. Prior to the first wash, filter pads were ground into a pulp with a glass rod in the solvent mixture. Samples were then centrifuged for 4 minutes at 1300 rpm at 4°C. The bottom organic layer was extracted from each sample using the double pipette technique and stored in separate, pre-cleaned tubes with 3 ml of methylene chloride. The extraction procedure was repeated three times, at each step the organic layer was pooled with the subsequent one.

Each lipid extract can contain many compounds of similar polarity but sometimes with important structural differences (Parrish, 1999). The FAMEs are usually incorporated into acyl lipid classes (i.e. triacylglycerol, glycolipid or phospholipid), and these fatty acids can be cleaved from their glycerol backbone and quantified. FAMEs were prepared by trans-esterifying the lipid extract in a solution of hexane (C_6H_{14}):boron trifluoride/methanol ($BF_3/MeOH$) at 95°C for 1 hour, or until the solution turned monophasic. Samples were then washed further with a solution of hexane and water (4:1), centrifuged for 5 minutes at 1500 rpm at 4°C. The top layer (FAME in hexane) was transferred into a corresponding new clean glass tube. This process was repeated a total of three times. Ten μl of an internal standard (19:0 FAME) working solution was added to the sample for calibration, and the samples were then evaporated to dryness and then re-dissolved with 250 μl of hexane. Samples were transferred to pre-labeled, pre-cleaned 2 ml amber glass vials with teflon-lined caps, flushed with nitrogen, capped and frozen (-80°C) until analysis.

The FAMEs were separated and quantified using gas chromatography on a
Trace GC2000 instrument (Thermoquest) equipped with a flame ionization detector.
Separation was performed on a DB-23 capillary column (Agilent Technologies, 25 m
x 0.25 mm internal diameter, 0.25 μm film thickness) with hydrogen as the carrier gas.
After injection (split ratio 1:24) at 60°C the temperature was held for 2 min and then
raised to 150°C at a rate of 20°C per minute, held for 2 minutes and then raised to
205°C at a rate of 1.8°C per minute, and finally raised to 230°C at a rate of 5°C per
minute. Most FAME peaks were identified by comparing their retention times with
those of authentic standards (Supelco Inc, Bellefonte, PA, USA).

Phytoplankton pigment content was measured from volumes of seawater
filtered onto GF/C Whatman filters and extracted in 96% ethanol in the dark for 24 h.
The pigment extract was stored frozen prior to analysis using high performance liquid
chromatography (HPLC) equipment. Using HPLC, pigments were proportioned into
the dominant algal groups (diatoms, dinoflagellates, cryptophytes, chlorophytes and
cyanophytes) according to the fraction of total chlorophyll a contributed by each taxa
(the diagnostic pigments are fucoxanthin, peridinin, alloxanthin, chlorophyll b, and
zeaxanthin). The HPLC equipment consisted of a 420 Waters fluorescence detector
(430 nm excitation light and 660 nm emission light) and a Spectra Physics ternary
pump (Model 880). Samples of 200 μl were injected via a Waters U6K injector valve,
and reversed-phase HPLC was performed on a 10 x 0.5 column packed with C18 4 μm
microsphere Chrompack.

3.2.3 Statistical analyses

One-way analysis of variance (ANOVA) was used to compare the total lipid
and individual fatty acid concentration of the three water types (plume, intermediate

and coastal). Significant differences among water types were further examined using the Fisher's protected least squares difference (PLSD). PLSD allows the pairwise comparison among a set of population means whose equality have been shown to differ in an ANOVA (Ott and Longnecker, 2001). Ordination by Principal Components Analysis (PCA) was then applied to reduce the complexity of the multivariate information in the matrix of fatty acid samples x sites to obtain a low dimensional picture of how the sites interrelate. For more details on ordination by PCA, refer to Jonson and Wichern (2002). Unidentified FAs were not included in the analyses. For all tests, a criterion of $P < 0.05$ was used to determine statistical significance.

3.3 Results

3.3.1 Lipid content of plume, coastal and intermediate waters

Results of fatty acids analyses appear in Table 3.1. Plume waters showed higher concentrations of total fatty acids (FAs) and most all individual FAs, although the total concentrations of FAs were not significantly different. The concentrations of FAs in coastal waters were higher than plume waters for the FAs 16:2n-4, 18:4n-3 and 22:6n-3. Individual FA concentrations in intermediate waters were higher than plume and coastal waters for 18:3n-1. FAs were then compiled according to major FA classes and fatty acid biomarkers by water type (Table 3.2). Individual fatty acid compounds, groups of compounds and their ratios were then used to distinguish the presence of various forms of biological material in the plume, intermediate and coastal waters. The FAs 18:2n-6 and 26:0, which were both present in our samples, and are commonly used as an indicator of the presence of terrestrial matter and terrestrial plants, were summed and used as markers for terrestrial material (Budge et al., 2001;

Table 3.1 Total lipid content (µg L^{-1}) and fatty acid composition (µg L^{-1}) for Elkhorn Slough plume, receiving coastal, and intermediate waters. Values represent the mean ± SE of four different samples.

Fatty Acids	Coastal (n=4)	Intermediate (n=4)	Plume (n=4)
Total fatty acid content (μ g L^{-1})	57.4 ± 15.8	104.7 ± 19.2	129.6 ± 19.0
12:0	3.40 ± 1.19	13.9 ± 1.98	11.2 ± 6.55
14:0	1.95 ± 0.48	3.44 ± 0.43	3.09 ± 0.89
15:0	0.27 ± 0.09	0.53 ± 0.26	1.18 ± 0.117
*iso*16	1.16 ± 0.56	6.07 ± 0.98	4.15 ± 2.54
16:0	9.90 ± 2.64	11.4 ± 2.83	20.2 ± 2.53
16:1n-9	0.34 ± 0.11	0.68 ± 0.14	0.74 ± 0.07
16:1n-7	2.15 ± 0.60	2.71 ± 0.85	5.55 ± 0.42
16:1n-5	0.32 ± 0.08	0.82 ± 0.09	0.71 ± 0.41
*iso*17	0.55 ± 0.33	0.29 ± 0.41	0.88 ± 0.2
16:2n-4	0.44 ± 0.14	0.54 ± 0.03	0.21 ± 0.31
17:0	0.57 ± 0.19	1.47 ± 0.31	1.75 ± 0.32
17:1	0.60 ± 0.20	1.41 ± 0.34	1.53 ± 0.46
18:0	2.81 ± 0.92	5.98 ± 1.7	12.4 ± 2.0
18:1n-9	1.90 ± 0.56	3.26 ± 0.52	4.44 ± 0.67
18:1n-7	2.03 ± 0.61	4.41 ± 0.71	7.54 ± 0.86
18:2n-6	0.90 ± 0.25	0.93 ± 0.24	1.29 ± 0.20
18:3n-4	0.88 ± 0.31	1.92 ± 0.34	1.97 ± 0.74
18:3n-1	0.95 ± 0.63	2.22 ± 1.1	2.81 ± 0.56
18:4n-3	1.38 ± 0.40	0.89 ± 0.25	1.11 ± 0.32
18:4n-1	0.15 ± 0.05	0.60 ± 0.74	0.98 ± 0.3
20:0	0.60 ± 0.19	1.38 ± 0.18	1.41 ± 0.5
20:1n-11	0.92 ± 0.32	1.79 ± 0.31	1.83 ± 0.7
21:0	0.78 ± 0.25	2.50 ± 0.33	2.44 ± 1.0
20:4n-3	0.83 ± 0.32	3.45 ± 0.46	2.29 ± 1.73
20:5n-3	3.11 ± 0.9	1.92 ± 0.83	3.72 ± 0.68
22:0	0.09 ± 0.03	0.32 ± 0.11	0.41 ± 0.12
21:n-9	0.48 ± 0.22	1.08 ± 1.25	2.32 ± 0.67
23:0	0.50 ± 0.18	0.82 ±v0.25	0.80 ± 0.22
22:4n-6	0.16 ± 0.09	0.47 ± 0.11	0.34 ± 0.16
22:5n-6	0.11 ± 0.05	0.37 ± 0.12	0.47 ± 0.09
24:0	0.34 ± 0.16	0.38 ± 0.19	0.59 ± 0.12
22:5n-3	0.19 ± 0.06	0.37 ± 0.11	0.57 ± 0.14
22:6n-3	4.45 ± 1.25	2.74 ± 1.18	4.00 ± 0.53
25:0	0.37 ± 0.2	0.48 ± 0.06	0.59 ± 0.08
26:0	1.25 ± 0.46	2.93 ± 0.48	2.23 ± 1.3
Unidentified	1.33 ± 0.29	2.52 ± 0.60	2.71 ± 0.51

Volkman et al., 1980). Similarly, our samples contained concentrations of 15:0, iso17, 17:0, 18:1n-7, and their sum, which commonly serves as bacteria-specific markers, were used as bacterial markers in our samples. Regression analysis between pigments from the HPLC analysis and fatty acids results were used to verify appropriate FA grouping or ratios for diatoms and dinoflagellates FA markers. The ratio $\Sigma16:1/16:0$ correlated well with increasing concentrations of the pigment fucoxanthin, (r = 0.75 p = 0.05) indicating a greater contribution of diatoms in the samples. The ratio 18:4n-3/16:1n-7 correlated reasonably with pigment concentrations of peridinin, a pigment prevalent in dinoflagellates (r = .80, p = 0.03). The respective FA ratios were used as indexes of diatoms and dinoflagellate abundance.

Table 3.2 Biomarkers and combination of fatty acids used to describe these markers.

Biomarker	Fatty Acid Ratio
Terrestrial Matter	18:2n-6 +26:0
Bacterial	15:0 + iso17 + 17:0 + 18:1n-7
Diatoms	$\Sigma16:1/16:0$
Dinoflagellates	18:4n-3/16:1n-7

The samples were dominated by saturated FAs (Figure 3.2) with even carbon number saturated 12:0-26:0 fatty acids. Both MUFAs and PUFAs were also present in the samples but in lower numbers. In all cases, the concentrations of FAs were higher in plume waters. While the mean concentrations of both SFAs and MUFAs were significantly different between the three water types, the concentrations of PUFAs were not (ANOVA, $P > 0.5$, Table 3.3). SFA concentrations between plume and intermediate waters were not significantly different while those between plume/coastal and intermediate/coastal waters showed a significant difference (Table 3.4). MUFA
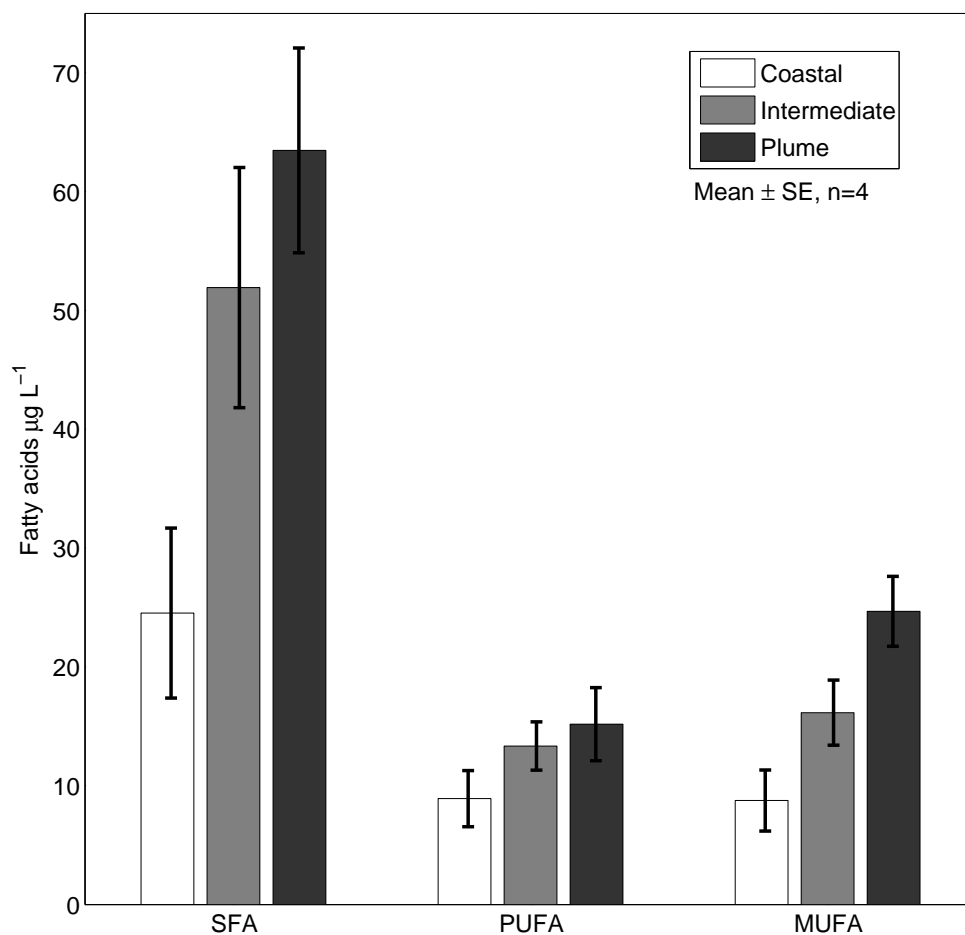
Figure 3.2 Major classes of fatty acids (μg L^{-1}) for the Elkhorn Slough plume, coastal and intermediate. Values represent the mean $\pm$ SE of four samples.

concentrations were significantly different between plume and coastal waters but not between intermediate and plume or coastal waters. Bacterial FA marker concentrations in plume waters were significantly greater than those in coastal and intermediate waters, while concentrations between intermediate and coastal waters were not significantly different (Figure 3.3; Table 3.4). Terrestrial matter showed no significant differences between plume, coastal or intermediate waters. Differences in

Table 3.3 Statistical summary from ANOVAs comparing the relative concentrations of fatty acids among the different water types coastal ocean, plume and intermediate, ns not significant, *, $P <= 0.05$, ** $P < 0.01$.

	$F_{3,9}$	P	
Total Fatty Acid Composition	4.15	0.05	ns
ΣSFAs	5.27	0.03	*
ΣMUFAs	8.37	0.008	**
ΣPUFAs	1.63	0.25	ns
ΣBacterial Markers	9.42	0.006	**
ΣTerrestrial Markers	1.17	0.359	ns
Algal Input	0.92	0.433	ns
Diatoms	7.17	0.014	*
Dinoflagellates	9.71	0.005	**

Table 3.4 Summary of protected least squared difference. The line indicates that there was no significant difference between water types.

	Coastal	Intermediate	Plume
SFAs		├──────────────┤	
MUFAs	├──────────────┤	├──────────────┤	
Bacteria	├──────────────┤		
Diatoms	├──────────────┤		
Dinoflagellates		├──────────────┤	
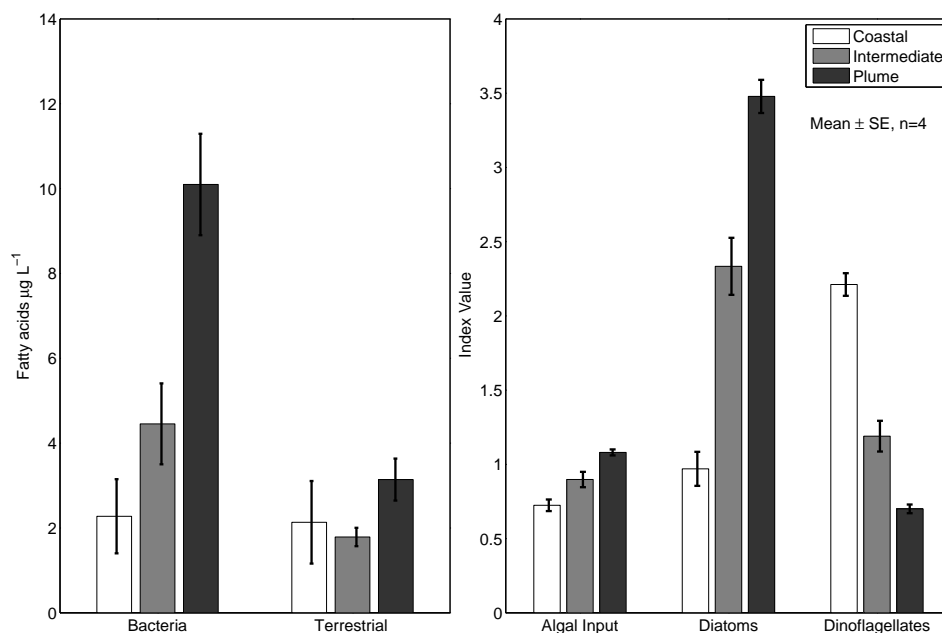
Figure 3.3 Fatty acid composition of samples collected from locations within the slough plume , coastal, and intermediate waters. Bacterial material is indicated by the sum of fatty acids 15:0, and 17:0 (iso and anteiso) and 18:1n-7. Terrestrial material is indicated by specific fatty acids 18:2n-6 and 26:0. The fatty acids ratios 16:1n-7/16:0 Σ16:1/16:0 and 18:4n-3 / 16:1n-7 are indicative of algal input, diatoms and dinoflagellates, respectively.

the algal input biomarker were not significantly significant between any of the water types. Diatom FA biomarker ratios showed a significant difference between plume and coastal waters, as well as intermediate waters, but there was no significant difference between intermediate and coastal waters. Dinoflagellate FA biomarker ratios in coastal waters showed a significant difference between plume and intermediate waters, yet there was no significant difference between plume and intermediate waters.

HPLC analysis describes in more detail the planktonic content of plume versus coastal waters and verifies the fatty acid analysis results. As in the fatty acid results, plume waters are higher in relative proportions of diatoms, while coastal waters are higher in relative proportions of dinoflagellates. The results further show that plume waters contain higher relative proportions of cryptophytes. Cyanophytes and chlorophytes, which made up a smaller component of the total pigment content of the samples, also showed a higher relative concentration in plume waters (Figure 3.4).
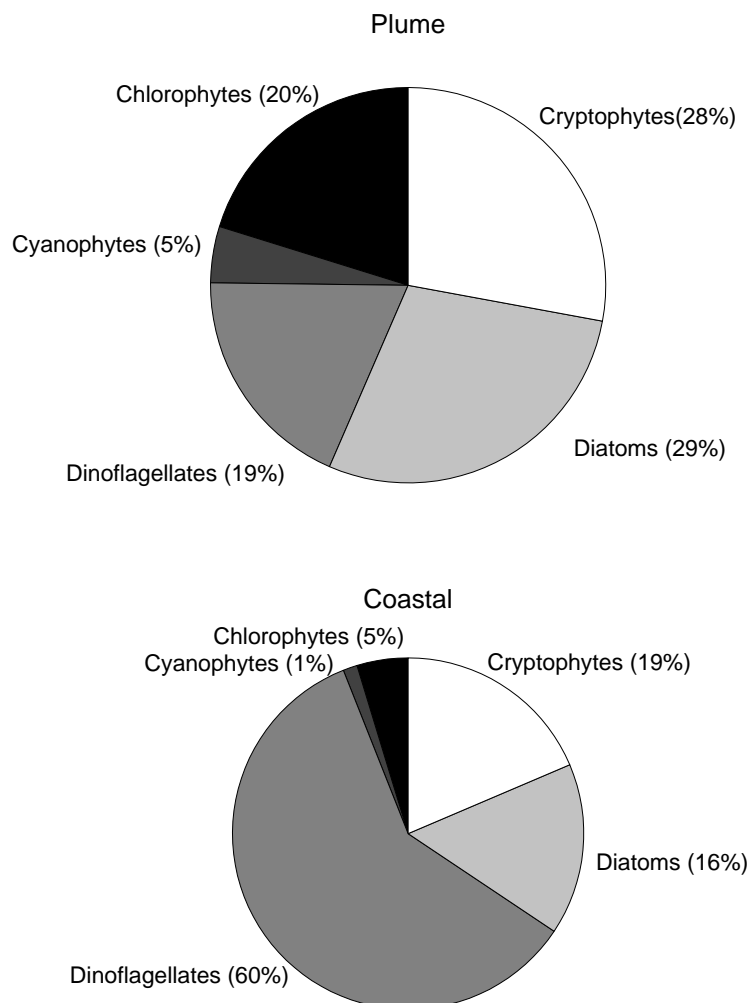
Figure 3.4 The average percentage of dominant algal groups in the slough plume versus ocean waters.

Ordination by principal component analysis by site further verifies differences in total FA concentrations between water types (Figure 3.5). Here, principal component analysis explained 91% of the total variance in the data using only two principal components. The first principal component (PC1) explained 73% of the total variance, while the second principal component (PC2) explained 18% of the total variance. Coastal waters showed a negative loading along PC1 and a positive loading along PC2. Plume waters generally showed a positive loading along PC1 and a negative loading along PC2. FA concentrations of intermediate waters clustered between plume and coastal waters, and this data indicates a separation of the biological differences between plume and coastal waters. In this plot, an outlier of intermediate water, heavily loaded in the positive direction along PC1 and PC2, dominates the graph. This is due to high concentrations of the SFA lauric acid (C12:0) in a sample of intermediate waters. Lauirc acid is a common FA in coconut and palm-kernel oil. This is likely a result of experimental error.
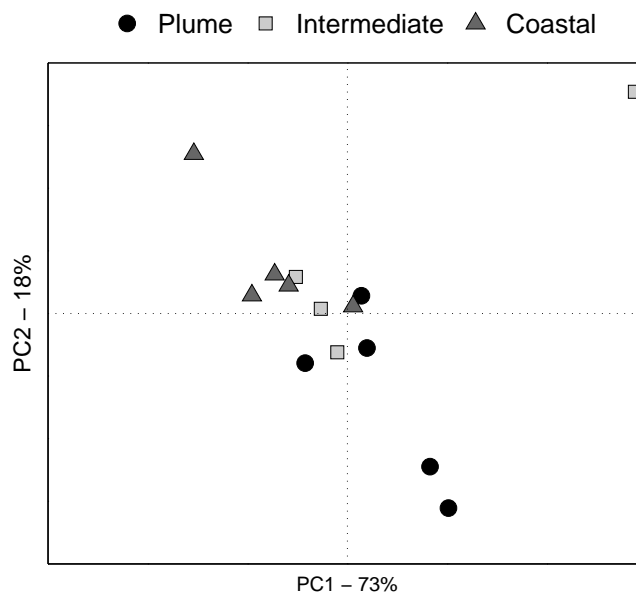
Figure 3.5 Principal components analysis of fatty acid data from plume, coastal and intermediate waters collected from Elkhorn Slough and Monterey Bay.

Underway mapping of plume waters, showed that the relative florescence of color dissolved organic matter (CDOM), percent optical transmission and the concentration of nitrate clearly distinguish plume from ocean waters (see Chapter 2). Values in the vicinity of each sampling station, of nitrate and CDOM were significantly higher in surface plume waters and decreased by over half when sampled at the coastal water stations. Likewise, low optical transmission indicates that the plume was rich in suspended sediments; however, the coastal waters were relatively clear in comparison. Physical properties of the plume waters (temperature and salinity) did not differ greatly, though plume expression was slightly cooler and less saline (Table 3.5).

Table 3.5 Mean values for underway surface water properties in the vicinity of the sampling locations.

	Temperature (°C)	Salinity (psu)	CDOM (rfu)	Fluorescence (rfu)	Transmission (%)	Nitrate (μM)
Coastal	13.5	32.1	0.25	0.2	48.8	20.6
Intermediate	13.5	32.1	0.36	0.15	20.2	28.5
Plume	13.3	31.4	0.77	0.17	12.2	50.1

Fatty acid biomarkers, which showed significant differences between plume and coastal waters, correlated with mean plume characteristics of CDOM, nitrate and transmission. Bacteria-specific FA markers, as well as the diatom biomarker index, showed a significant positive correlation with increases in CDOM and nitrate and a significant negative correlation with optical transmission (Figure 3.6). The
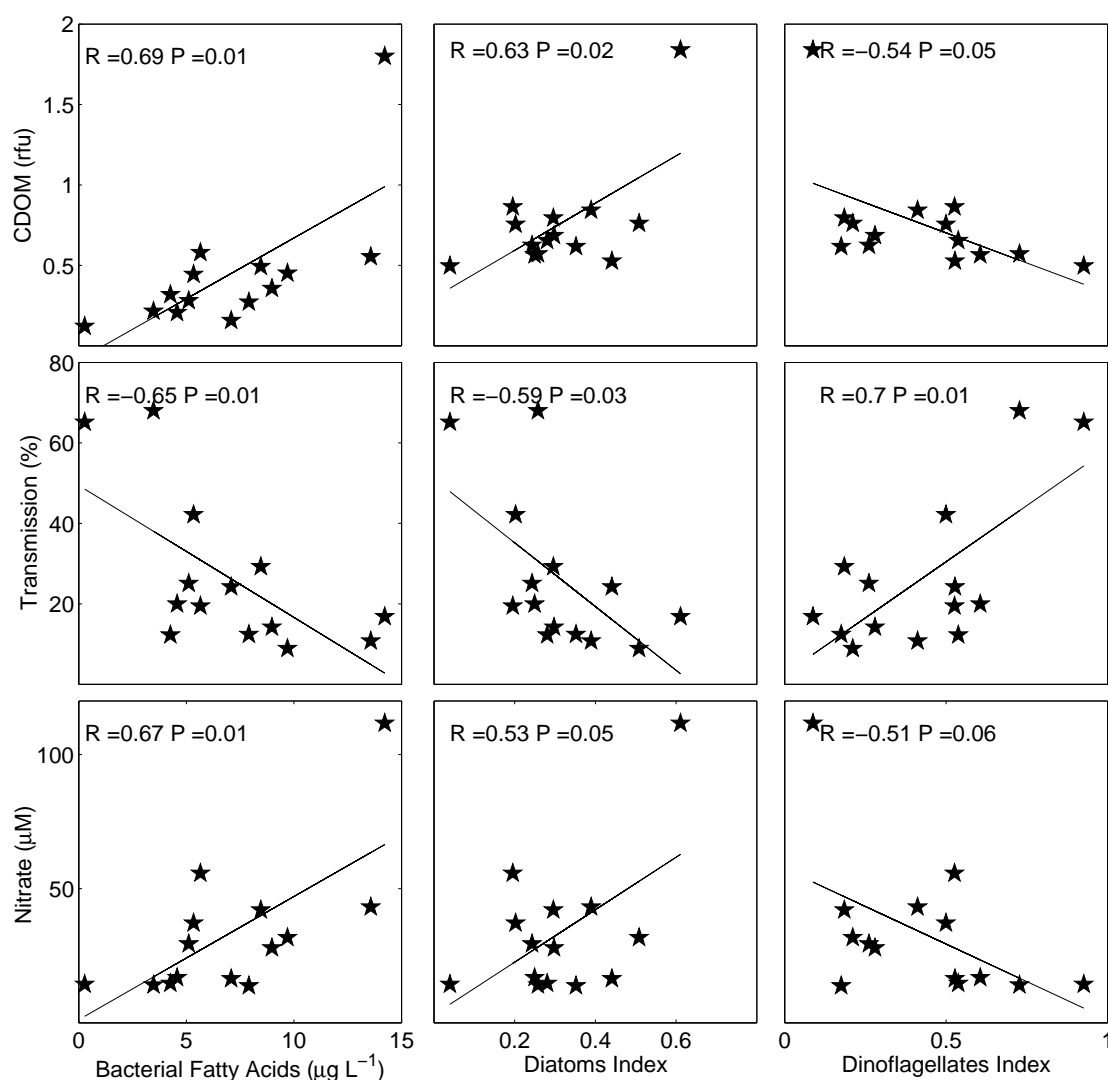
Figure 3.6 General patterns of fatty acid concentrations versus surface water properties.

dinoflagellate biomarker index showed the opposite general trend with the index ratio increasing with decreases in CDOM and nitrate concentrations and increases in optical transmission. This verifies that bacterial and diatom FA markers are prevalent in plume waters, while dinoflagellate markers are more prevalent in coastal ocean waters.

The tidal prism of Elkhorn slough has been measured to investigate the processes responsible for the erosion of wetland habitats within the slough, since it is the single most important factor determining currents within the slough. Broenkow and Breaker (2005) discuss the different measurements of the tidal prism made over the last several decades and they show that estimates of the tidal prism have increased from 2.65 x 10^6 m^3 in 1956 to 6.2 x 10^6 m^3 in 1993, a 134% increase over 37 years. The estimates of tidal prism for Elkhorn Slough shows a surprisingly linear increase over time with a slope of the linear trend of approximately 0.1 x 10^6 m^3 year^{-1} (Broenkow and Breaker, 2005). With approximately 6.2 x 10^6 m^3 of water leaving the slough on each tidal cycle and assuming 1.5 tidal prisms leave the slough each day, this translates to approximately 9.3 x 10^6 m^3 of water leaving the slough each day. This flux and biological content within the Elkhorn Slough plume appears to mix quickly with coastal waters showing a three-fold, quadratic decrease (y=0.86x^2- 5.4x +11 for bacteria and y=0.2x^2-1.2x+2.5 for diatoms) in concentration as soon as waters reach four kilometers from the harbor mouth (Figure 3.7). Nitrate and CDOM show similar mixing behavior, decreasing quickly before reaching the coastal sampling stations, where as transmission shows an almost linear increase (Figure 3.8).

3.4 Summary and Discussion

Elkhorn Slough exchanges water with Monterey Bay twice daily year round. Alterations to the mouth of the slough have contributed to an increase in the tidal prism and tidal erosion of the banks and the bottom of the slough, a positive feedback which has amplified over the years (Breaker and Broenkow, 2005). Water that enters the slough on an incoming tide is relatively clear bay water, however the plume that exits the slough on the ebb tide is significantly different. While, conservative properties (temperature and salinity) of these waters are fairly similar to surrounding
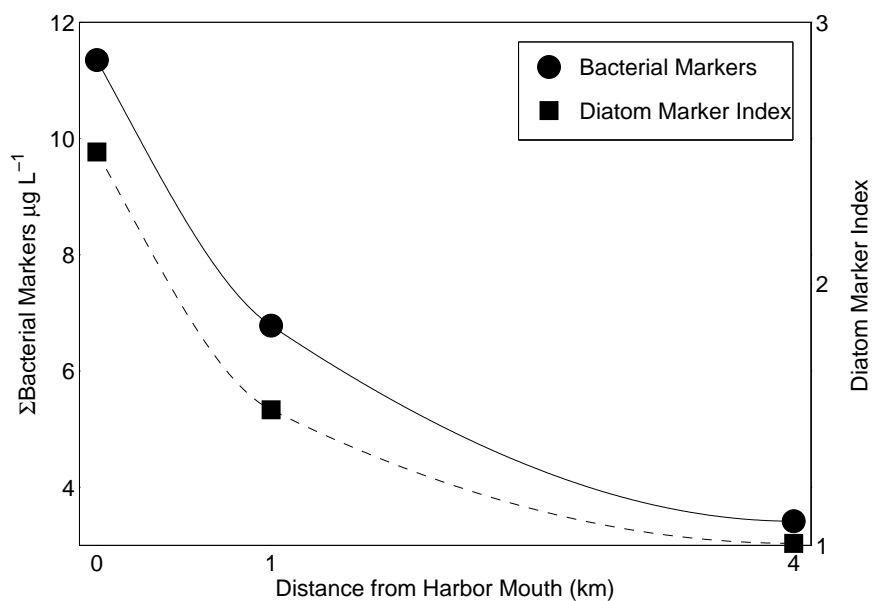
Figure 3.7 Change in concentration of bacterial fatty acids and diatom fatty acid markers with distance from the entrance of the Elkhorn Slough.
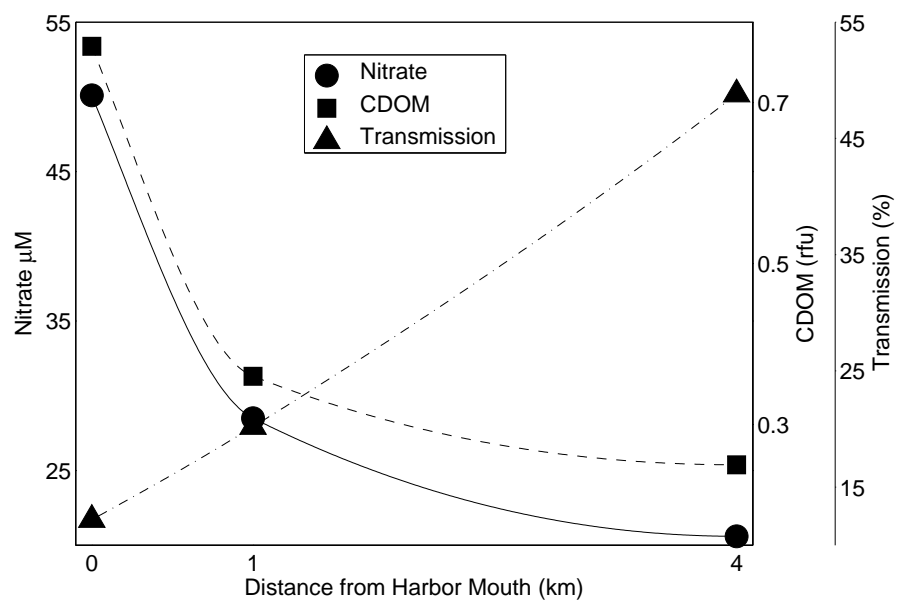
Figure 3.8 Change in mean value of surface water properties at water sampling locations with distance from the entrance of Elkhorn Slough.

bay waters, the outgoing plume expresses itself as biologically distinct from surrounding coastal waters.

A remarkable feature of the biological content of the plume waters is the abundance of bacteria-specific FAs. It is also noticeable that the increased concentration of bacterial FAs correlate with the concentrations of CDOM. Zou et al. (2004) showed that bacterial fatty acids are an important component of the DOM pool in estuarine and coastal waters. Bacteria release their cellular components into the DOM pool through several different ways: direct release from bacterial capsular material (Stoderegger and Herndl, 1998), viral lysis of free-living and particle-associated bacteria (Furhman, 1999), and heterotrophic grazing of flagellates on bacteria (Nagata and Kirchman, 1992). The FA content of the plume samples were also predominantly SFAs. This is also consistent with the results found by Zou et al. (2004) who found that even-carbon-number, SFAs dominated high-molecular-weight dissolved organic matter samples from estuarine and coastal waters. However, contrary to Zou et al. (2004) long chain (C22-C26) saturated fatty acids were found in Elkhorn Slough plume and coastal water samples, but made up only an average of 2.3% of the total samples. Shorter chain saturated fatty acids, especially 16:0, the most abundant fatty acid may be present in high quantities because of its origination in numerous marine and terrestrial cellular materials. Difference in terrestrial fatty acid concentrations were not different due to the recent breaching of the Pajaro and Salinas Rivers, changing the background condition of the nearshore waters of Monterey Bay (see Chapter 2).

The plume exiting the slough also showed elevated nitrate in comparison to the surrounding coastal waters (see Chapter 2). N-loading in the slough has been shown

to be both marine and land-based (Chapin et al., 2004; Fry et al., 2004). The main land-sources of N to the slough are thought to be in the form of nitrate from agricultural fields, dairy farms, and urban surface-water runoff. High nutrient, freshwater runoff enters the Elkhorn Slough after wet season storm events with rainfall greater than 1.5 cm (Caffrey et al., 2007). The duration and magnitude of these nutrient pulses depends on whether they occur early in the rainy season when they are rapidly flushed out of the system, or later in the rainy season when they can persist for weeks (Caffrey et al., 2007). Marine sources of nitrate are thought to enter the slough in the form of internal waves carrying water from ~100 m depth up the Monterey Submarine Canyon and into the lower section of the slough on every rising tide (Chapin, et al., 2004). During the dry season this source accounts for up to 80-90% of the nitrogen loading into the slough. This data shows that nutrient loading within the slough can be exported to the coastal ocean via the plume

Increased concentrations of nitrate correlated with increased concentrations of bacteria-specific FAs. The genus of nitrifying bacteria *Nitrobacter* is characterized by vaccenic acid (18:1n-7) as the main compound with up to 92% of the FAs (Lipski et al., 2001). Our plume samples showed that the mean concentration of vaccenic acid, in addition to the sum of bacterial-specific markers, was almost 4 times higher in our plume samples than in the coastal water samples. Iriate (2003) showed that bacterial production, herbivory, bacterivory and microbial community respiration were markedly high in the upper portions of shallow, tidally-influenced estuaries and that the degree of tidal flushing controlled the spatial variability of microbial abundance, herbivory, and respiration. Therefore, upper portions of the slough, which are less under the influence of tidal advection are likely to be more productive regions in terms of microbial and primary productivity. During extreme (spring and neap) tidal

flushing events, this microbial activity and primary productivity may be exported to the coastal ocean. Our sampling indicates that the average tidal range of 1.9 meters during the wet season was significant for the plume to serve as a mechanism of transport to enhance microbial biomass to the coastal ocean and Monterey Bay.

Results also showed that plume waters generally had higher concentrations of diatoms. This is likely the cause of increased nutrient loading in estuaries, which can lead to an increased abundance of benthic macroalgae and phytoplankton (Evgenidou, 1999). In their study, Evgenidou et al. (1999) showed that diatoms represented the dominant group in all three estuaries that they sampled and appeared in much greater concentrations than dinoflagellates. They indicate that nitrate enrichment in phytoplanktonic communities and higher growth rates may cause the domination of centric diatoms in estuaries. Welschmeyer et al. (2003) showed that the lower slough, near Monterey Bay, is dominated by a rich diversity of coastal phytoplankton including dinoflagellates, cyanophytes, green algae, and a high concentration of diatoms. They also showed that cryptophytes at the upper end of Elkhorn Slough can make up more than 75 percent of all the phytoplankton biomass. Microscopic analysis shows that the planktonic flora of upper Elkhorn Slough is relatively species poor, dominated by only one or two species of cryptophyte. The organically laden and dim light environment of estuaries, in general and Elkhorn Slough, more specifically, provide a suitable growth environment for cyptophytes and they were found in increased concentrations in the plume exiting the slough. Crytophytes have physiological adaptations that allow them to thrive in adverse and light-limited environments. These include photoacclimation to low light environments, mixotrophy, and motility across density gradients (Bergemann, 2004).

As shown here, the biogeochemical constituents of the slough waters are injected into the coastal waters and become entrained in the northward flowing, nearshore current of Monterey Bay (see Chapter 1) and quickly mix with the coastal waters. This flux has several potential consequences for the ecology of the bay. The introduction of bacteria can provide a food source for mixotrophic, dinoflagellate bloom producing populations of phytoplankton, such as *Akashiwo sanguinea* and *Cochlodinium sp.* (Jeong, et al., 2004, Jeong et al, 2005, Kudela et al. in review). Changes in the relative abundance of diatoms, dinoflagellates, and or cryptophytes under increasing nitrogen loading may have important implications for the receiving coastal waters, including influences on food web dynamics and biogeochemical transformation rates. Increased concentrations of CDOM and decreased optical transmission rates due to plume sediment loading change physical conditions (optical clarity) which may favor cryptophyte proliferation and also change the concentrations of specific nutritional fatty acids. As indicative of a mixing environment, Cohen et al., (1988) showed that the level of PUFAs, increases under nonlimiting light conditions. In contrast photo-inhibition and reduced light intensities reportedly lead to an accumulation of triacyglycerols (the major lipid storage product in algae) which is richer in saturated fatty acids and MUFAs. A decrease in PUFAs may have ecological implications for higher trophic levels. PUFAs are essential for optimal physiological performance in higher trophic levels. These essential fatty acids cannot be synthesized by organisms at rate sufficient to meet their basic biochemical requirements and, thus must be obtained through diet (Kainz et al 2004).

In summary, these results present evidence of an important land-sea interaction or biological link between Monterey Bay and the watersheds surrounding Elkhorn Slough. First, there is evidence that microbial activity and nutrient loading in the slough can be exported to the coastal ocean during wet season high tidal pulses.

77

Second, higher concentrations of diatoms and cryptophytes are exported to the coastal ocean via the Elkhorn slough plume. It is likely that the variability in the concentrations of cryptopytes depends on the reach of tidal mixing into the upper slough during extreme tidal exchanges such as spring and neap tides. Also, the mixing of the biologically derived material appears to be intense, on relatively short scale diminishing three-fold within four kilometers of the slough entrance. Finally, the introduction of increased concentrations of SFAs and MUFAs from the slough into the coastal ocean may present important consequences for ecosystem dynamics, such as affecting the dietary quality of foraging fish (Dalsgaard et al., 2003). Similar estuarine lagoons along the mid-latitude regions of North American most likely present similar important biological links across the land-sea interface. As agricultural and urban development, as well as climate change put increased environmental stress on estuaries, more research, monitoring and management efforts should be dedicated to understanding the delicate biogeochemical balance at this important land-sea interface.

CHAPTER 4

AN EVALUATION OF MODIS ALGORITHMS FOR MONITORING ANNUAL
AND SEASONAL PHYTOPLANKTON ABUNDANCE AND DINOFLAGELLATE
BLOOMS IN MONTEREY BAY, CALIFORNIA

4.1 Introduction

Recent advances in satellite and airborne remote sensing, such as
improvements in sensor and algorithm calibrations, processing techniques (Franz et
al., 2006) and atmospheric correction procedures (Wang and Shi, 2007) have provided
for increased coverage of remote-sensing, ocean-color products for coastal regions.
This opened the way for studying ocean phenomena and processes at finer spatial
scales, such as the interactions at the land-sea interface (Warrick et al., 2007), and
coastal red-tide and algal blooms (Ryan et al., 2005; Ryan et al., 2008; and Ryan et al.,
accepted). Human population growth and changes in coastal management practices
have brought about significant changes in the concentrations of organic and inorganic,
particulate and dissolved substances entering the coastal ocean. There is increasing
concern that these inputs have the potential to increase local concentration of
phytoplankton and cause harmful algal blooms (Epply et al., 1979; Anderson et al.,
2002; Spatharis et al., 2007). Evidence of impacts arising from these changes, such as
phytoplankton numbers and relative species abundance, and deep-water oxygen
declines) have been shown to occur more frequently in areas of restricted water
exchange (Jickells, 1998). It is important to utilize these new remote sensing
techniques to characterize the increase of algal blooms that have been documented in
coastal waters (Hallegraef et al., 2003; Hallegraef, 1993) and in upwelling areas
throughout the world (Kahru and Mitchell, 2008).

79

Dinoflagellate blooms in Monterey Bay appear to have increased in frequency and intensity over the last five years. Jester et al., 2008 noted a shift in dinoflagellate abundance in Monterey Bay beginning in 2002, with the relative proportion of dinoflagellates outnumbering other functional groups. Improved techniques of satellite and airborne remote sensing have been used to describe these blooms and how coastal processes have influenced the development, spread and retention of these blooms. Using airborne hyperspectral imagery, Ryan et al., (2005) illustrated the development of dense aggregations of dinoflagellates in water mass and internal wave frontal zones. Ryan, et al. (2008) used snapshots from various hyperspectral airborne sensors, along with images from the Medium Resolution Imaging Spectrometer (MERIS) to illustrate synoptic patterns of "extreme blooms" within the upwelling shadow (Graham and Largier, 1997) of Monterey Bay, which at times is an area of increased water residence time and reduced circulation. In their study, they also used MERIS imagery to produce long-term statistics to quantify extreme bloom intensity and identify a bloom incubation region within the northern waters of Monterey Bay. Ryan et al., (accepted) examined how the bay's bloom incubation area can interact with highly variable circulation to cause red-tide spreading, dispersal and retention. This examination used multiple remote-sensing and in situ data, including snapshots or daily images from the Moderate Resolution Imaging Spectrometer (MODIS).

In these studies of Monterey Bay, airborne and satellite imagery have been mainly used to provide snapshots of measuring the abundance of microscopic algae and to describe bloom processes. Another important element of understanding blooms is to develop an understanding of statistically significant, long-term patterns of phytoplankton abundance and potential variability of bloom activity in the bay. No published reports have examined the applicability of MODIS for looking at variability

of annual patterns of abundance and bloom activity in Monterey Bay. A limited number of studies have been published on the interpretation of satellite ocean-color imagery and the applicability of currently used satellite algorithms for the coastal waters of Monterey Bay. Due to the limited resolution of satellite sensors and atmospheric correction techniques, much of the work has focused on offshore in studies of the California Current system. Kudela and Chavez (2000) used satellite observations from the sea-viewing wide field-of-view sensor (SeaWiFS) to assess the impact of coastal runoff on biological and bio-optical properties of the coastal waters of central California during an El Nino year. They observed a 5-fold increase in SeaWiFS-derived chlorophyll concentrations, with a corresponding color dissolved organic matter (CDOM) extending 300 km offshore. The results demonstrate that during an El Nino event, the potential influence of riverine input on the bio-optical properties of the coastal ocean can extend far into the California Current system. Chavez (1995) used in situ and satellite-derived chlorophyll to assess the productivity of the California Current System and the Peru Current System, showing that while satellite and in-situ measurements yielded similar estimates for chlorophyll off California, the satellite yielded substantially lower concentrations off Peru. Kahru and Mitchell (2001), used chl a concentration derived from SeaWiFS and the Ocean Color and Temperature Scanner to evaluate the large-scale changes in surface patterns in the California Current. They detected significant increases in both chlorophyll and CDOM off central and southern California during the La Nina year of 1999 and identified statistically significant increasing trends of chlorophyll and CDOM from October 1996 to June 2000. These large-scale studies have contributed enormously to understanding patterns and variability of productivity of regional ecosystems. Satellite studies, along with regional ocean-observing systems have resulted in economic benefit for recreational activities including recreational fishing and boating, beach

81

recreation, maritime transportation, search and rescue operations, spill response, marine hazards prediction, offshore-energy, power generation, and commercial fishing (Kite-Powell, 2008).

The purpose of this chapter is to explore the utility of standard MODIS products, utilizing recently developed atmospheric correction capabilities of the high resolution NIR-SWIR bands, to understand phytoplankton and dinoflagellate bloom variability in Monterey Bay. The goals include: 1) to determine which standard product best quantifies phytoplankton biomass 2) to describe the spatial and temporal (inter-annual and seasonal) variability of these patterns using this product, and 3) to compare resulting annual and seasonal patterns to variables which may influence this productivity, including land-sea interactions. It is important to reiterate here that the point of this research was not to optimize algorithms to match local conditions (described below), but to provide an assessment of how well the commonly available products perform.

4.1.1 MODIS algorithms

We examined three algorithms that are MODIS standard output products using the SeaDAS software: two chlorophyll *a* (chl a) concentration algorithms (OC3M and Carder bio-optical model) and the chlorophyll fluorescence line-height product (O'Reilly, 2000; Carder et al., 1999; Letelier and Abbot, 1996). We considered these different algorithms because of the variability of oceanographic conditions that may cause different water types to be found in Monterey Bay. In general, oceanographic variability in Monterey Bay can be characterized as having three climatological periods: a spring/summer "upwelling" season, a summer/fall "oceanic" season and a "winter" Davidson Current season (Pennington and Chavez, 2000; see Chapter 1).

During any of these seasons, this open bay can be flushed by the oceanic waters of the California current (Ryan et al., 2005; Ryan et al., 2008b; Graham and Largier, 1997). These flushing events introduce Case-1 waters in which optical properties are dominated by chlorophyll and associated and covarying detrital pigments. During the winter months, rivers drain into the coastal ocean and introduce particulate and dissolved material which do not covary with chlorophyll (Case-2 waters). Waters that enter Monterey Bay during the upwelling period may introduce different particle size distributions of phytoplankton (Eisner and Cowles, 2005). During spring wind-driven upwelling of the turbid bottom boundary layer can result in Case-2 waters within and around the bay. During the fall, land flushing enhanced by rainfall significantly increases the occurrence of Case-2 waters during the same period in which dinoflagellate blooms occur most frequently. This optical complexity will influence remote sensing algorithm performance.

The MODIS FLH (fluorescence line height) linear baseline algorithm measures the the height of the reflectance peak caused by chlorophyll fluorescence in Case-1 waters. MODIS bands 13, 14, and 15, centered at 665.1, 676.7 and 746.3 nm, respectively with 10 nm band-width are used to estimate the FLH. The calculation estimates the difference between observed radiance for band 14 and a value at band 15 found by linearly interpolating between the radiances for bands 13 and 15 (Letelier and Abott, 1996). This can be written:

$$FLH = L_{14} - kL_{13} - (1 - k)L_{15}$$

where

Li = Radiance in Band i

and

$$k = (746.3 - 676.7)/(746.3 - 665.1)$$

for MODIS bands.

Fluorescence is one of the three energy release pathways, after the radiation of direct sunlight is absorbed by phytoplankton. The spectral feature of this fluorescence is well known and has a peak centered at 683nm (Letellier and Abbot, 1996; Babin et al., 1996). These features are usually approximated by a Guassian shape with a full width at half maximum (FWHM) of 25 nm (Gower et al., 1999). The FLH algorithm relies on a relatively narrow spectral region in the red portion of the spectrum, reducing the demands on sensor and atmospheric correction to produce accurate retrievals of water leaving radiance across the visible spectrum. This signal provides an alternative means of measuring chlorophyll concentrations and gives additional information on phytoplankton. Neville and Gower (1977) pioneered the measurement of sun-stimulated fluorescence from aircraft and their work prompted plans to develop the MODIS sensor to measure this signal. The amount of emitted fluorescence signal is expected to vary with variation in chl a pigment concentration, but it is also influenced by photoinhibition, phytoplankton species composition, physiological state, nutrient availability, light history and temperature (Kiefer, 1973; Falkowski and Kiefer, 1985). Fluorescence efficiency might vary across various water types.

The FLH algorithm has been used in place of empirical and semi-analytical band-ratio algorithms because it is less sensitive to interference caused by the presence of other absorbing suspended matter commonly found in surface waters and it does not saturate at high chlorophyll concentrations as do algorithms that rely on radiance measurements in the blue portion of the electromagnetic spectrum. Fluorescence-based algorithms tend to reliably estimate in situ chl a concentrations (from 0.1 to 82 mg m^{-3}), whereas standard spectral-ratio algorithms often give inconsistent estimates, probably caused by the interference of inorganic sediment and dissolved organic matter in these waters (Ahn, 2007). In coastal waters, the fluorescence signal can overlap with a strong NIR elastic scattering peak. The overlap occurs due to the confluence of strongly decreasing algal absorption, increasing water-absorption and density dependent scattering by phytoplankton cell structures (Schalles, 2006; Gilerson et al., 2007, Dierssen et al., 2006). When phytoplankton are present in high concentrations, strong scattering can cause the spectral peak to shift from 683 to between 700 and 710 nm. This measurement can be a particularly important for monitoring blooms in Monterey Bay because it succeeds in obtaining valid retrievals when the chlorophyll algorithms fail. Given the drawbacks of using the empirical and semi-analytical algorithms, which rely on absorption and reflectance in the blue green portion of the Electromagnetic Spectrum (EMS), FLH might provide a better alternative to study dinoflagellate bloom phenomena.

The MODIS OCM3 algorithm is a global, empirical algorithm that utilizes the spectral response in the blue and green portion of the electromagnetic spectrum to estimate surface-water chlorophyll concentrations. As chlorophyll concentrations in surface waters increase, reflectance in the blue portion of the EMS decreases dramatically, while reflectance in the green portion of the EMS decreases more

slowly. This is due to the presence of accessory pigments, which dominate absorption in the blue portion of the EMS. This empirical algorithm was derived from the regression of coincident ship and satellite observation of water-leaving radiance against shipboard observations of chl a. The algorithm was parameterized with an in situ data set (n = 2,853) and is described in O'Reilly et al. (2000). The chl a values in the in situ data set range from 0.008 - 90 mg m^{-3}

The MODIS OC3M algorithm can be written as:

$$\log_{10}(CHL) = 0.283 - 2.753R + 1.457R^2 + 0.659R^3 - 1.403R^4$$

where

$$R = \log_{10} R_{rs}(\lambda_{443})/R_{rs}(\lambda_{550}) > R_{rs}(\lambda_{490})/R_{rs}(\lambda_{550}).$$

This algorithm is an analog to the OC2 and OC4 algorithms developed for the Sea-viewing Wide Field-of-view Sensor (SeaWiFS). The OC algorithms have been used most extensively to characterize global chl a concentrations in case-1 waters. Since MB can, at times be characterized as having case-1 waters, I examined this algorithm. It is also the default chl a concentration product for the MODIS sensor. The OC algorithms were derived using an in situ data set with the approximate range of 0.01 < Chl < 75 mg m^{-3}. Generally, retrieved values much lower than 0.01 or higher than 100 mg m^{-3} are not trusted (Jeremey Werdell, Pers com).

In contrast to empirical algorithms, semi-analytical algorithms combine theoretical models of the relation of remote-sensing reflectance to backscatter/absorption ratios with empirical models of the dependence of absorption

and backscatter on oceanic constituents. Since these algorithms yield a set of simultaneous equations for quantities, such as chlorophyll concentration and CDOM absorption, this allows chlorophyll to be retrieved from both case-1 and case-2 waters. The Carder bio-optical model is a semi-analytical, bio-optical model of remote-sensing reflectance, $R_{rs}(\lambda)$, where $R_{rs}(\lambda)$ is defined as the water-leaving radiance, $Lw(\lambda)$, divided by the downwelling irradiance just above the sea surface, $E(\lambda,0^+)$. In the analytical approach, radiative transfer theory provides a relationship between upwelling radiance and the in situ constituents . Then, constituents and concentrations are derived from irradiance or radiance values measured at several wavelengths (Carder et al., 1999). This algorithm takes into account three different bio-optical domains: 1) high photoprotective pigment to chlorophyll ratio and low self-shading, or "unpackaged"; 2) low photoprotective pigment to chlorophyll ratio and high self shading, or "packaged;" an 3) a transitional or global average type. These domains are identified from space by comparing sea-surface temperature to nitrogen depletion temperatures (Kamykowski, 1987), the temperature above which nitrate concentration becomes negligible and indicates where a major transition in types of phytoplankton for each domain occur (Carder, 1999). Comparing SST to the nitrate-depletion temperature as an indicator of nutrient availability provides a space-based cue for evaluating whether upwelling or convective overturn has replenished the surface waters with nutrients from below the surface mixed layer. This changes the species and pigment composition of the phytoplankton assemblage observed, thus requiring adjustments in $a^*_{ph}(\lambda)$. These adjustments also compensate for the pigment-package effect whereby increased cell size and pigment per cell decreases $a^*_{ph}(\lambda)$ (Morel and Bricaud, 1981). Carder et al. (1999) showed that algorithm errors of 45% were reduced to 30% with this approach, with the greatest improvement occurring at the eastern and polar boundaries of basins.

The Carder algorithm development was initially focused on tropical, subtropical, and summer temperate environments and case-2 conditions; however, has evolved to accommodate global datasets (Carder et al, 2004). This case-2 algorithm is applicable in waters where other substances, which do not covary with chlorophyll, affect the optical properties. Such substances include gelbstoff, suspended sediments, coccolithophores, detritus, and bacteria. Since MB at times can exhibit qualities of case-2 waters, I examined this algorithm. Both of the OCM3 and the empirical portion of the Carder bio-optical model products as provided through SeaDAS processing were developed for global applications and are based on the NASA Bio-Optical Marine Algorithm Data set (NOMAD) (Werdell and Bailey, 2005).

4.2 Data and Methods

4.2.1 In situ measurements

Ground truth measurements of chlorophyll concentrations were used to assess the accuracy of the MODIS chlorophyll algorithm described above. The Biological Oceanography group at the Monterey Bay Aquarium Research Institute has been taking extracted chlorophyll measurements at three time-series stations in Monterey Bay and adjacent waters from 1989-present (Chavez et al., 2002). Time series cruises occurred at approximately 21 days intervals. Chl a and phaeopigments were determined by the fluorometric technique using a Turner Designs Model 10-005 R fluorometer that was calibrated with commercial chl a (Sigma). Samples for determination of plant pigments were filtered onto 25-mm Whatman GF/f glass fiber filters and extracted in 90% acetone in a freezer for between 24 and 30 hours (Vernick and Hayward, 1984). Other than the modification of the extraction procedure, the method used is the conventional fluorometric procedure of Holm-Hansen et al. (1965)

and Lorenzen (1966). Two other data sets were used to increase the number of in situ measurements in the Bay, those from the Center for Integrated Marine Technologies (CIMT) shipboard data (http://cimt.ucsc.edu) and those from Coastal Ocean Applications and Science Team (COAST) field surveys of 2006. Chlorophyll a values in these data sets were determined by the same techniques as above.

I applied the MODIS FLH algorithm to in situ reflectance spectra and compared these results to in situ chlorophyll measurements in order to quantify algorithm values across a range values. A hyperspectral tethered spectral radiometer buoy (HTSRB; Satlantic Inc.) was used to measure downwelling spectral irradiance above the sea surface $E_d(0^+)$ (350-800 nm, 2.5nm bandwidth) and upwelling radiance L_u at 0.7 m below the sea surface. The Satlantic sensors were factory calibrated prior to sampling. Collected radiometric data were processed using Satlantic's Prosoft software package according to manufacturer protocols. No dark corrections or self-shading corrections were applied to these data.   The HTSRB was deployed at specific stations in conjunction with discrete water samples for in situ chl a, determined using the methods described above. These spectra and chl a measurements were within the geographic limits of the Bay and were taken during a red-tide event on September 21 and 22, 2006. The FLH algorithm was applied to the in situ reflectance spectra to quantify the relationship between FLH and extracted concentrations over a range of surface chlorophyll values typical of dinoflagellate blooms.

4.2.2 Satellite data

Six years (2002–2007) of daily MODIS L1A data were downloaded from the L1 and Atmospheric Archive Distribution System (LAADS Web) at the Goddard

Space Flight Center. The MODIS data were processed from Level 1A using the SeaDAS software, by applying calibrations for ocean remote sensing developed by the MODIS Ocean Biology Processing Group (OBPG). The OBPG is responsible for the production and distribution of the ocean color data products from the MODIS sensor on Aqua and optimizes MODIS ocean color data by updating SeaDAS look up tables (LUTs). The LUTs are derived from analysis of the MODIS solar diffuser measurements, lunar observations, and on board lamps.   Additional improvements in the data products result from enhancements in the sensor calibration, atmospheric correction, and improved bio-optical algorithms.

Of the over 3050 files downloaded from the LAADS web and processed to level 1A, only 1369 contained coverage and contained some cloud free areas in the search region. Of the 1369 files, 673 files or 49% were deleted due to scene contamination by cloud edges or severe distortion by extreme sensor scan angles. The remaining 696 images were processed to mapped Level 3 chlorophyll *a* and chlorophyll fluorescence products. For the atmospheric correction required to derive products (FLH, chlorophyll), we computed true 250-m aerosol retrievals, extrapolated to the visible from the 859 nm band using a fixed aerosol model (maritime 90%) (Kahn et al., 2001; Franz et al., 2006). Resulting image data were mapped to a cylindrical projection. The true resolution of FLH, chlorophyll images are at best ~ 1 km at nadir; bilinear interpolation was used to generate 500 m resolution images. Images were further quality controlled, and those images containing cloud contamination or severe distortion from low scan angle were removed from the analysis.

As recommended by Bailey et al., (2002) satellite / in situ matchups were constrained to maximum 3-hour time offset. Pearson's correlation coefficients between the predictor variables (satellite algorithm) and the single common dependent variable (in situ) were computed. A test of heterogeneity among all coefficients and a confidence interval test for comparing each possible pair (FLH-OC3M, FLH-Carder, OC3M-Carder) of correlations were also conducted (Meng et al, 1992). The Fisher z transformation was applied to the correlation coefficients prior to testing to improve the normality of the correlation coefficients (Fisher, 1915). The superior performance of this transformation has been confirmed by Neill and Dunn (1975) and Stegier (1980). Long-term (2002-2007), annual and seasonal (oceanic, upwelling and winter) averages of daily imagery were produced for each product.

To examine forcing processes influencing the variability of observed chl a and fluroescence patterns, spatial means for Monterey Bay were then compared to upwelling indices, land-based nutrient measurements and cumulative wind stress. On a monthly basis, the Pacific Fisheries Environmental Laboratory generates indices of the intensity of large-scale, wind-induced coastal upwelling at 15 standard locations along the west coast of North America (Bakun, 1973). The indices are based on estimates of offshore Ekman transport driven by geostrophic wind stress. Geostrophic winds are derived from six-hourly synoptic and monthly mean surface atmospheric pressure fields. The pressure fields are provided by the U.S. Navy Fleet Numerical Meteorological and Oceanographic Center, Monterey, CA. Average annual and seasonal averages were calculated for 2002-2007. Land-based nutrient measurements are based on averaged measurements taken by the LOBO L01 mooring in the main channel of the Elkhorn Slough. Nitrate was measured by an in situ ultraviolet spectrophotometer (ISUS) (Johnson and Coletti, 2002). Hourly nitrate data of surface

waters (0.5 m) were downloaded from the LOBO Network Data Visualization (LOBOViz 3.0) (http://www.mbari.org/lobo/loboviz.htm) website. Data processed from these stations spanned the years 2004-2007. Annual seasonal averages were calculated from these data. Cumulative wind stress was calculated by summing the square of the V component of wind stress. Wind stress data were downloaded from the MBARI live access server (see Chapter 2). Seasonal averages were calculated for each of the environmental data sources for each year.

4.3 Results

4.3.1 Water optical properties

Upwelling radiance plots of in-water spectral measurements taken in dinoflagellate bloom waters and their corresponding extractive chlorophyll concentrations are shown in Figure 4.1. This data illustrates the shift in the peak from a fluorescence-based signal (683nm at 13 mg m^{-3}) to one dominated by an NIR peak due to elastic scattering by more highly concentrated dinoflagellate populations (700nm at 42 mg m-3) . Although the FLH algorithm is meant to measure the fluorescence peak at 683 nm, it is shown here that FLH algorithm can capture the shoulder of the shifting spectral peak produced by elastic scattering in the presence of elevated concentrations of dinoflagellates. The FLH measurement reasonably approximates the in situ chl a measurements ($r^2 = 0.72$). The spectra also maintain a persistent trough at ~665 nm, which provides a consistent anchor point for the FLH algorithm baseline. Extractive chlorophyll measured coincidently with spectral measurements in waters of ruddy discoloration show a chl a range between 13 to 42 mg m^{-3}.
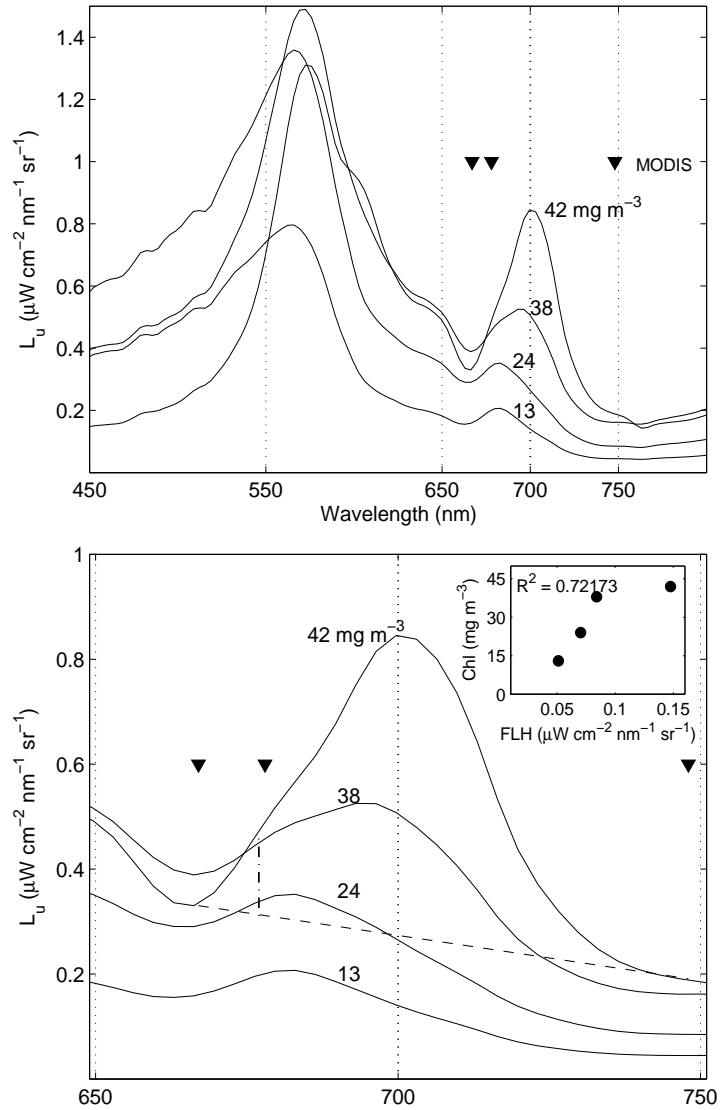
Figure 4.1: (Top panel) Spectral variability in water-leaving radiance (Lw) measured by an HSTRB in a red-tide bloom with increasing chl a concentrations (13, 24, 38 and 42 mg m^{-3}). The downward facing triangles show the center wavelengths of the MODIS bands used for fluorescence determination using the FLH algorithm. The bottom panel shows the same data, but only at the spectral range of 650 to 750 nm. The dashed lines show the FLH baseline and the measurement of the spectral peak above the baseline for spectra corresponding to a chl a concentration of 42 mg m-3. The inset shows the relationship and correlation between FLH calculated from the in situ spectra against the in situ chl a measurements.

4.3.2 *Extractive Chlorophyll and MODIS Algorithm Performance*

Due to varying sensor algorithm thresholds and quality flags, the number of extractive in situ points that matched with satellite coverage varied. Overall, the in situ chl a values ranged from 0.62 to 100.9 mg m^{-3} and the mean in situ measurements between the different algorithms were within a comparable range, 5.3, 5.2 and 6.5 mg m^{-3} for the corresponding matching points as determined by the FLH, OC3M and Carder algorithms. The relative frequency distribution of the log(chl a) measurements did not show a normal distribution and had a primary peak between log 0 to 0.5 mg m^{-3} and secondary peak at log 1 to 1.5 mg m^{-3} (Figure 4.2). This is largely due to the fact that the sampling effort of the BOG database targeted the vicinity of the M1 time series station at the mouth of the bay to coincide with satellite overpasses. Seventy-seven percent of the matched in situ observations of chl a were less than 5 mg m^{-3} and 94% observations less than 10 mg m^{-3}.
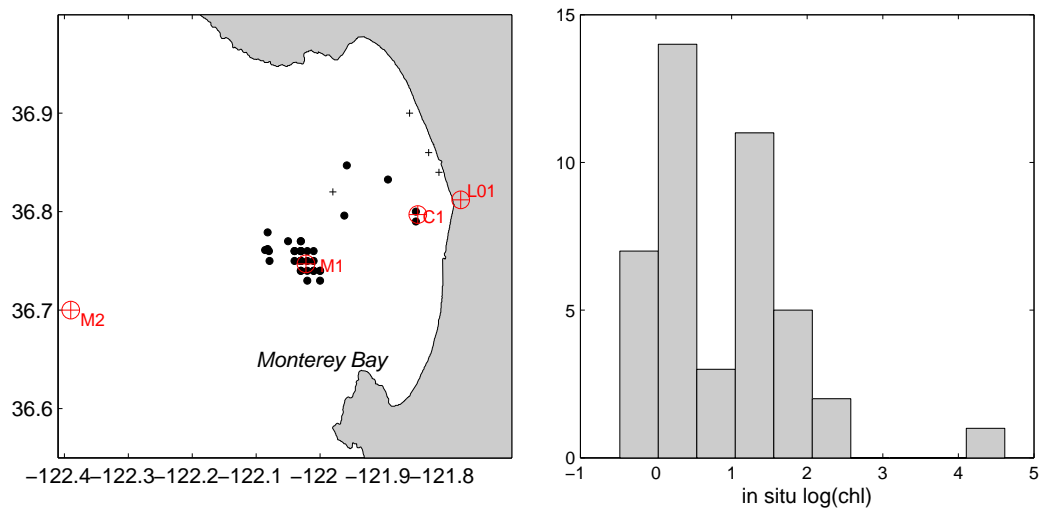
Figure 4.2: Left panel, the location of extractive chlorophyll sampling location (dots) and in situ spectral measurements (crosses). The location of time-series mooring locations as red markers. Right panel, the frequency distribution of log-transformed in situ chl a data.

The correlation is higher between FLH and in situ chl a than either the OC3M and Carder algorithms (r = 0.71, n = 43, Chl = 180*FLH-0.77) (Figure 4.3). However, tests of the equality of the correlation matrices (Meng et al., 1992) indicate that the correlations are not significantly different. The equality test first compares correlations between two or more predictor variables (FLH, OC3M and Carder) with a common dependent variable (in situ). The matchups were first reduced to similar sample sizes, including only those satellite / in situ pairs which occurred in all sets. In the reduced data set, correlations were relatively similar as the full datasets (r = 0 .71, r = 0.61 and r = 0.65 for FHL, CHL and Carder, respectively , n = 30). The test is a chi-squared test which can readily test the significance of the "heterogeneity" of the variables, or the degree to which the three correlations differ significantly among themselves. The calculated chi-squared result was less than the critical value at the 95% confidence interval (p > 0.5), an indication that all correlation coefficients are almost equal. Meng et al., (1992) derivation of Hotelling's t-test to compare individual pairs of correlation coefficients, which have a single common dependent variable was
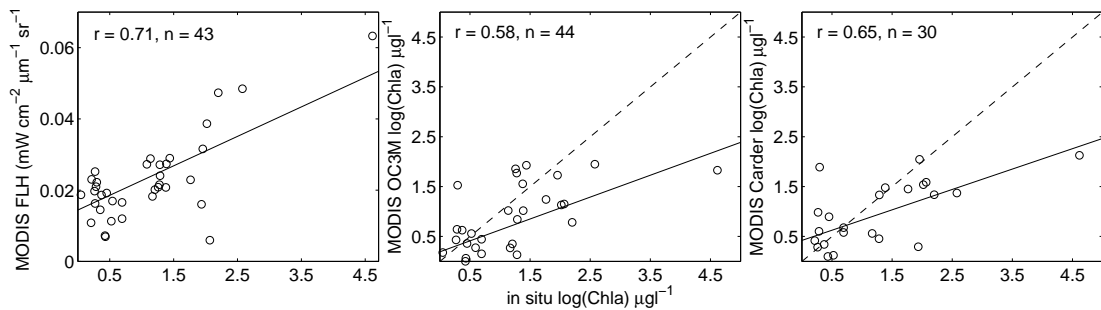
Figure 4.3: The relationships between FLH (left) OC3M chl a (middle) and Carder chl a (right) and log in situ chl a concentration. The best-fit line (solid) and the 1:1 line (dashed) are superposed.

then applied. The null hypothesis for Meng et al. (1992) test can be stated as such: Ho: correlation coefficients do not differ significantly. The result is a Z-statistic. For each of the pairs of correlations, the computed test statistic resulted in a p-value greater than the alpha value of 0.05. This indicates that the observation is consistent with the null hypothesis. The correlation coefficients do not differ significantly.

The correlations between in situ and derived chl a from OC3M and Carder algorithms are similar to those found in a comparable study in Monterey Bay (Kudela and Chavez, 2000). When the in situ data set and concurrent satellite matchup is reduced to represent only measurements less than 10 mg m^{-3}, the correlation between FLH and in situ chl a is less than the correlation between in situ measurements and chl a algorithm products (r = 0.48, 0.50 and 0.58 and n = 41, 42 and 28 for FLH, OC3M and Carder algorithms, respectively). Again the test of equality indicates no significant difference between the correlations ($p > 0.05$), suggesting that two data points in the in situ data set > 10 mg m^{-3} potentially drive the differences in correlation, while their ability to predict in situ chl a concentration is similar.

Estimates made by the OC3M algorithm appear to be higher than those provided by the Carder algorithm. The range in values were much greater for OC3M algorithm (0.442 – 174.89) than those of the Carder algorithm (0.0083- 27.36). For the higher values of chlorophyll, the OC3M algorithm frequently overestimated chlorophyll concentrations and in such cases the Carder algorithm produced no result. The Carder algorithm may do a better job of filtering out erroneous or over estimates.

Using three time-series stations, offshore station M2, M1 at the mouth of the bay, and C1 in the nearshore waters of the Bay, I compared mean in situ data to means

of the time series for each of the satellite products to understand which algorithm best characterized magnitudes in cross-shore gradient. Mean data from the BOG database at stations C1, M1, and M2 (n = 144, n = 115, n = 97) and the mean of a five pixel box size around each of these time series stations from the satellite imagery (n = 696) were compared (Table 4.1). In the nearshore waters, the mean, as measured at station C1 by the OC3M algorithm, overestimated the in situ measurements. The Carder algorithm did a much better job of estimating mean chl a in nearshore waters and at the offshore station M2. At station M1, in the mouth of the Bay, the OC3M algorithm performed better than the Carder algorithm. Overall, however, the correlation between the in situ

Table 4.1: Mean fluorescence and chl a concentrations at time series stations C1, M1 and M2 from in situ and satellite measurements.

Time-Series Station	In situ (mg m^{-3})	FLH	OC3M (mg m^{-3})	Carder (mg m^{-3})
C1	5.9	0.0284	11.1	5.6
M1	4.4	0.0226	3.8	2.9
M2	2.6	0.0202	2.0	2.5

and algorithm means across the offshore gradient correlated best with the FLH results (r = 0.96, r = 0.93, r = .90 for FLH, OC3M and Carder algorithms, respectively). In this case, an insufficient number of samples (n < 3) prohibits the comparison of the correlation coefficients (Meng et al, 1992).

4.3. Spatial and Temporal Variability

The spatial pattern in the long-term means of MODIS OC3M and Carder chl a products both show a shoreward increase of chl a concentrations, with the highest concentrations occurring as narrow strip along the coast of the northern Bay (Figure 4.4). The mean chl a estimated using the OC3M algorithm were generally higher than the estimations using the Carder algorithm. The mean of the FLH product shows a different spatial pattern with the highest signal dominating the northern half of the Bay. Smaller patches of high fluorescence signal occur in the southern and northwest
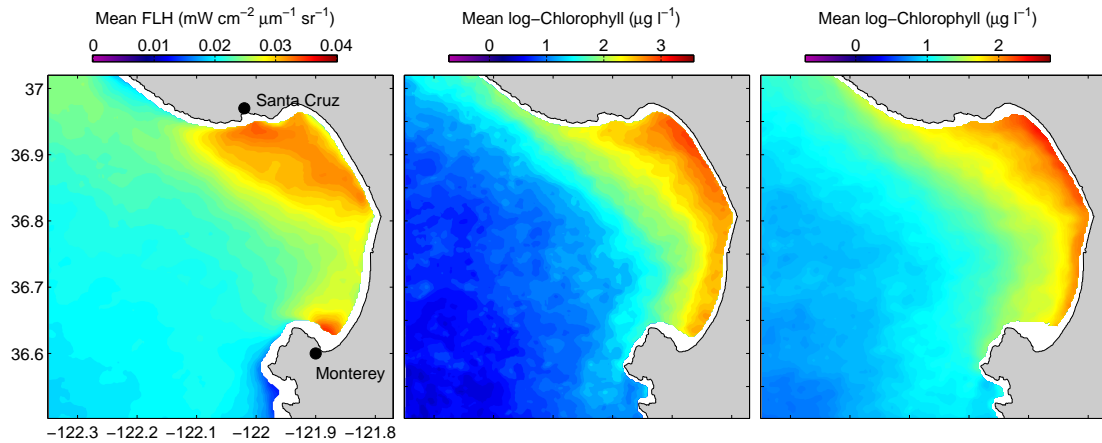
Figure 4.4: Mean FLH (left panel) and chla concentration composites from the OC3M (middle panel) and Carder bio-optical (right panel) for daily MODIS imagery from 2002-2007.

portions of the Bay, near the cities of Monterey and Santa Cruz. Within the northern Bay a diagonal stripe of higher signal appears to connect the nearshore area of the middle to the northwest corner of the Bay. The FLH signal does not suggest that there are higher concentrations of chl a hugging the coast in the northern Bay as they do in the means of the chl a algorithms.

The seasonal patterns of chl a concentration in Monterey Bay are illustrated by MODIS images averaged during the oceanic, upwelling and winter oceanographic seasons (Figure 4.5). All products generally suggest that the highest concentrations of chl a and fluorescence signal occur during the oceanic period (August-November), with the upwelling period (March- July) being the next season with the highest concentration of biomass. The lowest concentration of chl a and fluorescence signal occurs during the winter (December - February). Both the OC3M and Carder chl a algorithms show similar spatial patterns, a shoreward increase of chl a concentrations with the overall algal abundance decreasing in intensity between oceanic, upwelling and winter seasons, although the Carder algorithm has a lower overall mean than the OC3M algorithm.

Elevated concentrations of phytoplankton are evident in the northern portion of Monterey throughout all of the seasons. The lowest concentration of chl a appear offshore to the southwest of the entrance of Monterey Bay during winter. The seasonal FLH signal suggest a different spatial pattern than those illustrated by the chl a products. In the oceanic season composite, the highest FLH signal appears in the northern Bay and as a small patch in the southern Bay. A line of high FLH signal extends from the neashore region of the mid-Bay to the northwest corner of the Bay near Santa Cruz. This patch of high fluorescence, which appears relatively close to shore during the oceanic period moves offshore in the upwelling season composite. The winter months are characterized by a low FLH signal.

The interannual signal of FLH during the oceanic period appears in Figure 4.6. The oceanic season is also a period of interest due to the recent proliferation of dinoflagellate blooms in Monterey Bay (Jester, in press) and the FLH signal has been

99
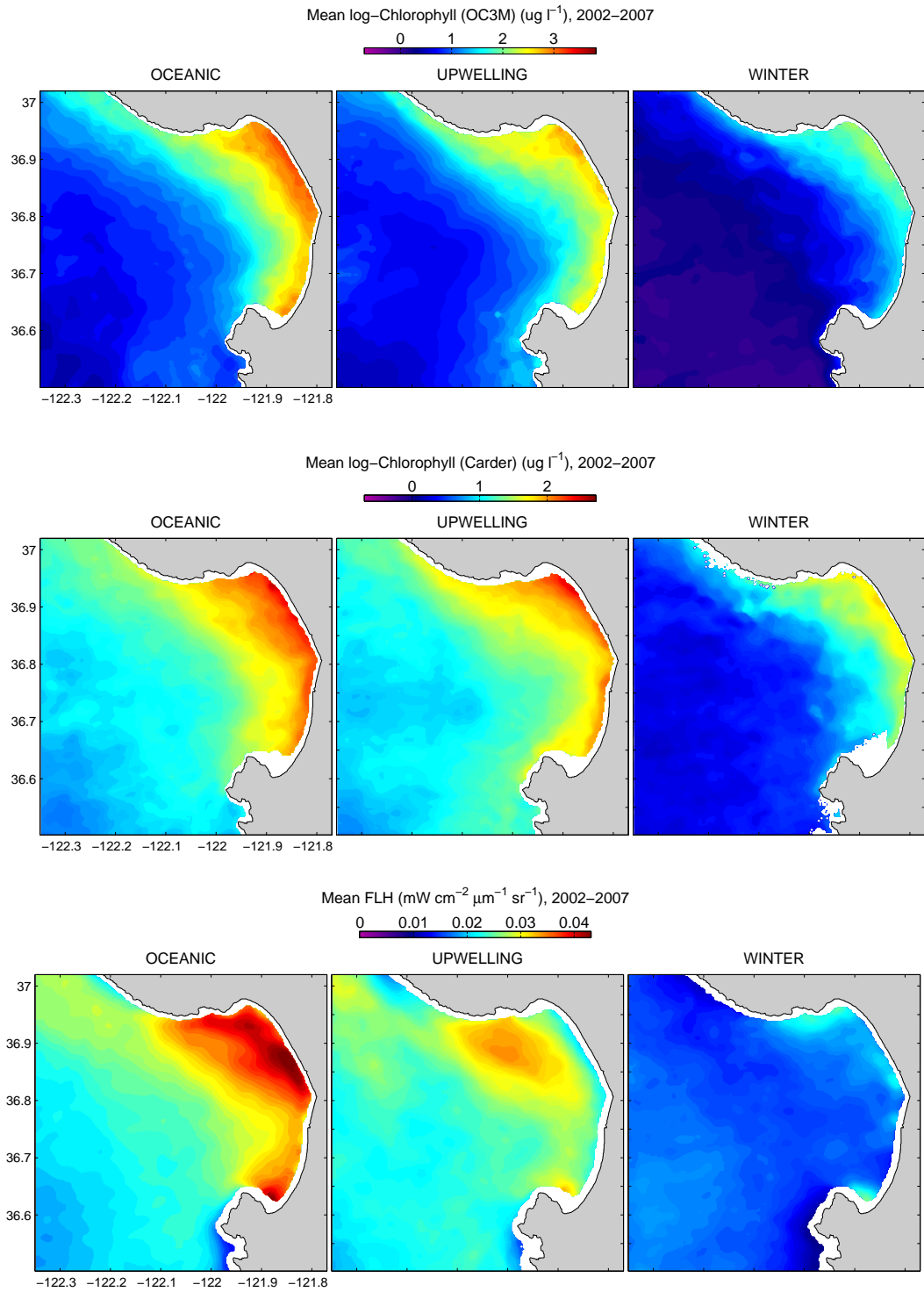
Figure 4.5: Seasonal (oceanic, upwelling and winter) patterns of chla concentrations (2002-2006) using the OC3M (top), Carder bio-optical model (middle) and Fluorescence Line Height (bottom) algorithms.
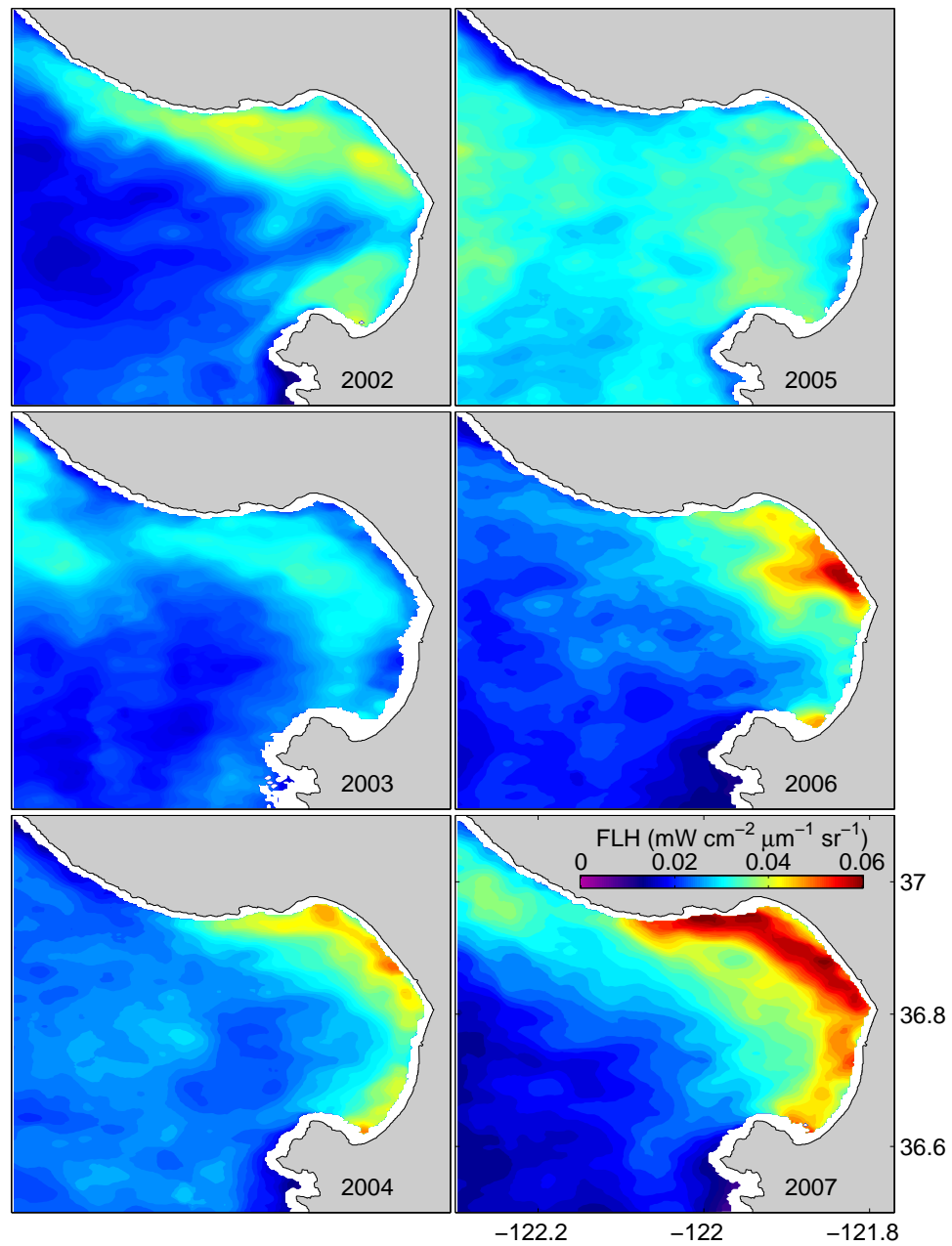
Figure 4.6: Interannual variability of phytoplankton fluorescence as measured by the MODIS FLH algorithm during the oceanic period (August-November) for Monterey Bay.

used to describe and trace dinoflagellate blooms (Hu et al, 2005). Generally, during the oceanic period between the years 2002-2007, the highest FLH signal occurs in the northern Bay, with evidence of a small patch of high FLH in the pocket of the southern Bay near Monterey. The highest Bay-wide signal occurred in 2006 and 2007. In 2002, 2006 and 2007, a high FLH signal appeared in the middle of the Bay near the mouths of the Elkhorn Slough and the Pajaro Rivers. This patch appears to extend in a northwesterly direction. In 2002 and 2003, the patch of high FLH extended from the mid-Bay past Santa Cruz with evidence of some of the signal being exported from the Bay. Both in 2004, 2006 and 2007, the mean signal does not extend past the northwestern most corner of the Bay, suggesting a retention of algal biomass during those years. Overall, there was a very low signal throughout the entire Bay in 2003 and 2005.

In an effort to understand what drives the interannual patterns of variability, I examined relevant environmental variables that are commonly monitored in Monterey Bay and Elkhorn Slough against the mean FLH signal within a box drawn around the outer limits of the Bay (Figure 4.7). The lowest oceanic period upwelling index which occurs in 2004, did not match up with the lowest bay-wide FLH signal, but it did coincide with the retention pattern of the FHL signal in the northern Bay. Consequently, the next lowest mean upwelling index, which occurs in 2007, shows a similar retention pattern but a much higher bay wide FLH signal. Cumulative wind stress during the oceanic period was highest in 2003 and 2004 and generally related to a low mean FLH signal. The bay-wide spatial patterns in 2003 and 2004 were characteristic of both the export and retention spatial patterns. Nutrient monitoring in the Elkhorn Slough, the main land-sea connection in Monterey Bay has only been in operation since 2004. The highest mean nutrient level during the oceanic period taken
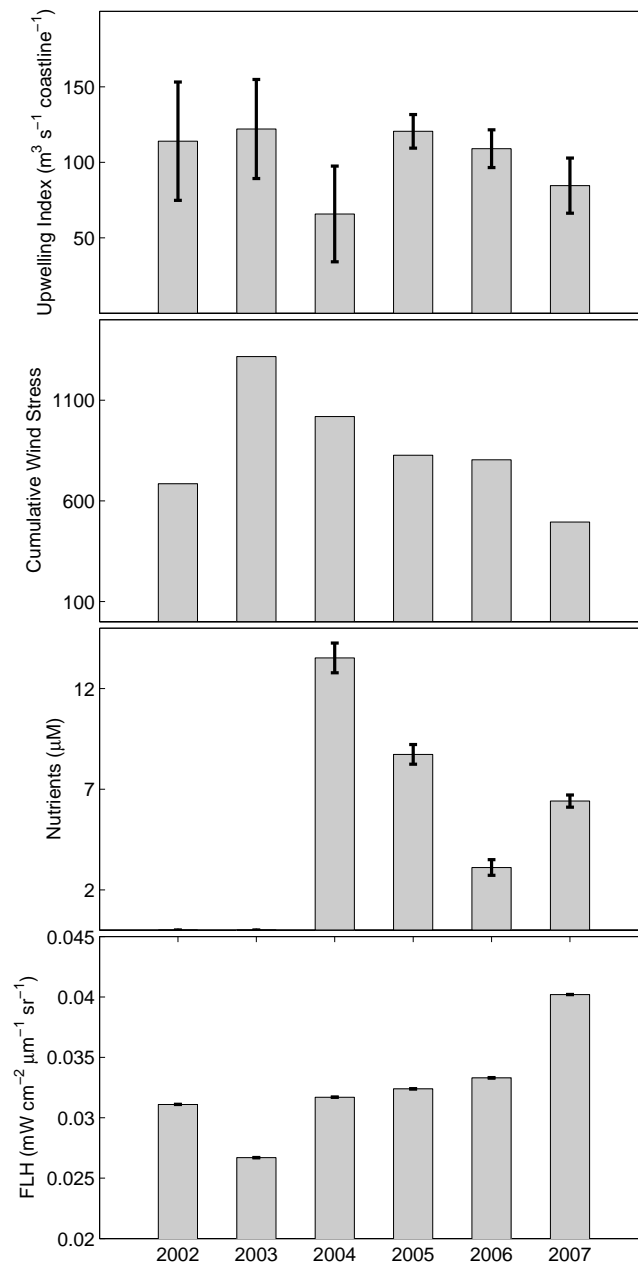
Figure 4.7: Annual oceanographic season means of environmental variables used to describe oceanographic phenomena in Monterey Bay. Mean upwelling index (top), cumulative wind stress at the M1 mooring (middle top), nitrate at the Elkhorn slough L01 mooring (middle bottom) and mean FLH derived from MODIS satellite imagery bottom).

at the L01 mooring occurred in 2004 and decreased to > 7 µM in 2005 and ~ 3 µM in 2006. The mean concentration then increased in 2007 back up to < 7 µM. The mean Bay-wide FLH signal did does not seem to match clearly with mean concentrations of nitrate measured at L01; however, the spatial pattern of FLH, especially in 2002, but also in 2006 and 2007, suggest a link between the mid-Bay, in the vicinity of the Elkhorn Slough, and transport in a northwesterly direction to the northern Bay. Representative drifter tracks, which mark the surface transport of outflow from the vicinity of the mouth of the Elkhorn Slough and the Pajaro River, indicate the highest signal of FLH during the oceanic period in the wake of these land-based sources of input (Figure 4.8).
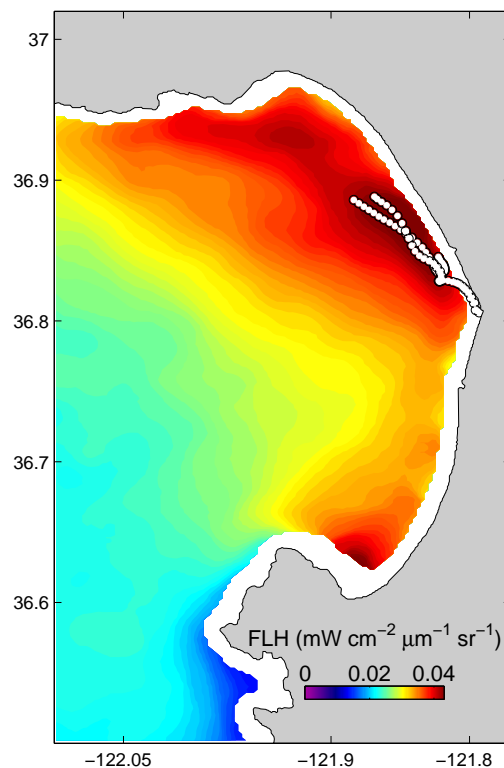
Figure 4.8 Mean oceanographic season FLH signal (2002-2006) with drifter tracks deployed at the Elkhorn Slough and Pajaro Rive mouths superimposed. The drifter tracks follow the highest FLH signal representing the highest phytoplankton abundance.

4.4 Summary

Chlorophyll-a concentrations derived from satellite remote-sensing images of ocean color provide a unique synoptic view of marine ecosystems. This information is of high relevance as it increases our understanding of ocean biogeochemistry, harmful algal blooms and fisheries. Another major value of ocean color lies in the long-term monitoring of the marine environment, which will improve the understanding of ecosystem functioning and help assess the response to anthropogenic pressures such as agriculture, urban development and global change. There are different types of algorithms which can be used to derive the proxies for phytoplankton biomass, which rely on various spectral properties of the upwelled radiance of the ocean surface. There are those which depend on the reflectance characteristics of the blue and green portion of the electromagnetic spectrum, either derived through regression of coincident ship and satellite observations or those which use a combination of theoretical and empirical models, where empirical relations allow the algorithm to adapt to change with season, geography and sea-surface temperature. Other algorithms rely on a measurement of chlorophyll-generated fluorescence and provide an alternative method for estimation of phytoplankton biomass, as well as for determination of other phytoplankton properties. The MODIS sensor aboard the Aqua satellite is equipped with channels in the blue, green and red portions of the EMR and therefore has the ability to measure phytoplankton biomass via the blue/green ratio empirical and semi-analytical algorithms as well as fluorescence. The purpose of this paper was to evaluate the use of MODIS Aqua imagery and in situ chlorophyll matchup data to understand which type of algorithm might serve as a better measure of phytoplankton biomass and thus serve as a more useful descriptor of seasonal and annual changes in phytoplankton patterns throughout the Bay. It is well know that satellite estimation of chl a in nearshore waters is complicated and that other optically

active substances such as detrital material, dissolved organic substances, and suspended sediments can interfere in this process. While algorithms utilizing the blue/green portions of the electromagnetic spectrum are sensitive to changes in concentrations of CDOM and suspended matter, the fluorescence signal is less sensitive to interference caused by the presence of these materials. It is likely that some fluctuations in fluorescence signal are probably caused by the physiological state of the phytoplankton, light condition, nutrients and temperature. Ahn and Shanmugan (2007) found that these effects were much less than those produced by suspended sediment and dissolved organic matter on chl a retrieval. However, Gilerson et al. (2006) has shown that in coastal waters the fluorescence signal might be confounded by density-dependent scattering of algal and non-algal particles.

Based on the results of in water optics and in situ match ups with satellite data, it appears that FLH may provide a similar estimate of phytoplankton biomass patterns for the surface waters of Monterey Bay as provided by the OC3M and Carder algorithms. Even at chl a concentrations > 10 mg m^{-3}, the MODIS FLH algorithm, which was designed to measure the fluorescence peak at 683 nm, captures the shoulder of the shifting reflectance peak and correlates reasonably well with measured chlorophyll concentrations between 13-42 mg m^{-3}. This is contrary to the results of Gower et al., (2004) whose modeling results illustrated that the FHL algorithm is only good for measuring chl a concentrations between 10-20 mg m^{-3}. FLH patterns first appeared to correlate better with the in situ chl a measurements than either the empirical OC3M or semi-analytical Carder algorithms though not significantly, as well as providing an equal or better estimate of the cross-shore chl a gradient. Even when the in situ data set was reduced to concentrations < 10 mg m^{-3}, the FLH correlated equally as well as the other chl a retrieval algorithms. In both cases there

106

was no significant difference between the equality of correlation coefficients. Regardless, the FLH algorithm might provide an equally robust tool for measuring relative patterns of phytoplankton biomass.

The difference in mean spatial patterns produced by three algorithms varied greatly. Overall mean patterns of chl a estimates by the OC3M and Carder algorithms suggest that chl a retrieval is affected by the presence of other non-covarying suspended particulate or color dissolved organic matter. Estimates in the nearshore waters are consistently higher throughout the entire Bay and show a gradual decrease with distance from shore. FLH patterns suggest more reasonable patterns in phytoplankton abundance and illustrate some of the coastal ocean dynamics that have been observed in Monterey Bay. In the overall mean FLH pattern, the northern Bay appears to be an area of higher phytoplankton biomass and reflects the characteristics of an upwelling shadow as described in Graham and Largier (1997). Such an area has higher retentive circulation and stratification with residence times, in the case of northern Monterey Bay, on the order of 8 days. Such residence times are comparable to semi-enclosed embayments even though, Monterey Bay is an open embayment. The stratification and coherent recirculation of this feature is likely to be very important for such biological processes as primary production, the dispersal and recruitment of larvae (Graham and Largier, 1997; Wing et al., 1995; Wing et al, 1998) and the development of harmful algal blooms (Moita et al., 2003, Ryan et al., 2008). In the FLH composite, the middle of the Bay exhibits lower concentrations of phytoplankton biomass, suggesting the intrusion of recently upwelled water (Rosenfeld, 1994). The FLH signal also identifies a retentive area in the southern Bay which stands out as an area of relatively higher phytoplankton biomass than surrounding waters. These retentive zones, associated with embayments near

107

upwelling systems have also been observed near Point Reyes and appear as areas of higher chl a concentrations (VanderWoude et al., 2006; Roughan et al., 2006).

Seasonal patterns of FLH show the on- and offshore movement of areas of high phytoplankton biomass between the oceanic and upwelling seasons. This suggests an increased cyclonic circulation throughout the Bay during the upwelling period causing phytoplankton to aggregate alongside the upwelling fronts which sweep from the north, near Point Ano Nuevo, across the mouth of the Bay (Rosenfeld, 1994). During the oceanic period, when wind relaxation events are more common and upwelling intensity deceases, reduced cyclonic circulation allow this patch of high biomass to remain closer to the nearshore regions. A closer examination of the spatial patterns during the oceanographic period suggests the presence of land-sea linkages. Representative drifter tracks, which mark the surface transport pattern of land-derived nutrients and material, indicate that the highest average intensity of phytoplankton abundance lies in the wake of land-sea exchange. Studies of a dinoflagellate blooms in Monterey Bay during the 2007 oceanic period indicated bloom inception where rain-induced flushing or agricultural lands entered the coastal ocean (Ryan, unpublished data).

A year-by-year comparison of the oceanic period FLH means suggests that the relative abundance of phytoplankton and the potential for dinoflagellate blooms in Monterey Bay can vary significantly between years. The seasonal composite for 2007 registered the highest mean FLH signal and represents the year during which Monterey Bay may have seen the highest bloom activity over the last six years. The annual composites of the oceanic season also show high patches of FLH in the nearshore waters of the northern Bay, highlighting the importance of this region as a

red-tide "incubator" (Ryan et al, 2008).   Also illustrated in these satellite composites is the potential land-sea linkage. Higher concentration of phytoplankton are evident in the vicinity of the land-based nutrient sources of the Pajaro River and Elkhorn Slough (e.g. 2004, 2006 and 2007) outflows and the cyclonic bay-wide circulation can transport these nutrients to the northern Bay incubation region (e.g. 2004 and 2007). It is difficult to understand whether any of the measured variables, upwelling index, cumulative wind stress or land-based nutrients directly contribute or are responsible for the observed patterns of phytoplankton abundance due to the limited time series which is currently available from MODIS.   However, MODIS is one of the few sensors which has the appropriate channel to measure this fluorescence response and therefore capable of making this comparison.

4.5 Conclusions

These results show that the MODIS FLH provides an equally robust estimate of phytoplankton abundance within Monterey Bay as do the empirical OC3M and the semi-analytical Carder chl a retrieval algorithms. However the spatial and longer-term temporal FLH patterns of phytoplankton abundance appear to illustrate coastal ocean processes and phenomena better than the chl a algorithms. The FLH algorithm also appears to be useful for chl a concentrations up to 42 mg m^{-3}, contrary to previously published results. Hu et al. (2005) used the MODIS FLH product to monitor red tide blooms off the east coast of Florida and showed that blue/green ratio algorithms may overestimate and may falsely identify high chl patches. For them MODIS FLH showed the highest correlation with near-concurrent in situ chl a concentration. This suggests that the FLH algorithm should be examined further as a potential tool for monitoring relative patterns of phytoplankton biomass during the oceanographic season when, in recent years, the high biomass of dinoflagellate blooms have been

prevalent throughout Monterey Bay. Though blooms have been observed and monitored as having concentrations as high as 600-1000 mg m^{-3}, numerous lower level blooms have been observed in the bay with significantly high concentrations of chlorophyll (~50mg m) and an associated ruddy discoloration of surface waters. Further work is necessary to understand the relative measure of the FLH signal in relation to chlorophyll values or phytoplankton cell counts through concerted efforts to match in situ measurements during blooms to satellite overflight. It is also necessary to understand how FLH responds to changes in solar irradiance across the different seasons, various aspects of phytoplankton physiology, nutrient concentrations, and temperature, to further understand the utility of the FLH algorithm for monitoring bloom patterns in the Bay.

REFERENCES

Ahn, Y-H, and P. Shanmugam. 2006. Detecting the red tide algal blooms from satellite ocean color observations in optically complex Northeast-Asia coastal waters. *Remote Sensing of Environment* 103: 419-437.

---. 2007. Derivation and analysis of the fluorescence algorithms to estimate phytoplankton pigment concentrations in optically complex coastal waters. *Journal of Optics A: Pure and Applied Optics* 9: 352-362.

Aiken, G.R., D.M. McKnight, R.L. Wershaw, and P. MacCarthy, eds. 1985. *Humic substances in soil, sediment and water: Geochemistry, isolation and characterization*. New York: Wiley.

Anderson, D.M., P.M. Glibert, and J.M. Burkholder. 2002. Harmful algal blooms and eutrophication: Nutrient sources, composition, and consequences. *Estuaries* 25: 704-726.

Arts, M.T., and B.C. Wainmann. 1999. *Lipids in freshwater ecosystesm*. New York: Springer-Verlag.

Babin, M., A. Morel, and B. Gentili. 1996. Remote sensing of sea surface sun-induced chlorophyll-a fluorescence: Consequences of natural variation in the optical characteristics of phytoplankton and the quantum yield of chlorophyll-a fluorescence. *International Journal of Remote Sensing* 17: 2417-2448.

Bachok, Z., P. Mfilinge, and M. Tsuchiya. 2006. Characterization of fatty acid composition in healthy and bleached corals. *Coral Reefs* 25: 545-554.

Bailey, S.W., C.R. McClain, P.J. Werdell, and B.D. Scheiber. 2000. *Normalized water-leaving radiance and chlorophyll a match-up analyses*. Ed. J. Hooker, and Firestone J.. NASA/ATM-2000-206892.

Bakun, A. 1973. *Coastal upwelling indices, westcoast of North America 1946-1971*. NOAA Tech. Rep.

Bay, S.M., B.H. Jones, and K.C. Schiff. 1999. Study of the impact of stormwater discharge on Santa Monica Bay. University of California, Los Angeles, CA; Sea Grant Progrma, Wrigley Institute for Environmental Studies.

Bergmann, T.I. 2004. The physiological ecology and natural distribution patterns of cyrptomonad algae in coastal aquatic ecosystems. Dissertation. New Brunswick Rutgers, The State University of New Jersey, January.

Boyer, E.W., C.L. Goodale, N. Jaworski, and R.W. Howarth. 2002. Effects of anthropogenic loading on riverine nitrogen export in the northeastern US. *Biogeochemistry* 57 & 58: 137-169.

Breaker, L.C., and W.W. Broenkow. 2004. The circulation of Monterey Bay and related processes. *Oceanography and Marine Biology: An Annual Review* 32: 1-64.

Breaker, L.C., W.W. Broenkow, W.E. Watson, and Y-H Jo. 2008. Tidal and non-tidal oscillations in Elkhorn Slough, California. *Estuaries and Coasts* 31, no. 2: 238-257.

Broenkow, W.W., and L.C. Breaker. 2005. *A 30-year history of tide and current measurements in Elkhorn Slough, California*. Scripps Instituion of Oceanography Library, November 18. Scripps Instituion of Oceanography Library. http://repositories.cdlib.org/sio/lib/8.

Broenkow, W.W., and W.M. Smethie. 1978. Surface circulation and replacement of water in Monterey Bay. *Estuarine and Coastal Marine Science* 6: 583-603.

Broglio, E., S.H. Jonasdottir, A. Calbet, H.H. Jakobsen, and E. Saiz. 2003. Effect of heterotrophic versus autotrophic food on feeding and reproduction of the calanoid copepod Acartia tonsa: relationship with prey fatty acid composition. *Aquatic Microbial Ecology* 31: 267-278.

Budge, S.M., and C.C. Parrish. 1998. Lipid biogeochemistry of plankton settling matter and sediments in Trinity Bay, Newfoundland. II. Fatty Acids. *Organic Chemistry* 29: 1547-1559.

Budge, S.M., C.C. Parrish, and C. McKenzie. 2001. Distriution of pigments and fatty acid biomarkers in particulate matter from the frontal structure of the Alboran Sea (SW Mediterranean Sea). *Organic Geochemistry* 29: 1547-1559.

Caffrey, J.M., T.P. Chapin, H.W. Jannasch, and J.C. Haskins. 2007. High nutrient pulses, tidal mixing and biological response in a small California estuary: Variability in nutrient concentrations from decadal to hourly time scales. *Estuarine, Coastal and Shelf Science* 71: 368-380.

Carder, K.L., F.R Chen, Z.P. Lee, S.K. Hawes, and D. Kamykowski. 1999. Semi analytic moderate-resolution imaging spectrometer algorithm for chlorophyll-a and absorption with bio-optical domains based on nitrate-depletion temperatures. *Journal of Geophysical Research* 104: 5403-5412.

Carder, K.L., F.R. Chen, J.P. Cannizzaro, J.W. Campbell, and B.G. Mitchell. 2004. Performance of the MODIS semi-analytical ocean color algorithm for chlorophyll-a. *Advances in Space Research* 33: 1152-1159.

Chadwick, B.D., and J.L. Largier. 1999a. Tidal exchange at the bay-ocean boundary. *Journal of Geophysical Research* 104, no. C12: 29,901-29,924.

---. 1999b. The influence of tidal range on the exchnage between San Diego Bay and the ocean. *Journal of Geophysical Research* 104, no. 12: 29,885-29,899.

Chapin, T.P., J.M. Caffrey, H.W. Jannasch, et al. 2004. Nitrate sources and sinks in Elkhorn Slough, California: Results from long-term continuous in situ nitrate analyzers. *Estuaries* 27, no. 5: 882-894.

Chase, Z., P. Strutton, and B. Hales. 2007. Iron links river runoff and shelf width to phytoplankton biomass along the U.S. West Coast. *Geophysical Research Letters* 34: 1-4.

Chavez, F.P. 1995. A comparison of ship and satellite chlorophyll from California and Peru. *Journal of Geophysical Research* 100, no. C12: 24,855-24,862.

Claustre, H., J-C. Marty, L. Cassiani, and J. Dagaut. 1988. Fatty Acid dynamics in phytoplankton and microzooplankton communities during a spring bloom in the coastal Ligurian Sea: ecological implications. *Marine Microbial Food Webs* 3, no. 2: 51-66.

Cohen, Z., A. Vonshak, and A. Richmond. 1988. Effect of environmental conditions on fatty acid composition of the red alga Porphyridium cruentum: correlation to growth rate. *Journal of Phycology*, no. 24: 328-332.

Colombo, J.C., N. Silverberg, and J.N. Gearing. 1997. Lipid biogeochemistry in the Laurentian Trough - II. Changes in composition of fatty acids, sterols and aliphatic hydrocarbons during early diagenesis. *Organic Geochemistry* 26, no. 3/4: 257-274.

Copeman, L.A., and C.C. Parrish. 2003. Marine lipids in a cold coastal ecosystem: Gilbert Bay, Labrdor. *Marine Biology* 143: 1213-1227.

Costanza, R., R. d'Arge, R. de Groost, et al. 1997. The value of the world's ecosystem services and natural capital. *Nature* 387: 253-260.

Cranwell, P.A. 1982. Lipids of aquatic sediments and sedimenting particulates. *Progress in Lipid Research* 21: 271-308.

da Cunha, C.L., E.T. Buitenhuis, C. Le Quere, X. Giraud, and W. Ludwig. Potential impact of changes in river supply on global ocean biogeochemistry. *Global Biogeochemical Cycles* 21: GB4007, doi:10.1029/2006GB002718.

Dalsgaard, J., M. St John, G. Kattner, D. Muller-Navarra, and W. Hagen. 2003. Fatty acid trophic markers in the pelagic marine. *Advances in Marine Biology* 46: 225-340.

Dierssen, H.M., R.M. Kudela, J.P. Ryan, and R.C. Zimmerman. 2006. Red and lack tides: Quantitative analysis of water-leaving radiance and perceived ocean color for phytoplankton, colored dissolved organic matter and suspended sediments. *Limnology and Oceanography* 51, no. 6: 2646-2659.

Eisner, L.B., and T.J. Cowles. 2005. Spatial variations in phytoplankton pigment ratios, optical properties, and environmental gradient in Oregon coast surface waters. *Journal of Geophysical Reseach* 110, C10S14, doi:10.1029/2004JC002614

Eittreim, S.L., J.P. Xu, M. Nobel, and B.D. Edwards. 2002. Towards a sediment budget for the Santa Cruz shelf. *Marine Geology* 181: 235-248.

Elwany, M.H.S., R.E. Flick, and S. Aijaz. 1998. Opening and closure of a marginal of southern California lagoon inlet. *Estuaries* 21, no. 2: 246-254.

Emmett, R., R. Llanso, J. Newton, et al. 2000. Geographic signatures of North American west coast estuaries. *Estuaries* 23, no. 6: 765-792.

Eppley, R.W., E.H. Renger, and W.G. Harrison. 1979. Nitrate and phytoplankton production in southern California coastal waters . *Limnology and Oceanography* 24, no. 3: 483-494.

Evgenidou, A., A. Konkle, A. D'Ambrosio, et al. 1999. Effects of increased nitrogen loading on the abundance of diatoms and dinoflagellates in estuarine phytoplanktonic communities. *Biological Bulletin* 197: 292-294.

Falkowski, P., and D.A. Kiefer. 1985. Chlorophyll a fluorescence in phytoplankton: Relationship to photosynthesis and biomass. *Journal of Plankton Research* 7: 715-731.

Fischer, H.B., E.J. List, R.C.Y. Koh, J. Imberger, and N.H. Brooks. 1979. *Mixing in inland and coastal waters*. New York, NY: Academic Press, Inc.

Fisher, R.A. 1915. Frequency distribution of the values of the correlation coefficient in samples of an indefinitely large population. *Biometrika* 10: 507-521.

Fofonoff, N.P., and R.C. Millard. *Algorithms for computation of fundamental properties of seawater*. UNESCO Technical Papers in Marine Science. Unesco Division of Marine Science, France.

Folch, J., M. Lees, and G.H. Sloane Stanley. 1957. A simple method for the isolation and purification of total lipides from animal tissues. *Journal of Biological Chemistry* 226, no. 1: 497-509.

Franz, B.A., P.J. Werdell, G.K. Meister, et al. 2006. MODIS land bands for ocean remote sensing applications. In . Proceedings Ocean Optics XVIII, Montreal, Canada, October 9-13, 2006.

Fry, B., A. Gace, and J.W. McClelland. 2003. Chemical indicators of anthropogenic nitrogen loading in four Pacific estuaries. *Pacific Science* 57, no. 1: 77-101.

Fulco, A.J. 1983. Fatty acid metabolism in bacteria. *Progress in Lipid Research* 22: 133-160.

Furhman, J.A. 1999. Marine viruses and their biogeochemical and ecological effects. *Nature* 399: 541-548.

Gao, Q-F, P.K.S Shin, G-H Lin, S-P Chen, and S.G. Cheung. 2006. Stable isotope and fatty acid evidence for uptake of organic waste by green-lipped mussels Perna viridis in a polyculture fish farm system. *Marine Ecology Progress Series* 317: 273-283.

Garvine, R.W. 1995. A dynamical system for classifying buoyant coastal discharges. *Continental Shelf Research* 15, no. 13: 1585-1596.

Gilerson, A., J. Zhou, S. Hlaing, et al. 2007. Fluorescence component in the
reflectance spectra from coastal waters. Dependence on water composition.
Optics Express 15, no. 24: 15702-15721.

Gower, J.F.R., R. Doerffer, and G.A. Borstad. 1999. Interpretation of the 685nm peak
in water-leaving radiance spectra in terms of fluorescence, absorption and
scattering, and its observation by MERIS. *International Journal of Remote
Sensing* 20, no. 9: 1771-1786.

Gower, J.F.R., C. Hu, G.A. Borstad, and S. King. 2006. Ocean color satellites show
extensive lines of floating Sargassum in the Gulf of Mexico. *IEEE
Transactions on Geoscience and Remote Sensing* 44, no. 12: 3619-3625.

Graham, W.M., and J.L. Largier. 1997. Upwelling shadows as nearshore retention
sites: the example of northern Monterey Bay. *Coastal Shelf Research* 17, no. 5:
509-532.

Hallegraeff, G.M. 1993. A review of harmful algal blooms and their apparent global
increase. *Phycologia* 32, no. 3: 79-99.

---. 2003. Harmful algal blooms: a global overview. In *Manual on Harmful Marine
Microalgae*, ed. G.M. Hallegraeff, D.M. Anderson, and A.D. Cembella, 25-49.
Paris: UNESCO.

Holm-Hansen, O.C., J. Lorenzen, R.W. Holmes, and J.D. Strickland. 1965.
Fluorometric determination of chlorophyll. *ICES Journal of Marine Science*
30, no. 3-15.

Howarth, R.W., D. Anderson, J. Cloern, et al. 2000. Nutrient pollution of coastal
rivers, bays, and seas. *Issues in Ecology* 7: 1-15.

Howarth, R.W., G. Billen, D.P. Swaney, et al. 1996. Riverine inputs of nitrogen to the
North Atlantic ocean: Fluxes and human influences. *Biogeochemistry* 35:
75-139.

Howarth, R.W., and R. Marino. 2006. Nitrogen as the limiting nutrient for
eutrophication in coastal marine ecosystems: Evolving views over 3 decades.
Limnology and Oceanography 51: 288-295.

Howarth, R.W., D.P. Swaney, E.W. Boyer, et al. 2006. The influence of climate on
average nitrogen export from large watersheds in the Northeastern United
States. *Biogeochemistry* 79: 163-186.

Hu, C., F.E. Muller-Karger, C. Taylor, et al. 2005. Red tide detection and tracing
using MODIS fluorescence data: A regional example in SW Florida coastal
waters. *Remote Sensing of Environment* 97, no. 3: 311-321.

Inman, D.L., and S.A. Jenkins. 1999. Climate change and the episodicity of sediment
flux of small California rivers. *Journal of Geology* 107: 251-270.

Iriate, A., I. Madariaga, M. Revilla, and A. Sarobe. 2003. Shot-term variability in microbial food web dynamics in a shallow tidal estuary. *Aquatic Microbial Ecology* 31, no. 2: 145-161.

Jeong, H.J., Y.D. Yoo, J.S. Kim, et al. 2004. Mixotrophy in the phototrophic alga Cochlodinium polykrikoides (Dinophycean): Prey species, the effects of prey concentration, and grazing impact. *Journal of Eukaryotic Microbiology* 51, no. 5: 563-569.

Jeong, H.J., Y.D. Yoo, J.Y. Song, et al. 2005. Feeding by phototrophic red-tide dinoflagellates : five species newly revealed and six species previ ously known to be mixotrophic. *Aquatic Microbial Ecology* 40, no. 2: 133-150.

Jester, R., M. Silver, G. Langlois, and V. Vigilant. 2008. A shift in the dominant toxin-producing species in central California alters phycotoxins in food webs. *Hamrful Algae* In press.

Jickells, T.D. 1993. Nutrient biogeochemistry of the coastal zone. *Science* 281: 217-222.

Johnson, J.W. 1973. Characteristics and behavior of Pacific coast tidal inlets. *Journal of the Waterways and Harbors and Coastal Engineering Division* 99, no. 3: 325-339.

Johnson, K.S., and L.J. Coletti. 2002. In situ ultraviolet spectrophotometry for high resolution and long-term monitoring of nitrate, bromide and bisulfide in the

ocean. *Deep-Sea Research I* 49: 1291-1305.

Johnson, R.A., and D.W. Wichern. 2002. *Applied multivariate statistical analysis*. 5th ed. Upper Saddle Rive, New Jersey: Prentice Hall.

Kahn, R., P. Banerjee, D. McDonald, and J. Martonchik. 2001. Aerosol properties derived from aircraft multiangle imaging over Monterey Bay. *Journal of Geophysical Reseach* 106, no. D11: 11,977-11,995.

Kahru, M., and B.G. Mitchell. 2008. Ocean color reveals increased blooms in various pats of the world. *EOS* 89, no. 19: 170.

Kainz, M., M.T. Arts, and A. Mazumder. 2004. Essential fatty acids in the planktonic food web and their ecological role for higher trophic levels. *Limnology and Oceanography* 49, no. 5: 1784-1793.

Kamykowski, D. 1987. A preliminary biophysical model of the relationship between temperature and plant nutrients in the upper ocean. *Deep Sea Research* A 34: 1067-1079.

Kaneda, T. 1991. Iso- and anteiso-fatty acids in bacteria: biosynthesis, function, and taxonomic significance. *Microbiology Review* 55: 288-302.

Kite-Powell, H., C. Colgan, and R. Weiher. 2008. Estimating the economic benefits of regional ocean observing systems. *Coastal Management* 36, no. 2: 125-145.

Kudela, R.M., and F.P. Chavez. 2000. The impact of coastal runff on ocean color
during an El Nino year in Central Caliornia. *Deep Sea Research II* 47:
1055-1076.

Kudela, R.M., and W.P. Cochlan. 2000. Nitrogen and carbon uptake kinetics and the
influences of irradiance for a red tide bloom off Southern California. *Aquatic
Microbial Ecology* 21: 31-47.

Kudela, R.M., J.P. Ryan, M.D. Blakely, J.Q. Lane, and T.D. Peterson. 2008. Linking
the physiology and ecology of Cochlodinium to better understand harmful
algal bloom events: a comparative approach. Harmful Algae 7, no. 3: 278-292.

Largier, J.L., J.T. Hollibaugh, and S.V. Smith. 1997. Seasonally hypersaline estuaries
in Mediterranean-climate regions. *Estuarine, Caostal and Shelf Science* 45:
789-797.

Lemos, R. T. , S. Bruno, and M. Los Huertos. 2007. Spatially varying temperature
trends in a Central California estuary. *Journal of Agriculture, Biological &
Environmental Statistics* 12, no. 3: 379-396.

Letelier, R.M., and M.R. Abbott. 1996. An analysis of chlorophyll fluorescence
algorithms for the Moderate Resolution Imaging Spectrometer (MODIS).
Remote Sensing of Environment 58: 215-223.

Lipski, A., E. Spiek, A. Makolla, and K. Altendorf. 2001. Fatty acid profiles of nitrite-oxidizing bacteria reflect their phylogenetic heterogeneity. *Systematic and Applied Microbiology* 24, no. 3: 377-384.

Lorenzen, C.J. 1966. A method for the continuous measurement of in vivo chlorophyll concentration. *Deep-Sea Research* 13: 223-227.

Lowe, P. 1999. Marsh loss in Elkhorn Slough, California: Patterns, mechanisms, and impact on shorebirds. M.S. Thesis, Moss Landing Marine Laboratories, San Jose State University.

Malzone, C.M. 1999. Tidal scour and its relation to erosion and sediment transport in Elkhorn Slough. M.S. Thesis, Department of Geology, San Jose State University.

Meng, X-L, R. Rosenthal, and D.B. Rubin. 1992. Comparing correlated correlation coefficeints. *Psychological Bulletin* 111, no. 1: 172-175.

Mertes, L.A.K., M. Hickman, B. Waltenberger, et al. 1998. Synoptic views of sediment plumes and coastal geography of the Santa Barbara Basin, California. *Hydrological Processes* 12: 967-979.

Mertes, L.A.K., and J.A. Warrick. 2001. Measuring flood output from 110 coastal watersheds in California with field measurements and SeaWiFS. *Geology* 29, no. 7: 659-662.

Meziane, T., and M. Tsuchiya. 2002. Organic matter in a subtropical mangrove-estuary subjected to wastewater discharge: origin and utilization by two macrozoobenthic species. *Journal of Sea Research* 47: 1-11.

Milke, L.M., V.M. Bricelj, and C.C. Parrish. 2004. Growth of post-larval sea scallops, Placopecten magellanicus, on microalgal diets, with emphasis on the nutirtional role of lipids and fatty acids. *Aquaculture* 234: 293-317.

Moita, M.T., P.B. Oliveira, J.C. Mendes, and A.S. Palma. 2003. Distribution of chlorophyll a and Gymnodinium catenatum associated with coastal uppwelling plumes off central Portugal. *Acta Oecologica* 24: S125-S132.

Mopper, K., and D.J. Kieber. Photochemistry and the cycling of carbon, sulfur, nitrogen and phosphorus. In B*iogeochemistry of Marine Organic Matter*, ed. D Hansell and C. Carlson. New York: Academic Press, Inc.

Morel, A., and A. Bricaud. 1981. Theoretical results concerning light absorption in a discrete medium, and application to specific absorption of phytoplankton. *Deep Sea Research* 28: 1375-1393.

Nagata, T., and D.L. Kirchman. 1992. Release of macromolecular organic complexes by heterotrophic marine flagellates. *Marine Ecology Progress Series* 83: 233-240.

Neill, J.J., and O.J. Dunn. 1975. Equality of dependent correlation coefficients. *Biometrics* 31: 531-543.

Neville, R.A., and J.F.R. Gower. 1977. Passive remote sensing of phytoplankton via chlorophyll alpha fluorescence. *Journal of Geophysical Research* 82, no. 24: 3487-3493.

Nichols, D.S., P.D. Nichols, and P. Virtue. Fatty acid, sterol and hydrocarbon composition of Antarctive sea ice diatom communities during the spring bloom in McMurdo Sound. *Antarctic Science* 5: 271-278.

Nichols, F.H., J.E. Cloern, S.N. Luoma, and D.H. Peterson. The modification of an estuary. *Science* 231: 567-573.

Noble, R.T., S.B. Weisberg, M.K. Leecaster, et al. 2003. Storm effects on regional beach water quality along the southern California shoreline. *Journal of Water and Health* 1, no. 1: 23-31.

NRC. 2000. *Clean Coastal Waters: Understanding and Reducing the Effects of Nutrient Pollution*. Washington, DC: National Academies Press.

O'Reilly, J.E. *SeaWiFS Postlaunch Calibration and Validation Analyses, Part 3*. NASA Tech. Memo. NASA Goddard Space Flight Center.

Ott, R.L., and M. Longnecker. 2001. *Statistical methods and data analysis*. 5th ed. Duxbury Thomspn lEarning.

Parrish, C.C.. 1999. Determination of total lipid, lipid classes, and fatty acids in aquatic samples. Eds M.T. Art and Wainman, C. In *Lipids in Freshwater Ecosystems*, 4-20. New York: Springer-Verlag.

Parrish, Christopher C., Raymond J. Thompson, and D. Deibel. 2005. Lipid classes and fatty acids in plankton and settling matter during the spring bloom in a cold ocean coastal environment. *Marine Ecology Progress Series* 286: 57-68.

Pennington, J.T., and F.R Chavez. 2000. Seasonal fluctuations of temperature, salinity, nitrate, chlorophyll and primary production at station H3/M1 over 1989-1996 in Monterey Bay, California. *Deep-Sea Research II* 47: 947-973.

Pond, D., R. Harris, R. Head, and D. Harbour. Environmental and nutritional factors determining seasonal variability in the fecundity and egg variability of Calanus helgolandis in coastal waters off Plymouth, UK. *Marine Ecology Progress Series* 143: 45-63.

Pond, S., and G.L. Pickard. 1983. *Introductory dynamical oceanography*. 2nd ed. Burlington, MA: Elsevier Butterworth-Heinemann.

Rein, F.A. 1999. An economic analysis of vegetative buffer strip implementation case study: Elkhorn Slouh, Monterey Bay, California. *Coastal Management* 27, no. 4: 377-390.

Rienecker, E.V., J.P. Ryan, M. Blum, et al. 2008. Mapping phytoplankton in situ using a laser-scattering sensor. *Limnology and Oceanography: Methods* 6: 153-161.

Roessler, P.G. 1990. Environmental control of glycerolipid metabolism in microalgae: commerical implicatio and future research directions. *Journal of Phycology* 29: 393-399.

Rosenfeld, L.K., F.B. Schwing, N. Garfield, and D.E. Tracy. 1994. Bifurcated flow from an upwelling center: a cold water source or Monterey Bay. *Continental Shelf Research* 14: 931-964.

Roughan, M., N. Garfield, J. Largier, et al. 2006. Transport and retention in an upwelling region: The role of across-shelf structure. *Deep Sea Research Part II* 53, no. 25-26: 2931-2955.

Ryan, J.P., H.M. Dierssen, R.M. Kudela, et al. 2005. Coastal ocean physics and red tides: An example from Monterey Bay, California. *Oceanography* 18, no. 2: 246-255.

Ryan, J.P., A.M. Fischer, R.M. Kudela, et al. 2008a. Influences of upwelling and downwelling winds on red tide bloom dynamics in Monterey Bay, California. *Continental Shelf Research* (accepted).

Ryan, J.P., J.F.R. Gower, S.A. King, et al. 2008b. A coastal ocean extreme bloom incubator. *Geophysical Research Letters* 35 L12602, doi:10.1029/2008GL03408.

Sargent, J.R, R.J Parkes, I. Mueller-Harvey, and R.J. Henderson. 1987. Lipid biomarkers in marine ecology. In *Micorbes in the Sea*. Chichester; Ellis Horwood; New York.

Sargent, J.R., and K.J. Whittle 1981. Lipids and hydrocarbons in the marine food web. In *Analysis of Marine Ecosystems*, ed. A.R. Longhurst, pp. 491-533, London:Academic.

Shalles, J.F. 2006. Optical remote sensing techniques to estimate phyotplankotn chlorophyll a concnetrations in caostal waters with varying suspended mater and CDOM concnetrations. In *Remote Sensing of Aquatic Coastal Ecosystem Processes: Science and Management Applications*, ed. L.L. Richardson and E.F. LeDrew, Chap 3. Springer.

Skreslet, S. 1986. *The role of freshwater outflow in coastal marine ecosystems*. Berlin: Springer-Verlag.

Sloan, N.A., K. Vance-Borland, and G. Carleton-Ray. 2007. Fallen between the cracks: Conservation linking land and sea. *Conservation Biology* 21, no. 4: 897-898.

Smith, R.E. 1974. The hydrography of Elkhorn Slough, a shallow california coastal embayment. M.A., Moss Landing Marine Laboratories an the Department of Natural Sciences, San Jose State University.

Spatharis, S., G. Tsirtsis, D.B. Danielidis, T.D. Chi, and D. Mouillot. 2007. Effects of pulsed nutrient inputs on phytoplankton assemblage structure and blooms in an enclosed coastal area. *Estuarine, Coastal and Shelf Science* 73, no. 3-4: 807-815.

Steiger, J.H. 1980. Tests or comparing elements of a correlation matrix. *Psychological Bulletin* 87: 245-251.

Stoderegger, K., and G.J. Herndl. 1998. Production and release of bacterial capsular material and its subsequent utilization by marine bacterioplankton. *Limnology and Oceanography* 43: 877-884.

Stommel, H., and H.G. Farmer. 1952. *On the nature of estuarine circulation*. Woods Hole Oceanographic Institute References, 52-51, 52-63, 52-88 (3 vols. Chapter 4).

Stubing, D., and W. Hagen. 2003. Fatty acid biomarker ratios - suitable trophic indicators in Antarctic euphausiids? *Polar Biology* 26: 774-782.

Valiela, I. 1992. Coupling of watersheds and coastal waters: an introduction to the dedicated issue. *Estuaries* 15: 429-430.

Vance, E., and J.E. Vance. 1985. *Biochemistry of lipids and membranes*. USA: Cummings Publishing Company, Inc.

VanderWoude, A.J., J.L. Largier, and R.M. Kudela. 2006. Nearshore retention of upwelled waters north and south of Point Reyes (northern California) - Patterns of surface temperature and chlorophyll observed in CoOPWEST. *Deep Sea Research Part II* 53, no. 25-26: 2985-2998.

Vernick, E.L., and T.L. Hayward. 1984. *Determining chlorophyll on the 1984 CalCOFI surveys*. California Cooperative Oceanic Fisheries Investgations.

Volkman, J.K., and R.C. [Ed.] Cambie. Fatty acids of microalgae used as feedstock in aquaculture. In *Fats for the Future*, 263-83. Chichester: Ellis Horwood.

Volkman, J.K., R.B. Johns, F.T. Gillian, and G.J. Perry. 1980. Microbial lipids of an intertidal sediment - I. Fatty acids and hydrocarbons. . *Geochimica et Cosmochimica Acta* 44: 1133-1143.

Walling, D.E. 2006. Human impact on land-ocean sediment transfer by the world's rivers. *Geomorphology* 79, no. 3-4: 192-216.

Wang, M., and W. Shi. 2007. The NIR-SWIR combined atmospheric correction approach for MODIS ocean color data processing. *Optics Express* 15, no. 24: 15722-15733.

Warrick, J.A., P.M. DiGiacomo, S.B. Weisberg, et al. 2007. River plume patterns and dynamics within the Southern California Bight. *Continental Shelf Research* 27: 2427-2448.

Warrick, J.A., L.A.K. Mertes, L. Washburn, and D.A. Siegel. 2004b. Dispersal forcing of southern California river plumes, based on field and remote sensing observations. *Geo-Marine Letters* 24: 46-52.

---. 2004. A conceptual model for river water and sediment dispersal in the Santa Barbara Channel, California. *Continental Shelf Research* 24: 2029-2043.

Washburn, L., K.A. McClure, B.H. Jones, and S.M. Bay. 2003. Spatial scales and evolution of stormwater plumes in Santa Monica Bay. *Marine Environmental Research* 56: 103-125.

Wasson, K., E. Van Dyke, R. Kvitek, J. Brantner, and S. Bane. 2001. Tidal erosion at Elkhorn Slough. *Ecosystem Observations for the Monterey Bay National Marine Sanctuary.* NOAA Monterey Bay National Marine Sanctuary, Monterey, California.

Welschmeyer, N., L. Younan, A. Thurber, and G. Wagner. 2003. Phytoplankton, Biodiversity and Invasive Species in Elkhonr Slough. *Ecosystem Observations for the Monterey Bay National Marine Sanctuary*. NOAA Monterey Bay National Marine Sanctuary, Monterey, California.

Werdell, P.J., and S.W. Bailey. 2005. An imporved in-situ bio-optical data set for ocean color algorithm development and satellite data product validation. *Remote Sensing of Environment* 98, no 1: 122-140.

Wing, S.R., L.W. Botsford, S.V. Ralston, and J.L. Largier. 1998. Meroplanktonic distribution and circulation in a coastal retention zone of the northern California upwelling system. *Limnology and Oceanography* 43, no. 7: 710-721.

Wing, S.R., J.L. Largier, L.W. Botsford, and J.F. Quinn. 1995. Settlement and transpot of benthic invertebrates in an intermittent upwelling region. *Limnology and Oceanography* 40, no. 2: 316-329.

Yankovsky, A.E., and D.C. Chapman. 1997. A simple theory for the fate of buoyant coastal discharges. *Journal of Physical Oceanography* 27: 1386-1401.

Zedler, J.B. 1996. Coastal mitigation in southern California: The need for a regional restoration strategy. *Ecological Applications* 6: 84-93.

Zou, L., X-C Wang, J. Callahan, et al. 2004. Bacterial roles in the formation of high-molecular-weight dissolved organic matter in estuarine and coastal waters: Evidence from lipids and the compound-specific isotopic ratios. *Limnology and Oceanography* 49, no. 1: 297-302.